

EVALUATION OF THE ROLE OF CORTISOL IN MODULATING SEASONAL CHANGES IN IMMUNITY

By

KAMAU PIERRE

A dissertation submitted to the

Graduate School – New Brunswick

Rutgers, The State University of New Jersey

In partial fulfillment of the requirements

For the degree of

Doctor of Philosophy

Graduate Program in Biomedical Engineering

Written under the direction of

Ioannis P. Androulakis

And approved by:

New Brunswick, New Jersey

October, 2017

ABSTRACT OF THE DISSERTATION

Evaluation of the role of cortisol in modulating seasonal changes in immunity

By KAMAU PIERRE

Dissertation Director:

Ioannis P. Androulakis

Inflammatory diseases such as asthma, rheumatoid arthritis (RA) and systemic vasculitis exhibit seasonality with higher prevalence and aggravated symptoms occurring during the winter months. Though the underlying causes remain to be elucidated, disease seasonality has been associated with circannual changes in antibodies, hormonal levels, acute phase reactants and numerous immunomodulatory components. For instance, RA risk biomarkers such as IL-6R mRNA, sIL-6 receptor and C-reactive proteins vary significantly throughout the year with peak expressions during the winter season. Apart from seasonal variation, the dynamics of functions such as cytokine production and hormone secretion display diurnal fluctuations that are entrained to the external 24-hour light/dark cycle. The light fraction of the light/dark cycle, or photoperiod, varies predictably throughout the year and is a robust environmental cue that synchronizes seasonal variations in neuroendocrine function. It is well established that cortisol, regulated via hypothalamic-pituitary-adrenal (HPA) axis activity and entrained to the external photoperiod, is a potent immunomodulator whose level varies seasonally. A

detailed experimental analysis of the role of the HPA axis in regulating seasonal changes in immune function is lacking due to the complex network of biological interactions. In this work, we developed a semi-mechanistic mathematical model to evaluate cortisol's role in modulating seasonal immunological plasticity. Our results indicate a shift from an anti- to a pro-inflammatory state as the seasons progress from summer through winter with elevated expression of the cortisol-activating enzyme 11 β -hydroxysteroid dehydrogenase type 1 (11 β -HSD1), an inflammatory disease biomarker, predicted for the winter season. Experimentally, the pro-inflammatory phenotype correlated with mitotic asynchrony is mitigated following glucocorticoid-induced cell resynchronization. A cortisol-dependent, time-of-day and seasonal variability in the synchronization of the molecular clock and cell cycle was predicted. These findings have major health implications as the misalignment of internal dynamics with environmental signals has been associated with inflammatory disease progression. The current model provides a framework for exploring the impact of asynchrony between the circadian and cell cycle oscillators, amongst cells in a population, on immune system dynamics. Knowledge of the underlying putative mechanisms governing seasonal and diurnal modifications of immune system dynamics can be applied to design more effective preventative and chronotherapeutic strategies addressing the development and advancement of a pro-inflammatory state.

Acknowledgements

This thesis became a reality due to the support of so many individuals. Firstly, I wish to thank **GOD** for the wisdom bestowed upon me as well as the strength and patience to pursue this academic endeavor to its completion. To my **FAMILY**, I would not be here if it were not for your sacrifices. I thank my father, **Brian**, for allowing me to develop into the man I am today. To my mother, **Merlyn**, I would need more than a lifetime to repay you for all that you did for me. I remain forever indebted. To my elder sisters, **Tricia** and **Kiesha**, you both easily assumed the role of “second mothers”. Always nurturing and protecting. I’ll always be your little brother. To **Sarah-Lee**, I applaud you for your patience and never-ending support. To my **FRIENDS** world-wide, I love you all. To my advisor, **Ioannis Androulakis**, I thank you for your guidance and vision. I thank my **Thesis Committee** for all their continued support. To all individuals, mentioned and unmentioned, I dedicate this work to you.

Table of Contents

ABSTRACT OF THE DISSERTATION	ii
Acknowledgements.....	iv
List of Tables	vii
List of Illustrations.....	viii
CHAPTER 1: Introduction	1
1.1: Photoperiod, circadian rhythms and immune activity	1
1.2: Seasonality, immune function and disease	4
1.3: Outline of the Dissertation.....	11
CHAPTER 2: HPA axis regulation of immune function to predict photoperiod-induced seasonality changes.....	13
2.1: Background.....	13
2.2: Approach.....	14
2.3: Seasonal Changes in Circadian Profiles and the Inflammatory Response	26
CHAPTER 3: The hepato-hypothalamic-pituitary-adrenal-renal axis: cortisol's production, metabolism and seasonal variation	35
3.1: Background.....	35
3.2: Approach.....	38
3.3: Seasonal Changes in Circadian Dynamics.....	48
3.4: Parameter sampling: <i>In silico</i> Population Generation, HSD11B1 KO and cluster analysis.....	56
3.5: Population seasonal changes in circadian dynamics.....	60
3.6: Sub-population classification and in-silico 11 β -HSD1 knockout.....	62
3.7: Sensitivity Analysis	75

3.8: Time scale Analysis	82
CHAPTER 4: Seasonal Entrainment of Physiological Oscillators.....	85
4.1: Entrainment of the peripheral molecular clock by a seasonally varying cortisol signal.....	85
4.1.1: Background.....	85
4.1.2: Approach.....	88
4.1.3: Seasonality of Entrainment and Intercellular Synchronization	90
4.2: Seasonal Entrainment of the Cell Cycle Oscillator	101
4.2.1: Background.....	101
4.2.2: Approach.....	104
4.2.3: Model Construction and Validation.....	107
4.2.4: Cell population cyclin oscillations and cell cycle mapping.....	109
4.2.5: Seasonal Populations, Perturbations and Future Considerations.....	118
CHAPTER 5: Conclusions	122
REFERENCES	124
APPENDIX.....	151
Table A1.....	151
Table A2.....	159
Table A3.....	161

Note: This work has been accepted in part for publication in *Physiological Genomics* and also submitted to the *Journal of Biological Rhythms*. The candidate is the original author of the material.

List of Tables

Table 1. Median values of each parameter arranged by cluster for the spring (baseline) model. ^{§¶Ω*} Same symbol indicates no significant difference between clusters.....	66
Table 2. Cluster regression coefficients for the spring model.	67
Table 3. Reference numbers and their corresponding parameter names for sensitivity analysis bar graph plots.....	78

List of Illustrations

Figure 1 .The modeled light profile for each season.	15
Figure 2. Schematic representation of our two compartment model.	15
Figure 3. Circadian rhythms for cortisol ($F_{\text{periphery}}$), pro-inflammatory mediator (P), pro-inflammatory receptor (R_P) and $BMAL1$	27
Figure 4. The amplitude (radial dimension) and phase (angular dimension) of the circadian rhythms for cortisol ($F_{\text{periphery}}$), pro-inflammatory mediator (P), pro-inflammatory receptor (R_P) and $BMAL1$ for each seasonal model.	28
Figure 5. Compass plot showing the seasonal differences of the amplitude (radial dimension) and phase (angular dimension) of R_{TLR4^*} in the unchallenged model.	29
Figure 6. Seasonal variations in the inflammatory response following in silico administration of acute doses of endotoxin (LPS dose of 0.5 a.u.) at each hour of the simulated day.	30
Figure 7. Diurnal profiles for cortisol and P_{max} for each seasonal model.	31
Figure 8. Circadian profiles of cortisol ($F_{\text{periphery}}$) and $BMAL1$ for each season in the unchallenged model.	32
Figure 9. Maximum pro-inflammatory mediator level (P_{max}) versus the time delay between LPS addition and the time-of-maximum response (ΔT_{max}) for each simulated season.	33
Figure 10. Profiles of R_{TLR4^*} for the unchallenged model and ΔT_{max} versus the time of LPS administration for each season.	33
Figure 11. Modified model schematic incorporating 11β -HSD dynamics and cortisol/cortisone metabolism.	39
Figure 12. Seasonal circadian profiles.	49
Figure 13. Seasonal and circadian variation of mechanisms regulating $F_{\text{periphery}}$ availability.	52
Figure 14. $F_{\text{periphery}}$ activation rate and circadian variation of 11β -HSD1 and E for the spring (baseline) model.	53
Figure 15. $F_{\text{periphery}}$ inactivation rate and circadian variation of 11β -HSD2 and $F_{\text{periphery}}$ for the spring baseline model.	55
Figure 16. Seasonal whisker plots for $F_{\text{periphery}}$ added or removed from the system by various mechanisms and the ratio of $F_{\text{periphery}}$ to E	61

Figure 17. Scatter plots of 741 subjects' $11\beta - HSD2$ versus $11\beta - HSD1$ amplitudes for all four seasons with each point color-coded by cluster association.	64
Figure 18. Cluster variation of spring parameter distributions for k_{8a} , k_{10a} and k_{12d} . ..	65
Figure 19. Cortisol fold change scatter plots.	69
Figure 20. Distributions of zenith fold changes for each season and cluster.	71
Figure 21. Distributions of nadir fold changes for each season and cluster.	72
Figure 22. Comparison of $F_{periphery}$ circadian profiles of each cluster for the spring model.	73
Figure 23. Cluster variation in $F_{periphery}$ activation for the spring (baseline) model under normal conditions.	74
Figure 24. Local sensitivity indices with respect to the amplitude of E	77
Figure 25. Local sensitivity indices with respect to the phase of E	78
Figure 26. Global sensitivity indices with respect to the amplitude of E	80
Figure 27. Global sensitivity indices with respect to the phase of E	80
Figure 28. Diurnal variation of time-scales for the spring model.	83
Figure 29. Seasonal distributions of Per-Cry _{mRNA} periods for the unentrained oscillators.	91
Figure 30. Seasonal distributions of Per-Cry _{mRNA} for the unentrained oscillators.	91
Figure 31. Seasonal circadian profiles of the unentrained Per-Cry _{mRNA} oscillators. ...	92
Figure 32. Seasonal circadian profiles of the pro-inflammatory mediator P with the unentrained molecular clock.	93
Figure 33. Seasonal distributions of Per-Cry _{mRNA} periods for the entrained oscillators.	94
Figure 34. Seasonal distributions of Per-Cry _{mRNA} phases for the entrained oscillators.	97
Figure 35. Seasonal circadian profiles of the entrained Per-Cry _{mRNA} oscillators.	99
Figure 36. Seasonal circadian profiles of the pro-inflammatory mediator P with the entrained molecular clock.	100
Figure 37. Modified model schematic incorporating the cell cycle component.	106
Figure 38. Seasonal circadian profiles for cyclin/Cdk complexes.	108
Figure 39. Seasonal circadian profiles for cyclin/Cdk complexes following the removal of the entraining signals.	109

Figure 40. Representative circadian profiles of the molecular clock and cell cycle..	110
Figure 41. Seasonal circadian profiles of <i>CYCD</i>	112
Figure 42. Cell cycle phase determination.....	113
Figure 43. Spring distribution for duration of cell cycle phases.....	114
Figure 44. Bar graph depicting circadian and seasonal variations in cell cycle progression.	115
Figure 45. Seasonal and circadian variation in cell cycle synchronization and cortisol levels.	117
Figure 46. Seasonal differences in cell cycle synchrony following cortisol perturbation.	120

CHAPTER 1: Introduction

1.1: Photoperiod, circadian rhythms and immune activity

Biological activities of organisms have evolved to achieve synchrony between processes and the environment with the periodicity of numerous physiological functions paralleling the 24-hour light-dark cycle. This synchrony ultimately confers a survival advantage (Toh 2008). Strains of cyanobacteria, for instance, with a circadian period similar to their exposed light-dark cycle are favored to survive over others (Ouyang, Andersson et al. 1998). In animals, activities such as feeding behavior, the sleep-wake cycle, body temperature and hormone secretion are under circadian control whereby they oscillate with a period approximating 24 hours. The precise timing of these activities are regulated by an endogenous molecular clock. The mammalian master circadian pacemaker is located in the suprachiasmatic nucleus (SCN) of the anterior hypothalamus. The SCN is a complex network of approximately 20000 neurons and is entrained to the diurnal light-dark cycle by communication with retinal ganglion cells (RGCs) present within the eye (Newman, Walker et al. 2003). The photic signal is integrated within the SCN and translated into neuronal and humoral signals that ultimately regulate the timing of biological processes. While the SCN is the central pacemaker, autonomous oscillators in the periphery also temporally coordinate physiological functions. The intrinsic molecular clock mechanism present in both the SCN and the periphery is contingent on an auto-regulatory transcription-translation feedback loop comprising core genes which include *Per1*, *Per2*, *Cry*, *Cry2*, *Clock* and *Bmal1* (Takahashi, Hong et al. 2008). Though

entrainable to external cues, or zeitgebers, the endogenous clock regulates circadian activity in the absence of external signals.

Circadian hormones such as melatonin and glucocorticoids (cortisol in humans), regulated by SCN activity, act as circadian signal transduction mediators that modulate immune function (Mavroudis, Scheff et al. 2013). Melatonin, produced by the pineal gland, is typically considered to be immunoenhancing whereby it promotes pro-inflammatory cytokine production (Srinivasan, Maestroni et al. 2005). Furthermore, pinealectomized animals tend to display impaired immune function including inhibition of natural killer cell activity, attenuation of IL-2 production and diminished humoral responses (Carrillo-Vico, Reiter et al. 2006). Glucocorticoids (GCs) are generally characterized as anti-inflammatory as they repress transcription of pro-inflammatory genes encoding for cytokines such as IL-1 β , IL-2, IL-3, IL-6, IL-11 and TNF- α , inhibit macrophage secretion of inflammatory mediators and also repress the activation, proliferation and survival of T-lymphocytes (Barnes 1998). Deviating from the stereotypical anti-inflammatory classification, GCs have also been ascribed pro-inflammatory traits. Stimulation of human peripheral blood mononuclear cells with dexamethasone increases expression of pro-inflammatory receptors such as IL-1R1, the IL-6 type receptor gp130 subunit, IFN- α R, IFN- γ RI, IFN- γ RII and TNF receptor family members (Galon, Franchimont et al. 2002). It is now currently believed that in the periphery GCs bestow both “permissive” and “suppressive” effects such that basal GC concentrations are pro-inflammatory while elevated concentrations of GCs are anti-inflammatory (Sorrells and Sapolsky 2007).

Various functions and parameters of immune function display diurnal fluctuations which include cytokine secretion, leukocyte trafficking, pathogen detection sensitivity and phagocytic ability (Scheiermann, Kunisaki et al. 2013). Although it is highly possible that the SCN coordinates the timing of these immune activities, cellular oscillators in the periphery have been shown to regulate facets of immune function. Keller et al. (Keller, Mazuch et al. 2009) identified the existence of circadian clock proteins in the lymph nodes, spleen and peritoneal macrophages of mice. Additionally, secretion of IL-6 and TNF- α by spleen macrophages following endotoxin administration at different circadian times displayed a time-of-day sensitivity. The inflammatory response was comparable for both the control and adrenalectomized mice and suggests a fundamental role of the peripheral oscillators in regulating immune function; independent of a systemic signal. The influence of peripheral clock genes (PCGS), and the proteins they encode, on inflammatory responses is well documented. Myeloid-specific BMAL1 deficient mice exhibit enhanced activity of NF- κ B, a pro-inflammatory gene inducer, and enhanced production of IL-1 β , INF- γ and IL-6 (Gibbs, Blaikley et al. 2012, Nguyen, Fentress et al. 2013, Curtis, Fagundes et al. 2015). CLOCK is often complexed with the NF- κ B subunit p65 and overexpression of CLOCK increases transcriptional activity of NF- κ B (Spengler, Kuropatwinski et al. 2012). Per2 mutant mice express less Tlr9 mRNA (Silver, Arjona et al. 2012) which is fundamental for pathogen recognition. Increased production of IL-6 and Cxcl1 by BMDM from Cry1/Cry2 double KO mice was observed (Narasimamurthy, Hatori et al. 2012).

While the PCGs oscillate autonomously and coordinate dynamics in the periphery, they are also regulated by signals such as feeding schedule and glucocorticoids (Mohawk, Green et al. 2012). Treating primary mouse mesenchymal stem cells (MSCs) with dexamethasone stimulates transcriptional oscillation of core clock components like Per1-3, Cry1-2 and Bmal1 mRNA (So, Bernal et al. 2009). The entraining effects of GCs on peripheral oscillators have been recently investigated whereby 16 healthy volunteers were administered exogenous doses of Cortef, a synthetic GC (Cuesta, Cermakian et al. 2015). This study found that GC exerted no effects on the central clock but following their assessment of PBMCs, observed an increased expression of Per1 and that the phases of mRNA expression for Bmal1 and Per2-3 were shifted by 9.5 – 11.5 hours.

Current evidence suggests that while immune function may be diurnally regulated via peripheral molecular clock components, these PCGs, and by extension immune activity, can be entrained to a systemic signal such as cortisol. It is possible, therefore, that photoperiod changes could potentially alter immune functionality indirectly by modulating the circadian dynamics of cortisol secretion.

1.2: Seasonality, immune function and disease

Alterations in physiological function correlate with environmental seasonal changes and for the winter season, in temperate regions, the adjustment of anatomical, metabolic and neuroendocrine function promote survival against stressful conditions. Birds, for instance, increase their body fat as a thermoregulatory response to the colder winter season (Wu, Zhou et al. 2015). Physiological adjustments to changing seasons

occur progressively and so animals use changing environmental cues such as rainfall patterns, temperature and photoperiod to anticipate seasonal change. Of these, photoperiod is the most predominantly used cue that can synchronize physiological seasonal changes (Hazlerigg and Wagner 2006).

In most vertebrates, immune function displays a circannual rhythm and varies cyclically throughout the year. The “winter immunoenhancement hypothesis” contends that immune activity is enhanced in anticipation of the winter season (Nelson 2004). This hypothesis speculates that by the reinforcement of immune function, the organism is better prepared to survive against the stresses of winter which include colder temperatures and limited food supply. The absence of this seasonal-specific modification would otherwise compromise the animal’s immune competence. Given the variety of immune components, it is particularly challenging to broadly characterize the seasonality of all immune responses which differ between species. Most of the experimental work investigating mammalian immune function seasonality is conducted using rodents. Intra-annual variation in innate, humoral and cell-mediated immunity has been confirmed using field studies on cotton rats (Lochmiller, Vestey et al. 1994) and prairie voles (Sinclair and Lochmiller 2000). Immune regulation originating from different environmental stressors, however, may affect immune responses differently. Additionally, these stressors are not of consistent strength from year to year and so may lead to inconsistencies when comparing responses between similar seasons. The popular belief, however, is that innate immunity is repressed and that acquired immunity is augmented during the winter season (Demas and Nelson 2012). Due to this variability,

attention has shifted to specific signals, primarily the photoperiod, which could be simulated within laboratory conditions to explore these seasonal changes.

A vast majority of these laboratory experimental studies investigating the photoperiod-induced seasonal changes in immune function focus on melatonin. Melatonin secretion increases during the shorter photoperiod winter season and can contribute to seasonal immune function changes (Demas and Nelson 2012). Strains of inbred mice have been investigated to explore the role of melatonin in mediating photoperiod changes in immune activity (Yellon and Tran 2002). C3H/HeN mice display a pronounced melatonin circadian rhythm and their B cell and T cell numbers are increased when transferred from longer to shorter days; which simulates a seasonal change from summer to winter. C57/BL6 mice, on the contrary, fail to exhibit photoperiod induced melatonin profile changes and do not display immunological photoperiodism (Bhat, Hamm et al. 2003). Challenging Siberian hamsters with acute endotoxin administration under short day (SD) conditions results in an attenuated febrile response when compared to hamsters exposed to long day (LD) conditions. A reduction in body temperature and fever duration could be mimicked under LD conditions by exposing the hamsters to daily melatonin injections four hours before darkness (Bilbo and Nelson 2002). These injections simulate the SD melatonin signal. Following the administration of an acute endotoxin dose, SD Siberian hamsters exhibited enhanced leukocyte counts and an attenuated behavioral sickness response (nest building suppression, anorexia, cachexia) when compared to their LD counterparts. Pinealectomized (PINx) SD Siberian hamsters, however, did not exhibit these responses

(Wen, Dhabhar et al. 2007). In the LD group, leukocyte counts and the sickness response were not affected by PINx. Photoperiod-induced seasonal immunological changes have also been attributed to variation in gonadal and thyroid activity (Stevenson and Prendergast 2015). Siberian hamsters exposed to SD conditions undergo gonadal regression and their testosterone secretion is inhibited. These changes are concurrent with sickness response diminution (Prendergast, Baillie et al. 2008). While thyroid hormone T₃ (triiodothyronine) and T₄ (thyroxine) concentrations in serum display seasonality in humans (Smals, Ross et al. 1977, Hassi, Sikkila et al. 2001), assessment of seasonality on model mammalian organisms are limited. T₃ and T₄ concentrations in Siberian hamsters are invariant to photoperiod changes (O'Jile and Bartness 1992). In the lymphocytes assessed from SD hamsters, an increased localization of T₃ in the cytoplasm was observed (Stevenson, Onishi et al. 2014). A T₃ compartmentalization shift may seasonally modulate lymphocyte activity or differentiation.

Despite it being shown that SD photoperiod increases glucocorticoid concentrations in Siberian hamsters (Bilbo, Dhabhar et al. 2002), tests assessing the involvement of HPA axis activity in regulating photoperiod-induced immune activity is extremely scarce. Both control and medulla adrenalectomized (ADMEDx) Siberian hamsters showed comparable splenic masses that were not unaffected by changing photoperiod exposure (Demas, Drazen et al. 2002). Quantifying immune function by serum IgG concentration measurements, ADMEDx attenuated the immune response but only under LD exposure conditions.

Mechanisms describing seasonal changes in physiological function are yet to be thoroughly investigated. Based on measurements from serum, plasma and saliva samples from humans, the general belief is that cortisol levels are elevated during winter (Walker, Best et al. 1997, Persson, Garde et al. 2008, Hadlow, Brown et al. 2014) . Additionally, concentrations of IL-6 and its soluble IL-6 receptor (sIL-6R) display seasonality with increased levels detected in the winter season (Maes, Stevens et al. 1994). A seasonal gene expression using PBMCs characterized winter as “pro-inflammatory” with augmented levels of IL-6R mRNA, sIL-6R and C-reactive proteins expressed during that time (Dopico, Evangelou et al. 2015). Elevated levels of these inflammatory components are associated with various diseases such rheumatoid arthritis (Uson, Balsa et al. 1997, Keul, Heinrich et al. 1998, Robak, Gladalska et al. 1998), ulcerative colitis, Crohn’s disease (Mitsuyama, Toyonaga et al. 1995), allergic asthma (Doganci, Eigenbrod et al. 2005). Of note, the incidence or exacerbation of symptoms in diseases like coronary heart disease (Douglas, Dunnigan et al. 1995) and rheumatoid arthritis (Schlesinger and Schlesinger 2005) also display seasonality that peak during the winter and spring months. These diseases are further characterized by diurnal fluctuations in activity which peak in the late night/ early morning (Rocco, Barry et al. 1987, Haus, Sackett-Lundeen et al. 2012). For instance, in patients suffering from rheumatoid arthritis, the peak concentrations of TNF and IL-6 are augmented by an order of magnitude with phase delayed pro-inflammatory cytokine circadian rhythms (Cutolo and Straub 2008).

In the assessment of innate immune function seasonality, an ex-vivo study was conducted on PBMCs obtained from 15 human volunteers (Khoo, Chai et al. 2011).

Samples were collected throughout the course of one year and challenged with acute endotoxin doses. An increased inflammatory response, quantified by pro-inflammatory cytokine expression, was observed when cells were stimulated in winter. In this ex-vivo study, an attenuated inflammatory response in the summer was attributed to elevated serum vitamin D₃ levels. Vitamin D₃ is immunosuppressive, inhibiting human monocyte production of cytokines such as IL-1, IL-6, and TNF- α (Almerighi, Sinistro et al. 2009, Khoo, Chai et al. 2011) as well as B cell and T-cell proliferation (Aranow 2011). A majority of the body's vitamin D₃ is produced by the skin following exposure to UV-B radiation which also varies seasonally with photoperiod. Higher vitamin D₃ levels in the summer season correlates with the longer photoperiod (Bolland, Grey et al. 2007). It is likely that vitamin D₃ could mediate seasonal immunological plasticity, however its impact on immune function remains controversial. A human in-vivo experimental endotoxemia study found no correlation between the endotoxin induced inflammatory response and plasma vitamin D₃ levels (Kox, van den Berg et al. 2013). Also, while the activity of rheumatoid arthritis (RA), ankylosing spondylitis (AS) and osteoarthritis (OA) displayed seasonality, a lack of correlation was established between disease activity and serum vitamin D₃ concentrations which failed to display seasonal variation (Yazmalar, Ediz et al. 2013). While vitamin D₃ insufficiency is considered as a biomarker for RA and OA (Grazio, Naglic et al. 2015), it is possible that confounding factors such as sunscreen use, skin pigmentation and dietary practice alter the body's availability of vitamin D₃ (Nair and Maseeh 2012) consequently rendering it challenging to establish a compelling relationship between vitamin D₃ and immune function.

Other than photoperiod, environmental changes such as temperature and humidity may seasonally modulate immune function. The lower temperature and humidity of the winter season may contribute to the peak incidence of respiratory tract infections (RTIs) (Eccles 2002, Mourtzoukou and Falagas 2007, Makinen, Juvonen et al. 2009). Enhanced cooling of the respiratory epithelium during the winter can repress mucociliary clearance (Salah, Dinh Xuan et al. 1988) and leukocyte phagocytic activity (Salman, Bergman et al. 2000) which compromises respiratory defenses against infection. Impaired barrier function, coupled with overcrowding (Lofgren, Fefferman et al. 2007) and augmented efficiency of respiratory droplet transmission (Lowen and Steel 2014) may result in peak RTI incidence during the winter. Temperature and humidity are also known to regulate symptom severity of RA (Patberg and Rasker 2004, Iikuni, Nakajima et al. 2007, Abasolo, Tobias et al. 2013) with joint pain and stiffness increasing during rainy and cold weather. It has been postulated that joint pain and stiffness may be a result of greater muscle stiffening around joints in response to the colder temperatures (Abasolo, Tobias et al. 2013).

Experimental evidence clearly conveys that environmental changes promote the seasonality of immunological function. While it is likely that temperature and humidity may contribute to immune activity plasticity, and ultimately the seasonality of disease incidence, photoperiod appears to be a dominating factor influencing immune function. Rodent data, especially from Siberian hamster studies, implicate photoperiod-induced melatonin signal changes as the primary putative seasonal immunomodulator. The effects of cortisol, another circadian signal transduction immune regulator, have been

experimentally overlooked. Considering the role of cortisol, this work proposes to assess the influence of seasonally varying photoperiods on neuroendocrine-immune axis activity. It is anticipated that this study will provide insight into the seasonally changing dynamics of this axis and ultimately may be used to predict the seasonality of immune function and disease.

1.3: Outline of the Dissertation

The seasonal assessment conducted involves the step-wise development and refinement of a semi-mechanistic mathematical model structure as we expand the domain of our investigation. In Chapter 2, a base-line seasonal model is developed and we focus on examining the effects of circannual changes of photoperiods in regulating HPA axis activity. The photoperiod-induced seasonally varying cortisol signal on moderating the downstream dynamics of peripheral clock genes (molecular clock), pro-inflammatory cytokine dynamics and innate immune function is investigated. In Chapter 3, we incorporate cortisol metabolism dynamics and explore the activities of the metabolic enzymes $11\beta - HSD1$ and $11\beta - HSD2$ and their ability to regulate cortisol's bioavailability and affect HPA axis function in a circadian and seasonal dependent context. In Chapter 4, the modeling framework is expanded to consider intercellular variability among cells in a population. The robustness of seasonally varying systemic signals in effectively synchronizing the dynamics of a cell population is assessed. The deleterious effects of internal oscillator misalignment with the environmental signal is

discussed and we consider further developments of the cell cycle model. In Chapter 5, the project's major findings and future directions are addressed.

CHAPTER 2: HPA axis regulation of immune function to predict photoperiod-induced seasonality changes

2.1: Background

Studies investigating the seasonal fluctuations of cortisol concentrations have found no change (Kanikowska, Sugeno et al. 2009), increased concentrations in spring and summer (Matchock, Dorn et al. 2007) and elevated levels in the winter season (Walker, Best et al. 1997, Persson, Garde et al. 2008, Hadlow, Brown et al. 2014). These conflicting reports are attributed to factors such as age and a lack of significant environmental variation throughout the year. In a 13 year study, assessing serum cortisol levels from 27569 subjects, it was found that a delay in the time of sunrise, most pronounced during winter, correlated with an increase in cortisol (Hadlow, Brown et al. 2014). Furthermore, this sunrise delay also correlated with a phase delay in cortisol's circadian rhythm (Vondrasova, Hajek et al. 1997). Apart from cortisol, an increased expression of pro-inflammatory immune components has also been observed with elevated concentrations of IL-6R mRNA, sIL-6R and C-reactive proteins measured during the winter (Maes, Stevens et al. 1994, Dopico, Evangelou et al. 2015). Interestingly, expression of BMAL1 mRNA, encoding for the anti-inflammatory peripheral clock protein, was minimal during the winter (Dopico, Evangelou et al. 2015). Based on these findings, there appears to be an overall systemic adaption to environmental cues that ultimately modulates immunological function. This motivates the development of a semi-mechanistic model that accounts for the effects of seasonal

photoperiod changes at both the central and peripheral level which can provide insight for understanding the circannual fluctuation of immune function dynamics.

2.2: Approach

The system was modeled with two compartments: the central and peripheral. The central compartment comprises the HPA axis and its activity regulates the dynamics of *CRH*, *ACTH* and cortisol (F_{HPA}) while an immune subsystem constitutes the periphery. HPA axis rhythms are regulated by the light/dark (L/D) cycle. To model changes in seasonality, the photoperiod was altered for each season. Summer was modeled with a photoperiod of 16 (16L/8D) and winter with a photoperiod of 8 (8L/16D) (Bodenstein, Gosak et al. 2012). Spring was modeled with 12L/12D and autumn with 10L/14D (Pidwirny 2006). Light was modeled as a step function with an intensity of 1 during the light phase (L) and an intensity of 0 during the dark phase (D). Figures 1A, 1B, 1C and 1D depict the seasonal light profiles. Entrained to the photoperiod, cortisol is output from the HPA axis and regulates clock gene and immune function dynamics. A schematic of our model is shown in Figure 2. Parameter values and their descriptions are included in Table A1 of the Appendix.

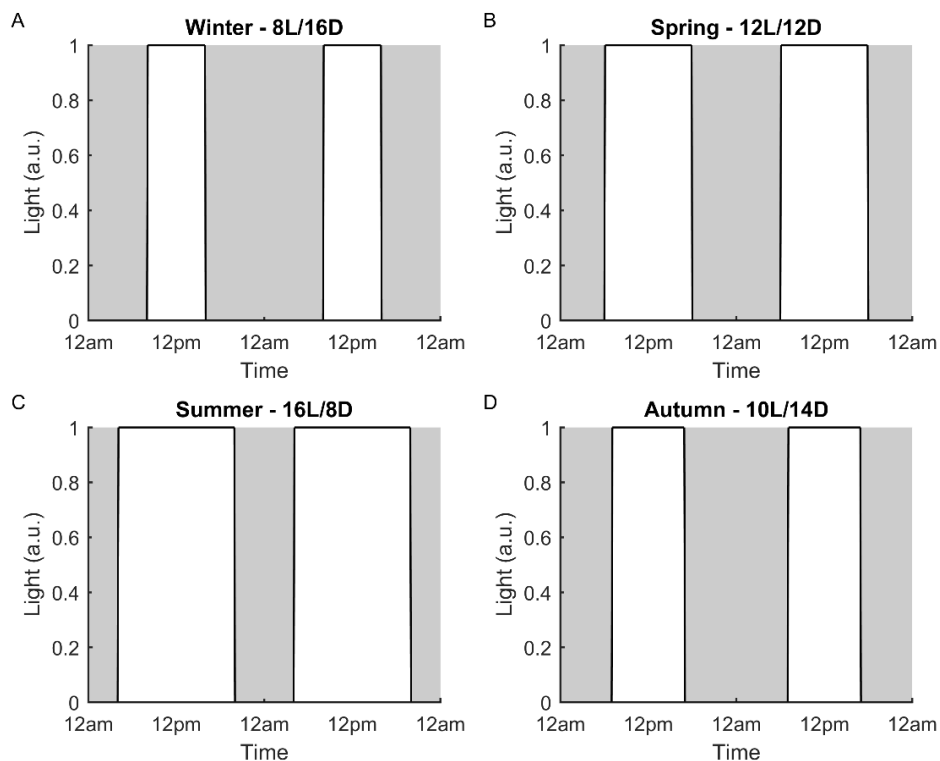


Figure 1. The modeled light profile for each season.

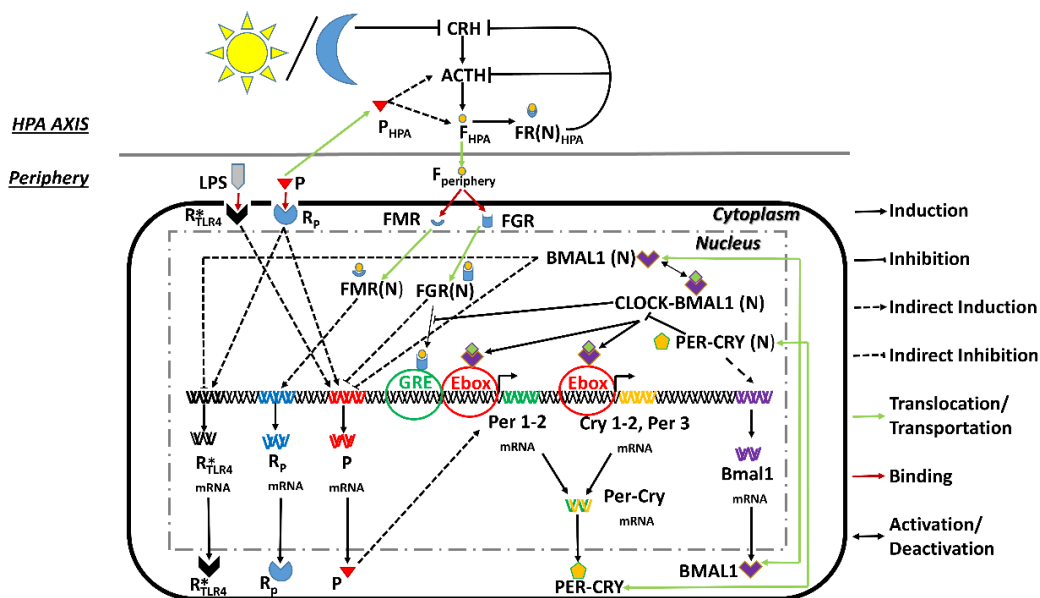


Figure 2. Schematic representation of our two compartment model.

Light entrainment and cortisol dynamics in the HPA axis

The circadian profiles of CRH , $ACTH$ and F were mathematically modeled using Equations 1 – 3. These core equations were adapted from our earlier work (Mavroudis, Corbett et al. 2014) and parameters optimized to improve the goodness of fit between cortisol’s modeled circadian profile and experimentally measured human data (Hermann, von Aulock et al. 2006). A variety of factors including neurotransmitters, peptide hormones, and even CRH are known to positively regulate CRH release (Majzoub 2006). We have assumed these CRH secretagogues converge to yield a constant inducing input signal (In_{CRH}) which triggers CRH production. Following production, CRH (Equation 1) stimulates the anterior pituitary to release $ACTH$ (Equation 2). $ACTH$ then triggers the release of F_{HPA} from the adrenal cortex (Equation 3). Cortisol (F_{HPA}) levels are regulated by a negative feedback mechanism whereby cortisol binds to its glucocorticoid receptors in the hypothalamus and anterior pituitary. The cortisol-receptor complex (FR) then translocates into the nucleus ($FR(N)$) and inhibits production of both CRH and $ACTH$. The signal transduction pathway involving the formation of the nuclear cortisol-receptor complex is described using Equations 4 – 7; derived from a corticosteroid pharmacodynamic model (Ramakrishnan, DuBois et al. 2002). Transcription of the receptor mRNA ($mRNA_{R,HPA}$, Equation 4) is downregulated by cortisol. The receptor mRNA is then translated (R_{HPA} , Equation 5) and binds to cortisol in the cytoplasm to form the cortisol-receptor complex (FR_{HPA} , Equation 6) which is rapidly translocated to the nucleus ($FR(N)_{HPA}$, Equation 7) and induces its effects via glucocorticoid responsive element (GRE) binding.

$$\frac{dCRH}{dt} = \frac{k_{p1}}{K_{p1} + FR(N)_{HPA}} - \frac{V_{d1} \cdot CRH \left(1 + \frac{V_{season} \cdot light}{1 + light}\right)}{K_{d1} + CRH} \quad (1)$$

$$\frac{dACTH}{dt} = \frac{k_{p2} \cdot CRH}{K_{p2} + FR(N)_{HPA}} \left(1 + k_{fp} \cdot P_{HPA}\right) - \frac{V_{d2} \cdot ACTH}{K_{d2} + ACTH} \quad (2)$$

$$\frac{dF_{HPA}}{dt} = \frac{k_{p3} \cdot ACTH}{c_{season} \cdot K_{p3} + ACTH} \left(1 + k_{fp} \cdot P_{HPA}\right) - \frac{V_{d3} \cdot F_{HPA}}{K_{d3} + F_{HPA}} \quad (3)$$

$$\frac{dmRNA_{R,HPA}}{dt} = k_{synRm} \left(1 - \frac{FR(N)_{HPA}}{IC_{50Rm} + FR(N)_{HPA}}\right) - k_{deg} \cdot mRNA_{R,HPA} \quad (4)$$

$$\frac{dR_{HPA}}{dt} = k_{synR} \cdot mRNA_{R,HPA} + R_f \cdot k_{re} \cdot FR(N) - k_{on} \cdot F_{HPA} \cdot R_{HPA} - k_{dgrR} \cdot R_{HPA} \quad (5)$$

$$\frac{dFR_{HPA}}{dt} = k_{on} \cdot F_{HPA} \cdot R_{HPA} - k_T \cdot FR_{HPA} \quad (6)$$

$$\frac{dFR(N)_{HPA}}{dt} = k_T \cdot FR_{HPA} - k_{re} \cdot FR(N)_{HPA} \quad (7)$$

$$\frac{dP_{HPA}}{dt} = \frac{1}{\tau} (P - P_{HPA}) \quad (8)$$

$$\frac{dF_{periphery}}{dt} = \frac{1}{\tau} (F_{HPA} - F_{periphery}) \quad (9)$$

Acute bright light exposure downregulates cortisol (Jung, Khalsa et al. 2010) and a decrease in the SCN-mediated secretion of arginine vasopressin (AVP) increases cortisol levels (Kalsbeek, van der Vliet et al. 1996). Assuming that cortisol downregulation is mediated by AVP, cortisol production was regulated via degradation of *CRH* by light. Critical modifications were made to the central Goodwin oscillator model (Equations 1 – 3) to investigate the influence of external seasonal changes. Cortisol's activity, mediated by its glucocorticoid receptor, is immune suppressive and the HPA axis regulates rising pro-inflammatory cytokine levels by consequently increasing

cortisol production (Petrovsky, McNair et al. 1998, Leonard 2006). Alternatively, cytokines are known for their HPA-axis inductive effects. The mechanisms of cytokine action on the HPA axis can be via direct binding to receptors or via indirect pathways involving neurotransmitters. To overcome the complexity of cytokine influence, the $ACTH$ and F_{HPA} production terms were stimulated with the pro-inflammatory mediator (P) using an indirect response (IDR) model (Equations 2 and 3). IDRs are typically used to describe dynamic responses to factors by mechanisms that are unknown or complex (Sharma and Jusko 1998). This inflammatory mediator (P) is a generic variable that represents the combined effects of pro-inflammatory cytokines.

Seasonal analysis on SCN neuronal activity from mice and rat hypothalamic slice explants have identified that the synchronization of firing patterns among neurons increase with decreasing photoperiod (Schaap, Albus et al. 2003, Rohling, Wolters et al. 2006, VanderLeest, Houben et al. 2007, Meijer, Michel et al. 2010). The increased synchrony among neuronal activity results in higher amplitude signals. To account for the photoperiod dependence of SCN electrical activity, a multiplicative coefficient (V_{season}) was included in the Michaelis-Menten, light-mediated, degradation term of CRH which characterizes the maximum activity of the SCN. The V_{season} parameter, indicative of the SCN ensemble amplitude, decreases with increasing photoperiod; based on rat neuronal electrophysiological measurements (Schaap, Albus et al. 2003). From their human seasonal study, Walker et al. (Walker, Best et al. 1997) concluded that the rate of cortisol production was diminished during the winter season. The seasonality of cortisol's production rate was accounted for with the use of a seasonally varying Michaelis constant

of cortisol production: $c_{season} \cdot K_{p3}$ (Equation 3). The c_{season} parameters are numerically equal to V_{season} and decreases with increasing photoperiod. A higher c_{season} for the winter season represents a lower binding affinity which reduces the rate at which the maximum rate of production is achieved.

A transit compartment model was used to describe a delay in transport of P and F_{HPA} between compartments. A transient delay (τ) of 15 minutes (Equations 8 and 9) was selected. A time delay between $ACTH$ secretion of cortisol's production is well established (Papaikonomou 1977) and so we assumed a similar delay existed for transport between the central and peripheral compartments. The value of this delay term was selected from a previous numerical simulation study (Walker, Terry et al. 2010).

Glucocorticoid and Mineralocorticoid receptor dynamics in the periphery

After diffusing into the cytoplasm, cortisol binds to and activates two receptors; the mineralocorticoid (MR) and the glucocorticoid (GR) receptors. Activation of these receptors involves the release of heat shock proteins, hyperphosphorylation and receptor conformational changes (Ramakrishnan, DuBois et al. 2002). Here we consider hyperphosphorylation to be the rate-determining step (Tyson, Chen et al. 2003) for both receptors (Equations 10 and 13). Following binding to cortisol, both ligand-receptor complexes (Equations 11 and 14) translocate into the nucleus (Equations 12 and 15) and induce their effects via binding to their respective GREs. The variation in the binding affinities of cortisol to both receptors (Sapolsky, Romero et al. 2000) was modeled by setting the dissociation constant of the mineralocorticoid receptor (K_{MR}) to a lower value

than that of glucocorticoid receptor (K_{GR}). Similar reaction kinetics governing binding and translocation into the nucleus were assumed for both receptors. The equations and parameters described here were adapted from our previous work (Mavroudis, Corbett et al. 2015) and parameters were estimated based on human cortisol and inflammatory cytokine experimental diurnal profiles from (Petrovsky, McNair et al. 1998).

$$\frac{dMR}{dt} = k_{MR} \left(\frac{\left(1 + \frac{k_{F,MR} \cdot F_{periphery}}{K_{F,MR} + F_{periphery}}\right) (MR_T - MR)}{K_{MR} + MR_T - MR} \right) - \frac{k_{MR,deg} \cdot MR}{K_{MR,deg} + MR} - k_{b,MR} \cdot F_{periphery} \cdot MR + k_{r,MR} \cdot FMR(N) \quad (10)$$

$$\frac{dFMR}{dt} = k_{on,MR} F_{periphery} \cdot MR - k_{T,MR} FMR \quad (11)$$

$$\frac{dFMR(N)}{dt} = k_{T,MR} FMR - k_{re,MR} FMR(N) \quad (12)$$

$$\frac{dGR}{dt} = k_{GR} \left(\frac{\left(1 + \frac{k_{F,GR} \cdot F_{periphery}}{K_{F,GR} + F_{periphery}}\right) (GR_T - GR)}{K_{GR} + GR_T - GR} \right) - \frac{k_{GR,deg} \cdot GR}{K_{GR,deg} + GR} - k_{b,GR} \cdot F_{periphery} \cdot GR + k_{r,GR} \cdot FGR(N) \quad (13)$$

$$\frac{dFGR}{dt} = k_{on,GR} F_{periphery} \cdot GR - k_{T,GR} FGR \quad (14)$$

$$\frac{dFGR(N)}{dt} = k_{T,GR} FGR - k_{re,GR} FGR(N) \quad (15)$$

Peripheral Clock Gene dynamics with cortisol entrainment

Here, a network of transcriptional and translational feedback loops to describe the activity of the autonomous peripheral oscillations was incorporated. These equations

were developed previously and validated against mRNA and protein concentrations from rodent data (Becker-Weimann, Wolf et al. 2004). In this model, *Per* and *Cry* mRNAs and proteins were represented by the same variables due to their phase of nuclear accumulation (Kume, Zylka et al. 1999), their coexistence in a nuclear complex (Reppert and Weaver 2002), their comparable regulation by *CLOCK – BMAL1* and negative regulation of *CLOCK – BMAL1* activity (Jin, Shearman et al. 1999, Shearman, Sriram et al. 2000). The transcription of *Per – Cry* genes is stimulated by the binding of the *CLOCK – BMAL1* heterocomplex to an E-Box Enhancer (Equation 16). The translated *PER – CRY* complex (Equation 17) translocates to the nucleus (Equation 18) and inhibits *CLOCK – BMAL1* transcriptional stimulation of its own genes; consequently forming a negative feedback (Equation 16). *Bmal1* transcription (Equation 19) is indirectly stimulated by the *PER – CRY(N)* nuclear complex. The translated *BMAL1* protein (Equation 20) translocates into the nucleus (Equation 21) and binds to the *CLOCK* protein to form the *CLOCK – BMAL1* heterocomplex (Equation 22). In this model, *CLOCK* protein levels were assumed constant since *Clock* mRNA concentrations do not fluctuate diurnally (Keller, Mazuch et al. 2009).

Glucocorticoid entrainment of clock gene mRNA expression is well documented (So, Bernal et al. 2009). Human treatment with oral doses of exogenous GC phase shifted *Per 2*, *Per 3* and *Bmal1* mRNA expression by approximately 9.5 – 11.5 hours (Cuesta, Cermakian et al. 2015). The *FGR(N)* additive term in Equation 16 accounts for this entrainment. *CLOCK – mediated* acetylation inhibits the transcriptional activity of the

glucocorticoid receptor and so $CLOCK - BMAL1(N)$ was included in denominator of the entrainment term to describe this repressive effect (Charmandari, Chrousos et al. 2011).

The PCG dynamic equations have been revised to include the effects of seasonality and the pro-inflammatory cytokine influence. Treatment of human hepatoma cells with IL-6 (Motzkus, Albrecht et al. 2002), rheumatoid synovial (Yoshida, Hashiramoto et al. 2013) and monocytic THP-1 (Perez-Aso, Feig et al. 2013) with $TNF-\alpha$ enhances $Per1$, $Cry1$ and $Cry2$ mRNA expression. Cytokine feedback into our $Per - Cry$ transcription (Equation 16) was accounted for by applying an indirect stimulation term. Greater dermal blanching following topical glucocorticoid treatment (Walker, Best et al. 1997) and increased number of glucocorticoid receptor binding sites (Blackhurst, McElroy et al. 2001) during the winter indicate an increased sensitivity during this time. Glucocorticoid sensitivity seasonality was modeled by using a Hill response type function (Zhang, Bhattacharya et al. 2013) to describe the $FGR(N)$ entraining effects on $Per - Cry$ transcription. The Hill coefficients (n_{season}) are numerically equal to the V_{season} (and c_{season}) coefficients and increase with decreasing photoperiod to reflect an increased sensitivity in the winter.

$$\frac{dPer-Cry_{mRNA}}{dt} = \frac{v_{1b}(CLOCK-BMAL1+c)}{k_{1b}(1+(\frac{PER-CRY(N)}{k_{1l}})^p)} (1 + k_f \cdot P) - k_{1d} \cdot Per - Cry_{mRNA} + k_c \frac{FGR(N)^{n_{season}}}{CLOCK-BMAL1} \quad (16)$$

$$\frac{dPER-CRY}{dt} = k_{2b} \cdot Per - Cry_{mRNA}^q - k_{2d} \cdot PER - CRY - k_{2t} \cdot PER - CRY + k_{3t} \cdot PER - CRY(N) \quad (17)$$

$$\frac{dPER-CRY(N)}{dt} = k_{2t} \cdot PER - CRY - k_{3t} \cdot PER - CRY(N) - k_{3d} \cdot PER - CRY(N) \quad (18)$$

$$\frac{dBmal1_{mRNA}}{dt} = \frac{v_{4b} \cdot PER-CRY(N)^r}{k_{4b}^r + (PER-CRY(N))^r} - k_{4d} \cdot Bmal1_{mRNA} \quad (19)$$

$$\frac{dBMAL1}{dt} = k_{5b} \cdot Bmal1_{mRNA} - k_{5d} \cdot BMAL1 - k_{5t} \cdot BMAL1 + k_{6t} \cdot BMAL1(N) \quad (20)$$

$$\begin{aligned} \frac{dBMAL1(N)}{dt} = k_{5t} \cdot BMAL1 - k_{6t} \cdot BMAL1(N) - k_{6d} \cdot BMAL1 + k_{7a} \cdot CLOCK - BMAL1 - \\ k_{6a} \cdot BMAL1(N) \end{aligned} \quad (21)$$

$$\frac{dCLOCK-BMAL1}{dt} = k_{6a} \cdot BMAL1(N) - k_{7a} \cdot CLOCK - BMAL1 - k_{7d} \cdot CLOCK - BMAL1 \quad (22)$$

Diurnal Rhythm of the Pro-Inflammatory Mediator and its Receptor

Equations 23 to 27 describe the dynamics associated with the pro-inflammatory mediator production and receptor activity. These equations and their parameters were obtained from previous work (Mavroudis, Corbett et al. 2015) and parameters were independently estimated based on experimental data (Petrovsky, McNair et al. 1998). Further refinements to the model were made to describe the PCG influence and seasonality on pro-inflammatory dynamics. The indirect inhibition term in the transcription of the pro-inflammatory mediator's mRNA (Equation 23) reflects cortisol's suppressive effects which occur via the cortisol-glucocorticoid receptor complex $FGR(N)$. Similar to the glucocorticoid entrainment term in the $Per - Cry$ transcription (Equation 16), a Hill response type function is again used to model seasonal glucocorticoid sensitivity changes. In contrast to the previous model, $BMAL1$ is employed as the anti-inflammatory mediator of the immune system's circadian control. $BMAL1(N)$ inhibition of the pro-inflammatory mediator mRNA expression was

simulated via an indirect response. The autocatalytic regulation of cytokine levels on their own transcription have been accounted for by including indirect stimulation via the pro-inflammatory ligand-receptor complex. Following transcription, the pro-inflammatory mediator is then translated (Equation 24). Cortisol's upregulation of pro-inflammatory receptor levels were modeled by the indirect stimulation term in Equation 25 which occurs via the $FMR(N)$ complex. This receptor is then translated (Equation 26) and binds to the pro-inflammatory mediator (Equation 27).

$$\frac{dmRNA_P}{dt} = k_{mRNA_{P_{in}}} \left(1 - \frac{k_{fr} \cdot FGR(N)^{n_{season}}}{K_{fr} + FGR(N)^{n_{season}}} \right) \cdot \left(1 - \frac{k_{pc} \cdot BMAL1(N)}{K_{pc} + BMAL1(N)} \right) \cdot (1 + PR) - k_{mRNA_{P_{out}}} \cdot (mRNA_P) \quad (23)$$

$$\frac{dP}{dt} = k_{in_P} \cdot mRNA_P - k_{out_P} \cdot P \quad (24)$$

$$\frac{dmRNA_{R_P}}{dt} = k_{mRNA_{R_P_{in}}} \left(1 + \frac{k_{fr2} \cdot FMR(N)}{K_{fr2} + FMR(N)} \right) - k_{mRNA_{R_P_{out}}} \cdot (mRNA_{R_P}) \quad (25)$$

$$\frac{dR_P}{dt} = k_{in_{R_P}} \cdot mRNA_{R_P} - k_{out_{R_P}} \cdot R_P - k_d \cdot P \cdot R_P \quad (26)$$

$$\frac{dPR}{dt} = k_d \cdot P \cdot R_P - k_{out} \cdot PR_P \quad (27)$$

Innate Immune Function Seasonality

Seasonality assessment of the innate immune response was conducted by integrating an endotoxemia model previously developed within our lab into the study (Equations 28 – 31, (Foteinou, Calvano et al. 2009, Foteinou, Calvano et al. 2010, Scheff, Calvano et al. 2010, Scheff, Mavroudis et al. 2011)). This model was developed using human experimental data and a detailed description of the model can be found here (Foteinou,

Calvano et al. 2009). *LPS*, the endotoxin, when added (Equation 28), binds to the active form of the toll-like 4 receptor (R_{TLR4}^*). Here, R_{TLR4}^* represents a receptor hetero-complex comprising TLR4, CD14 and MD-2. This receptor complex is transcribed in Equation 29, translated in Equation 30 and results in the formation of the $LPSR_{TLR4}^*$ ligand-receptor complex (Equation 31) after binding with *LPS*. $LPSR_{TLR4}^*$ then promotes transcription of the pro-inflammatory mediator mRNA. Equation 32 shows the modified version of the pro-inflammatory mediator transcription equation which includes the inducible effect of $LPSR_{TLR4}^*$. In Equation 29, it was assumed that R_{TLR4}^* exhibits circadian rhythmicity as $mRNA_{R_{TLR4}^*}$ is entrained indirectly by *BMAL1*. Circadian rhythmicity of TLR4 is absent in mice macrophages (Keller, Mazuch et al. 2009, Silver, Arjona et al. 2012, Gibbs, Ince et al. 2014) and in human monocytes and neutrophils (Lancaster, Khan et al. 2005). However, circadian regulation of components at all levels of the *LPS* – *TLR4* response pathway exists (Keller, Mazuch et al. 2009). It was therefore hypothesized that the active form of the TLR4 receptor complex (R_{TLR4}^*) is under circadian influence and so an IDR term was used to model the suppressive effects of *BMAL1* (N) on the transcription of $mRNA_{TLR4}^*$.

$$\frac{dLPS}{dt} = k_{LPS,1} \cdot LPS(1 - LPS) - k_{LPS,2} \cdot LPS \quad (28)$$

$$\frac{dmRNA_{TLR4}^*}{dt} = k_{LPS,3} \cdot \left(1 + k_{mRNA_{R_{TLR4}^*}} \cdot PR\right) \cdot \left(1 - \frac{k_{pc} BMAL1(N)}{K_{pc} + BMAL1(N)}\right) - k_{LPS,4} mRNA_{TLR4}^* \quad (29)$$

$$\frac{dR_{TLR4}^*}{dt} = k_{syn} \cdot mRNA_{TLR4}^* + k_2 \cdot LPSR_{TLR4}^* - k_1 \cdot LPS \cdot R_{TLR4}^* - k_{syn} \cdot R_{TLR4}^* \quad (30)$$

$$\frac{dLPSR_{TLR4}^*}{dt} = k_1 \cdot LPS \cdot R_{TLR4}^* - k_3 \cdot LPSR_{TLR4}^* \quad (31)$$

$$\begin{aligned} \frac{dmRNA_P}{dt} = & k_{mRNA_{P_{in}}} \left(1 - \frac{k_{fr} \cdot FGR(N)^{n_{season}}}{K_{fr} + FGR(N)^{n_{season}}} \right) \cdot \left(1 - \frac{k_{pc} \cdot BMAL1(N)}{K_{pc} + BMAL1(N)} \right) \cdot (1 + PR) \cdot (1 + \\ & k_{p, LPSR_{TLR4}^*} \cdot LPSR_{TLR4}^*) - k_{mRNA_{P_{out}}} \cdot (mRNA_P) \end{aligned} \quad (32)$$

2.3: Seasonal Changes in Circadian Profiles and the Inflammatory Response

The data presented in this section are a result of numerical integration of the model equations (Equations 1 – 32).

Figures 3 and 4 illustrate the circadian rhythms and amplitude/phase plots for cortisol ($F_{periphery}$), the pro-inflammatory mediator (P), pro-inflammatory receptor (R_p) and $BMAL1$. As the photoperiod decreased, the amplitudes of $F_{periphery}$, P and R_p increased. The opposite was predicted for $BMAL1$ as its amplitude was highest during the summer when the photoperiod was the largest. The prediction of a heightened cortisol amplitude in the winter is in accordance with experimental findings (Walker, Best et al. 1997, Persson, Garde et al. 2008, Hadlow, Brown et al. 2014). Higher amplitude oscillations for the pro-inflammatory mediator (P) is comparable to the peak winter expression observed in the human IL-6 seasonal study by (Maes, Stevens et al. 1994). Additionally, R_p and $BMAL1$ predictions are in line with the seasonal mRNA expression data (Dopico, Evangelou et al. 2015).

Our model predicted a phase delay in the circadian rhythms for all variables with decreasing photoperiod. This phase delay for cortisol agrees with experimental data as a

delay in cortisol's morning rise was detected when comparing winter to summer profiles (Vondrasova, Hajek et al. 1997).

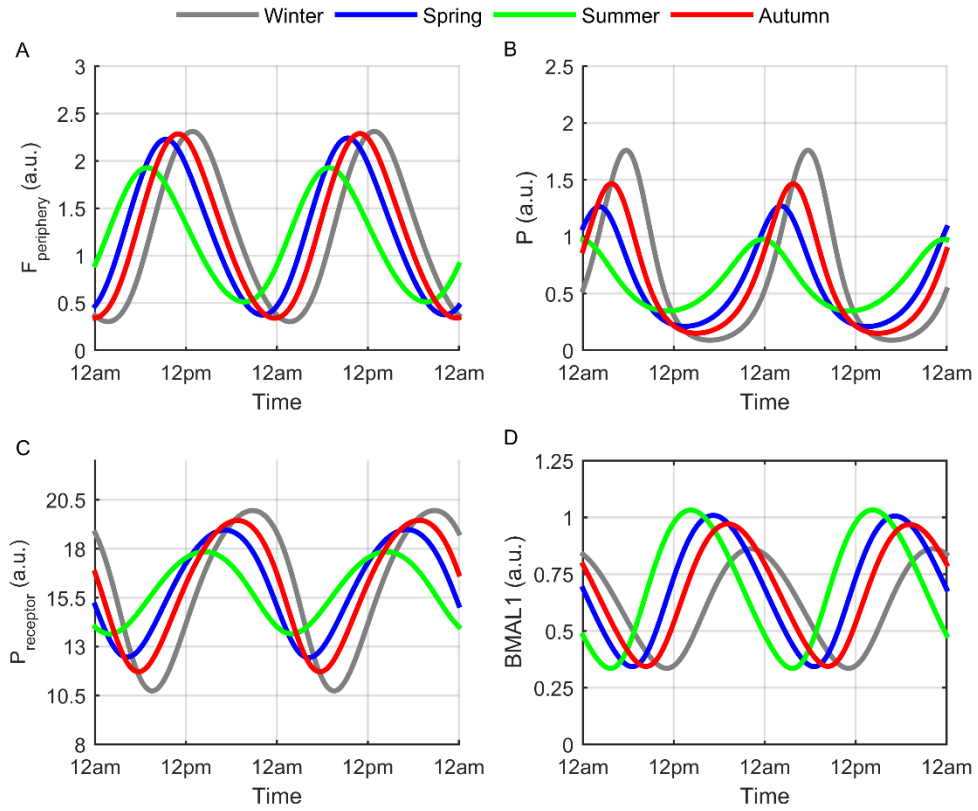


Figure 3. Circadian rhythms for cortisol ($F_{\text{periphery}}$), pro-inflammatory mediator (P), pro-inflammatory receptor (R_p) and BMAL1.

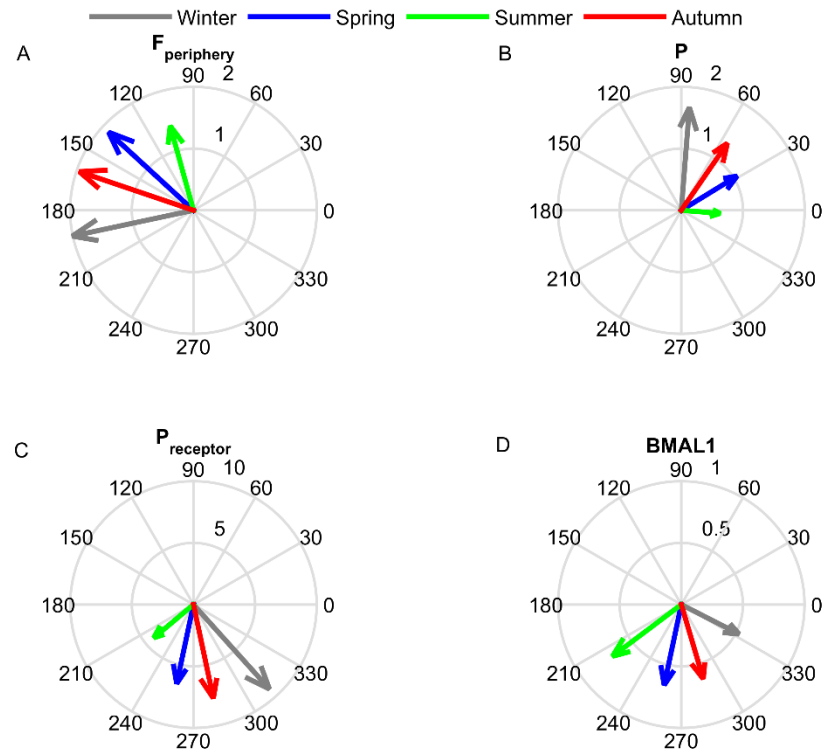


Figure 4. The amplitude (radial dimension) and phase (angular dimension) of the circadian rhythms for cortisol ($F_{periphery}$), pro-inflammatory mediator (P), pro-inflammatory receptor (R_p) and BMAL1 for each seasonal model.

Figure 5 illustrates the R_{TLR4}^* amplitude/phase plots for each season in the *LPS* –unchallenged (control) model. As was found from the human ex-vivo endotoxin stimulation study (Khoo, Chai et al. 2011), our model predicted the highest circadian amplitude of R_{TLR4}^* during the winter season. The summer model R_{TLR4}^* rhythm displayed a phase advancement and a diminished oscillatory amplitude (green vector).

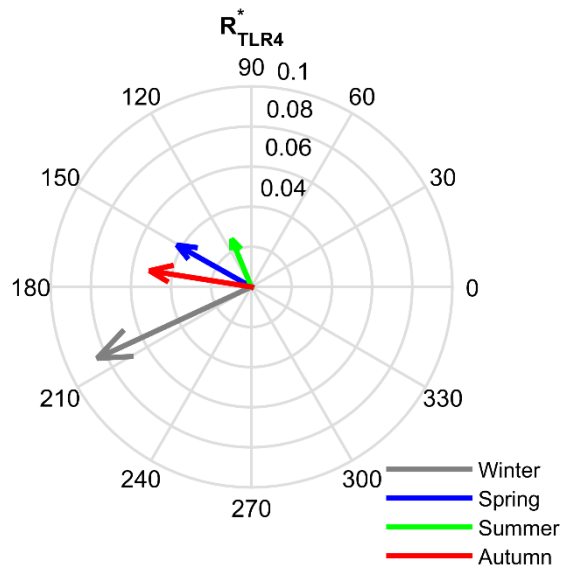


Figure 5. Compass plot showing the seasonal differences of the amplitude (radial dimension) and phase (angular dimension) of R_{TLR4}^* in the unchallenged model.

To assess the seasonal and circadian sensitivities of the inflammatory response, we administered *in silico* acute *LPS* doses at each hour of a simulated day. The magnitude of the inflammatory response was evaluated for each treatment time by computing the maximum pro-inflammatory mediator level (P_{max}) attained following *in silico* treatment. Figure 6 depicts the circadian fluctuation of P_{max} for winter, spring, summer and autumn after low dose *in silico* endotoxin treatment ($LPS = 0.5 a. u.$). The model predicts an exacerbated response in the winter versus other seasons; comparable to the human *ex-vivo* stimulation studies (Khoo, Chai et al. 2011).

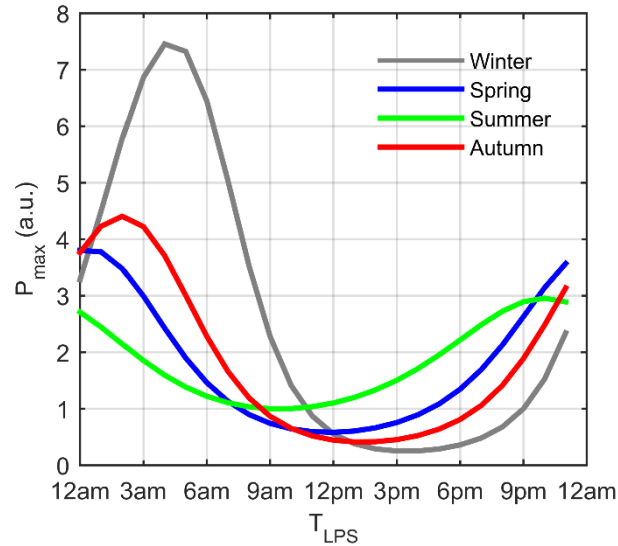


Figure 6. Seasonal variations in the inflammatory response following *in silico* administration of acute doses of endotoxin (LPS dose of 0.5 a.u.) at each hour of the simulated day.

P_{max} profiles as well as control cortisol circadian rhythms for each season are illustrated in Figure 7. Our simulated findings reveal that the magnitude of the inflammatory response is more extensive when *LPS* is added at times near cortisol's trough while a more attenuated response occurs with treatment at times near cortisol's peak. Similar findings were found in our previous work (Mavroudis, Corbett et al. 2015). Investigating more thoroughly, it is observed that the extent of the inflammatory response is also contingent on whether cortisol's rhythm is in the ascending or descending phase with a more pronounced response occurring with treatment during cortisol's ascending phase; even at similar cortisol levels. While it was previously contended that these findings were due to cortisol's immune-permissive and immune-suppressive effects, *BMAL1*, the anti-inflammatory circadian clock protein, also contributes to these circadian and seasonally sensitive responses.

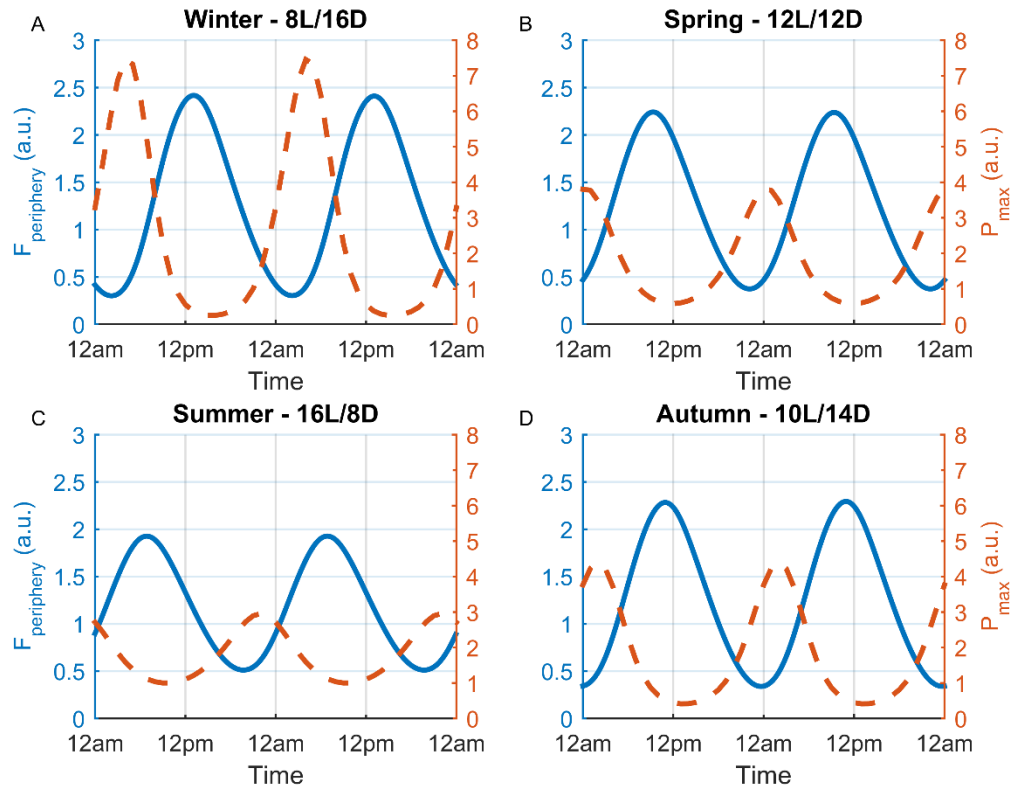


Figure 7. Diurnal profiles for cortisol and P_{max} for each seasonal model.

In Figure 8, the circadian profiles for cortisol ($F_{periphery}$) and $BMAL1$ for the unchallenged seasonal models are represented. Although higher amplitude $BMAL1$ oscillations in the summer promote a heightened anti-inflammatory state, the phase of oscillations also modulates the system's inflammatory response. $BMAL1$'s zenith occurs during the descending phase of cortisol which consequently produces a more diminished inflammatory response in comparison to a response triggered during cortisol's ascending phase, when the levels of $BMAL1$ are lower.

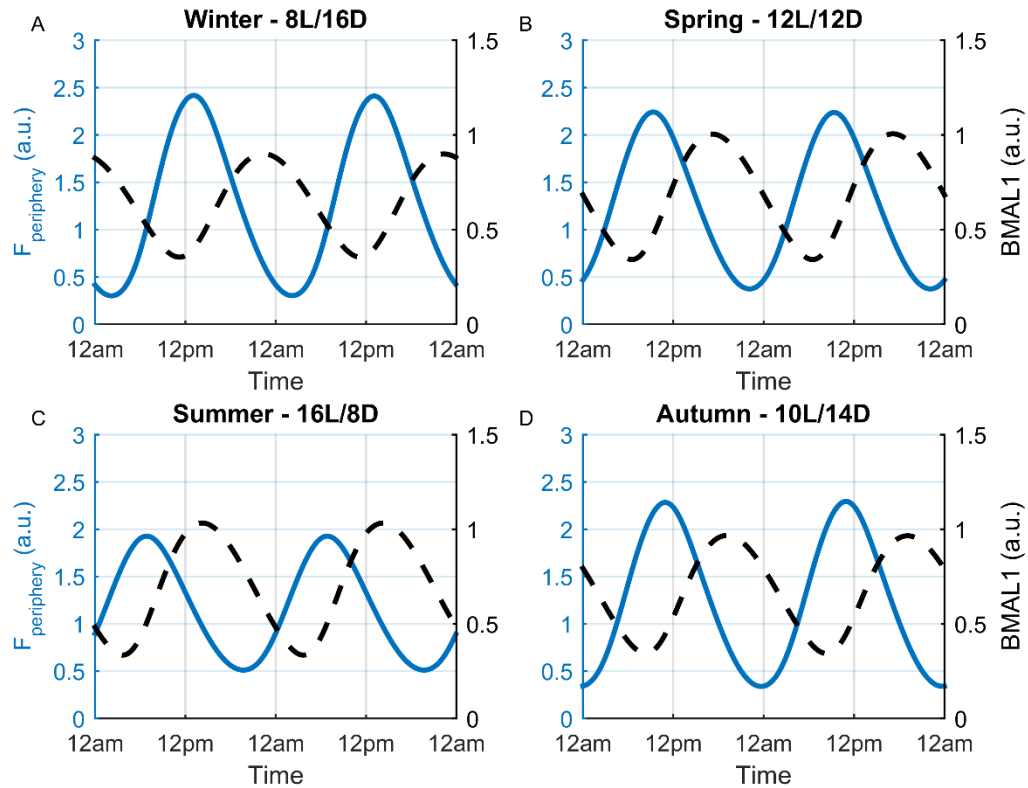


Figure 8. Circadian profiles of cortisol ($F_{periphery}$) and BMAL1 for each season in the unchallenged model.

The temporal responsiveness (ΔT_{max}) of the system to in silico *LPS* treatment was then assessed. ΔT_{max} was computed as the difference between the time of *LPS* addition and the time of P_{max} . Figure 9 depicts seasonal plots for P_{max} versus ΔT_{max} values. The magnitude of the inflammatory response is seemingly independent of the time required to mount the response. Figure 10 depicts the rhythmic profiles of R_{TLR4}^* of the control model and ΔT_{max} versus the time of *LPS* treatment. These plots illustrate that the inflammatory response time is negatively correlated with the circadian rhythm of R_{TLR4}^* . Higher R_{TLR4}^* levels provide more *LPS* binding sites which enhances the rapidity of the inflammatory response. Alternatively, a more delayed response occurs when R_{TLR4}^* levels are low.

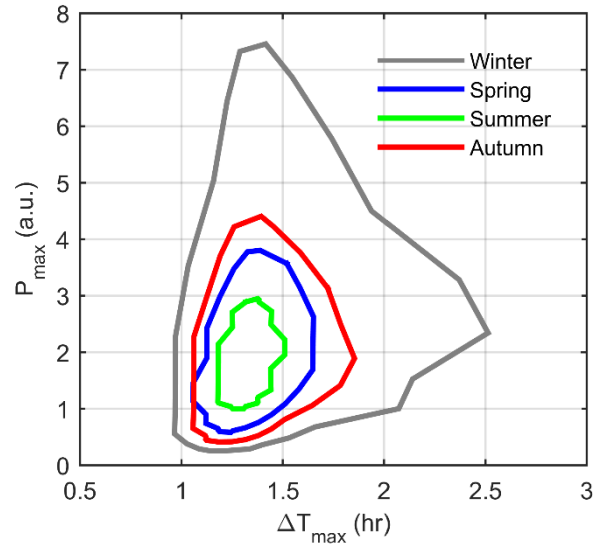


Figure 9. Maximum pro-inflammatory mediator level (P_{max}) versus the time delay between LPS addition and the time-of-maximum response (ΔT_{max}) for each simulated season.

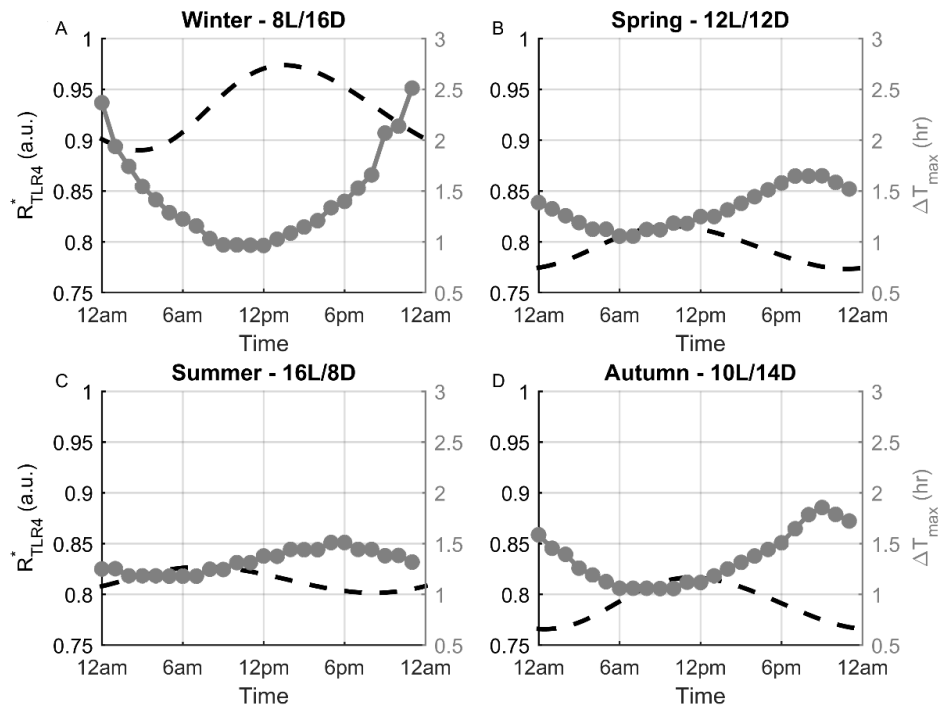


Figure 10. Profiles of R_{TLR4}^* for the unchallenged model and ΔT_{max} versus the time of LPS administration for each season.

In summary, the model provides predictions that are in agreement with several experimental observations: Firstly, it predicts that seasonal changes in photoperiod and the plasticities of SCN activity, adrenal function and glucocorticoid sensitivity can regulate changes in activity of the neuroendocrine-immune axis. Overall, the findings characterize the winter season as “pro-inflammatory dominant” with increased circadian amplitude of $F_{periphery}$, R_P , P and R_{TLR4}^* . Conversely, despite reduced amplitude cortisol oscillations, the model predicted a pronounced anti-inflammatory state in the summer when $BMAL1$ amplitude oscillations were highest and the amplitude of R_P , P and R_{TLR4}^* rhythms were lowest. The in silico seasonal endotoxemia assessment revealed both a circadian and seasonal sensitivity of innate immune function whereby a more exacerbated inflammatory response was predicted following simulated LPS treatment during the winter. A time-of-day sensitivity analysis revealed that the system was more susceptible to inflammatory triggers at times when both cortisol and $BMAL1$ levels were low. The amplitude and phase of these two anti-inflammatory mediators are therefore critical in regulating both the seasonal and time-of-day sensitivities of the inflammatory response. Finally, our model predicts that while R_{TLR4}^* regulates the response time of the system, the magnitude of the inflammatory response is heavily reliant on the circadian rhythms of $F_{periphery}$ and $BMAL1$ and to a lesser extent on the oscillatory profile of R_{TLR4}^* .

CHAPTER 3: The hepato-hypothalamic-pituitary-adrenal-renal axis: cortisol's production, metabolism and seasonal variation

3.1: Background

Apart from being centrally regulated by the HPA axis and the SCN, GC availability in the periphery is controlled by the activity of an enzymatic system comprising 11β -hydroxysteroid dehydrogenase (HSD), 20β -oxoreductase, 6β -hydroxylase, 5β -reductase, 5α -reductase, and 3α -HSD (Gathercole, Lavery et al. 2013). Of these, the 11β -HSD family, which consists of 11β – *HSD1* and 11β – *HSD2*, has been identified as core modulators of GC bioavailability. In humans, these intracellular gatekeepers of GC action catalyze the reciprocal conversion between cortisol and its inactive metabolite, cortisone (Chapman, Holmes et al. 2013). 11β – *HSD2* is NAD^+ dependent, catalyzes the oxidation of cortisol to cortisone, and is localized in aldosterone sensitive tissues such as the kidneys, colon and salivary glands. 11β – *HSD1* is NADPH dependent, present in metabolically active tissues like the central nervous system (CNS), liver, skeletal muscle and adipose tissue, and catalyzes the regeneration of cortisol from cortisone. The deactivation of cortisol by 11β – *HSD2* serves to prevent the illicit stimulation of the mineralocorticoid receptor by cortisol whereas the regeneration by 11β – *HSD1* amplifies cortisol action (Seckl and Walker 2001). Altered 11β – *HSD1* activity and expression has been associated with metabolic syndrome (Esteves, Kelly et al. 2014), rheumatoid arthritis (RA) (Hardy, Rabbitt et al. 2008), systemic lupus erythematosus (SLE), pleuritis, acute interstitial pneumonitis (Ichikawa, Yoshida et al. 1977) and

depression (Dekker, Tiemeier et al. 2012). Although a local increase in $11\beta - HSD2$ gene expression was observed in peripheral blood mononuclear cells (PBMCs) obtained from RA patients (Olsen, Sokka et al. 2004), defective $11\beta - HSD2$ expression and/activity is commonly associated with apparent mineralocorticoid excess (AME); a disease characterized by symptoms such as hypertension, hypokalemia, and low plasma renin activity (White 2001). Gene-expression studies in mice emphasize the profound influence of $11\beta - HSD1$ in regulating HPA axis dynamics as the knockout of this gene can result in the elevation of basal *ACTH*, corticosterone levels, and exacerbation of the acute restraint stress response (Harris, Kotelevtsev et al. 2001, Carter, Paterson et al. 2009). Restoration of the corticosterone profile and reversal of the aggravated stress response to control conditions is conferred by crossing the $11\beta - HSD1$ deficient mice with transgenic $11\beta - HSD1$ overexpressing mice (Paterson, Holmes et al. 2007).

The regulation of GC dynamics is therefore multi-tiered; controlled at both the central and peripheral levels, with the central clock (i.e. the SCN) entrainable to external agents such as the light-dark cycle or the degree of temperature. These zeitgebers, or environmental cues, can therefore modulate physiological processes by way of the SCN. In temperate regions, the length of the light phase in the light-dark cycle predictably fluctuates throughout the year. The photoperiod, or light fraction of the day, which decreases toward winter and then increases from winter through summer is a robust environmental entrainer that regulates various seasonal metabolic and endocrine changes (Hazlerigg and Wagner 2006). Peak cortisol concentrations in the winter (Walker, Best et al. 1997, Persson, Garde et al. 2008, Hadlow, Brown et al. 2014) reflect this seasonal

plasticity of endocrine function. Furthermore, elevation of the ratio of cortisol to cortisone urinary metabolites and enhanced sensitivity to topical GC application in the winter suggests the amplification of GC action by augmented $11\beta - HSD1$ activity (Walker, Best et al. 1997) .

A coordinated balance between stress-induced and basal regulatory mechanisms governing GC secretion is imperative for homeostasis (Dedovic, Duchesne et al. 2009) and abnormal cortisol dynamics is associated with RA (Perry, Kirwan et al. 2009), advanced stages of breast cancer (Sephton, Sapolsky et al. 2000), type 2 diabetes (Lederbogen, Hummel et al. 2011), cardiovascular disease mortality (Kumari, Shipley et al. 2011) and behavioral disorders such as post-traumatic stress disorder and depression (Sriram, Rodriguez-Fernandez et al. 2012). In addition, coronary heart disease (Douglas, Dunnigan et al. 1995), inflammatory diseases such as rheumatoid arthritis (Schlesinger and Schlesinger 2005) and seasonal affective disorder (winter depression) (Lam and Levitan 2000) display seasonal variation with elevated incidence and intensified symptoms occurring in the winter season. Experimental restrictions limit the comprehensive evaluation of the underlying mechanisms contributing to aberrant cortisol profiles in disease states, disease and cortisol production seasonality, and the regulatory influence of cortisol metabolism on HPA axis activity. Procedures to accurately quantify expression of $11\beta - HSDs$ are invasive, requiring tissue explantation, while in-vivo measurements of enzyme activity are extensive and typically involve radiation exposure (Andrew, Smith et al. 2002, Basu, Singh et al. 2004, Hughes, Manolopoulos et al. 2012). In this chapter, we employ a mathematical modeling approach to further develop the

understanding of the underlying dynamics. To the authors' knowledge, no mathematical model currently exists that explores the dynamics of 11β -hydroxysteroid dehydrogenase activities or its contributions to HPA axis activity. With cortisol as the representative effector molecule, and extending from our previous modeling efforts (Pierre, Schlesinger et al. 2016), our integrated model explores the influence of the hepato-hypothalamic-pituitary-adrenal-renal axis (HHPAR)(Edwards 2012) in modulating both baseline and seasonal neuroendocrine-immune system dynamics.

3.2: Approach

Figure 11 depicts our model schematic that has been modified to account for 11β -HSD dynamics as well as the activation and deactivation of cortisol. The central compartment is entrained to the external light/dark cycle. Cortisol in the periphery ($F_{periphery}$) entrains the molecular clock components and modulates the dynamics of the pro-inflammatory mediator (P) and its receptor (R_p). Peripheral cortisol availability is also regulated by the enzymatic activities of $11\beta - HSD1$ and $11\beta - HSD2$.

Modified Central Compartment

Physiologically, adrenal production of cortisol occurs in the periphery in conjunction with the activation and deactivation regulated by $11\beta - HSD1$ and $11\beta - HSD2$ present within the hepatic and renal subsystems of our model. We therefore described an $F_{periphery}$ variable instead (Equation 3) that is synthesized in the periphery and then transported back to the central compartment ($F_{central}$, Equation 4). Using a transit compartment model, we assumed a delay (τ) of 15 minutes as was employed in the

previous model with cortisol transported from the central to peripheral compartment. Modified parameter values and their descriptions are included in Table A2 of the Appendix.

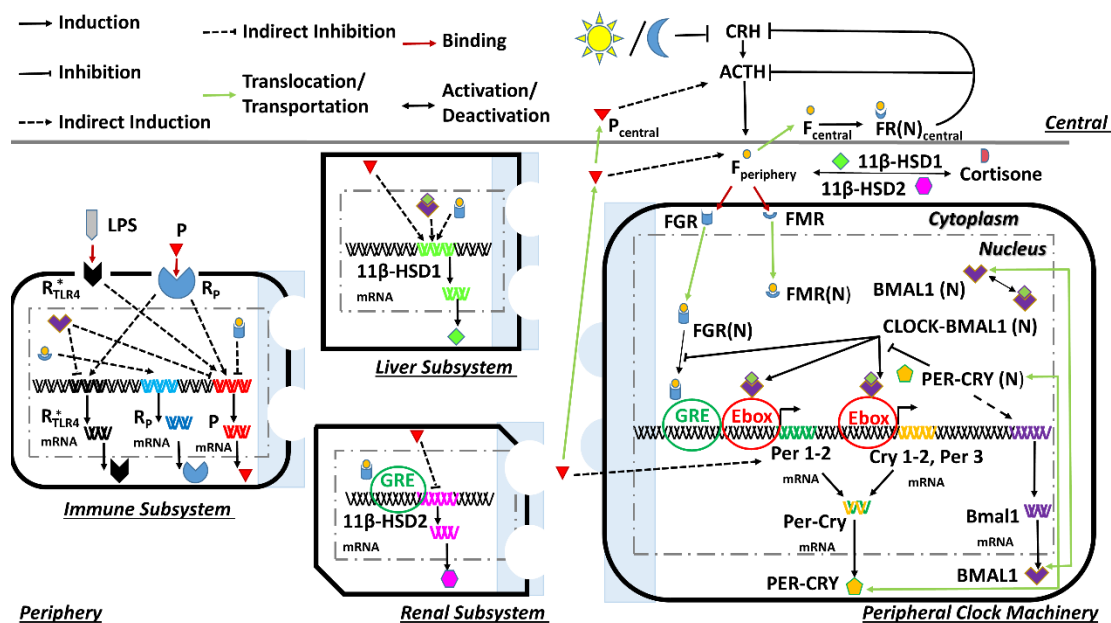


Figure 11. Modified model schematic incorporating 11β -HSD dynamics and cortisol/cortisone metabolism.

The reported effects of light exposure on cortisol concentrations include no change (Rüger, Gordijn et al. 2006), increased (Scheer and Buijs 1999, Leproult, Colecchia et al. 2001) and decreased levels (Jung, Khalsa et al. 2010). These inconsistencies may be attributed to differences in light intensity, duration of exposure and the phase of light presentation. Vasopressin (VP), a SCN secreted circadian hormone (Forsling, Montgomery et al. 1998, Kostoglou-Athanassiou, Treacher et al. 1998) released during the light period is considered to confer an inhibitory effect on HPA axis activity (Kalsbeek, Fliers et al. 2010). Corticosterone production is inhibited in male Wistar rats treated with VP and treatment with a VP antagonist increases production

(Kalsbeek, van der Vliet et al. 1996). Depressed patients, characterized by HPA axis hyperactivity, display reduced levels and amplitudes of VP mRNA (Zhou, Riemersma et al. 2001). Assuming that the inhibitory effect of VP is light-mediated and acts via *CRH*, cortisol's secretion was regulated via degradation of *CRH* by light (Equation 1). We described the light response using a Michaelian function as photosensitive RGCs exhibit response saturation (Berson, Dunn et al. 2002).

Sigmoidal dose response curves, describing an initial exponential growth phase that eventually slows and plateaus as saturation occurs, have been used to relate the cortisol secretion response to *ACTH* (Demitrack, Dale et al. 1991, Keenan, Roelfsema et al. 2004, Bousquet-Melou, Formentini et al. 2006). This ultrasensitive cortisol response was modeled using a Hill function with a seasonal coefficient n_{season} that reflects seasonal changes in adrenal sensitivity to *ACTH* (Equation 3). In sand rats, *in vivo* administration of *ACTH* elicits greater cortisol secretion in the winter versus the summer months (Amirat and Brudieux 1993) and corticosterone production is more elevated in Fischer 344 Rats challenged with *ACTH* in short photoperiods/days (SD) versus long days (LD) (Otsuka, Goto et al. 2012). The SCN has been identified as a critical regulator of adrenal sensitivity as SCN lesioning eliminates the diurnal variation in *ACTH*-induced corticosterone secretion in rats (Sage, Maurel et al. 2002). In mice, acute light exposure can stimulate corticosterone secretion and regulate the expression of transcription factor genes of steroid synthesizing enzymes via an *ACTH*-independent, SCN-sympathetic nervous system-dependent mechanism (Ishida, Mutoh et al. 2005). The light induced response was abrogated with SCN lesioning and adrenal denervation suggesting that the

SCN-sympathetic nervous system is pivotal in photic regulation of adrenal function. The electrical activity of the SCN displays seasonal adaptation to photoperiod changes such that the duration of electrical activity is extended in long days (LD) and compressed in shorter days (SD) (Meijer, Michel et al. 2010). Seasonal population changes in SCN neuronal electrical activity may be attributed to phase differences between neurons and/or variations in individual neuronal activity. No significant differences, however, were found to exist between individual SD and LD mice neuronal activity profiles despite the observation of compressed population activity following SD exposure (VanderLeest, Houben et al. 2007). Via computational modeling, it has been revealed that the phase relationships among neuronal activities accounts for the photoperiod-induced population waveform changes (Rohling, Wolters et al. 2006) and that the narrowly synchronized SD neuronal population activity pattern is associated with a high amplitude rhythm (Schaap, Albus et al. 2003). We hypothesized, therefore, that augmented SCN activity during the SD winter season promotes enhanced sympathetic signaling which enhances adrenal sensitivity to ACTH. The Hill coefficient n_{season} was set to increase with decreasing photoperiod to reflect this seasonal variation.

Enzymatic activation and inactivation of cortisol via $11\beta - HSD1$ and $11\beta - HSD2$ activity was also accounted for in our description of $F_{periphery}$ dynamics.

Estimated parameters of Equations 1-3 as well as those describing cortisol metabolism in the periphery (Equations 28 – 32) were optimized to improve the goodness of fit between cortisol's normalized spring model circadian profile (baseline) and diurnal serum cortisol

measurements (Hermann, von Aulock et al. 2006). The redefined equations describing light entrainment and cortisol dynamics are shown in Equations 1 through 9 below.

$$\frac{dCRH}{dt} = \frac{k_{p1} \cdot In_{CRH}}{K_{p1} + FR(N)_{central}} - \frac{V_{d1} \cdot CRH \left(1 + \frac{light}{1 + light}\right)}{K_{d1} + CRH} \quad (1)$$

$$\frac{dACTH}{dt} = \frac{k_{p2} \cdot CRH}{K_{p2} + FR(N)_{central}} \left(1 + k_{fp1} \cdot P_{central}\right) - \frac{V_{d2} \cdot ACTH}{K_{d2} + ACTH} \quad (2)$$

$$\frac{dF_{periphery}}{dt} = \frac{k_{p3} \cdot ACTH^{n_{season}}}{K_{p3}^{n_{season} + ACTH^{n_{season}}}} \left(1 + k_{fp2} \cdot P\right) + \frac{k_{cat1} \cdot 11\beta - HSD1 \cdot E}{K_{mF} + E} - \frac{k_{cat2} \cdot 11\beta - HSD2 \cdot F_{periphery}}{K_{mE} + F_{periphery}} - \frac{V_{d3} \cdot F_{periphery}}{K_{d3} + F_{periphery}} \quad (3)$$

$$\frac{dF_{central}}{dt} = \frac{1}{\tau} (F_{periphery} - F_{central}) \quad (4)$$

$$\frac{dmRNA_{R,central}}{dt} = k_{synRm} \left(1 - \frac{FR(N)_{central}}{IC_{50Rm} + FR(N)_{central}}\right) - k_{dgrRm} \cdot mRNA_{R,central} \quad (5)$$

$$\frac{dR_{central}}{dt} = k_{synR} \cdot mRNA_{R,central} + R_f \cdot k_{re} \cdot FR(N) - k_{on} \cdot F_{central} \cdot R_{central} - k_{dgrR} \cdot R_{central} \quad (6)$$

$$\frac{dFR_{central}}{dt} = k_{on} \cdot F_{central} \cdot R_{central} - k_T \cdot FR_{central} \quad (7)$$

$$\frac{dFR(N)_{central}}{dt} = k_T \cdot FR_{central} - k_{re} \cdot FR(N)_{central} \quad (8)$$

$$\frac{dP_{central}}{dt} = \frac{1}{\tau} (P - P_{central}) \quad (9)$$

The equations describing the peripheral mineralocorticoid and glucocorticoid receptor dynamics, the peripheral molecular clock dynamics with cortisol entrainment, and the diurnal rhythm of the pro-inflammatory mediator and its receptor were kept the same as in the previous chapter.

11 β -hydroxysteroid dehydrogenase and cortisone dynamics

Equations 28 and 29 describe the transcription and translation of 11 β – HSD1 while Equations 30 and 31 characterize the transcription and translation of 11 β – HSD2.

The translated $11\beta - HSD2$ and $11\beta - HSD1$ enzymes catalyze the interconversion between cortisone (E , Equation 32) and cortisol ($F_{periphery}$, Equation 3). The CCAAT-enhancer-binding proteins (C/EBPs) is a family of transcription factors composed of 6 members, from C/EBP- α to C/EBP- ζ , and are the only factors directly involved in promoting $11\beta - HSD1$ transcription following endocrine, inflammatory and metabolic stimuli (Chapman, Holmes et al. 2013). C/EBP α and C/EBP β are predominantly expressed in the liver with lower levels of C/EBP δ expressed under basal conditions (Lekstrom-Himes and Xanthopoulos 1998). C/EBP regulation of $11\beta - HSD1$ expression is complex whereby C/EBP α is a potent activator of $11\beta - HSD1$ and C/EBP β is a weak activator (Williams, Lyons et al. 2000). Additionally, C/EBP β acts a relative inhibitor of C/EBP α . Under basal conditions in the liver, the ratio of C/EBP α to C/EBP β is high which favors enhanced $11\beta - HSD1$ transcription. In response to inflammatory triggers such as TNF- α (Yin, Yang et al. 1996) and LPS treatment (Alam, An et al. 1992), nuclear localization and transcription of C/EBP α decreases. Alternatively, TNF- α , IL-6 and LPS treatment increases the nuclear localization, expression and transcription of C/EBP β (Alam, An et al. 1992, Yin, Yang et al. 1996, Niehof, Streetz et al. 2001). Administration of dexamethasone, increases the transcription rate and transcript levels of C/EBP β mRNA without affecting C/EBP α mRNA levels (Matsuno, Chowdhury et al. 1996). As is evident from the GC, pro-inflammatory cytokine and LPS administration studies, C/EBP α is essential for basal regulation of $11\beta - HSD1$ and C/EBP β is crucial for regulation under high-stress scenarios.

CLOCK – BMAL1 directly regulates *C/EBP α* transcription and the expressions of both *C/EBP α* (Kawasaki, Doi et al. 2013) and *C/EBP β* mRNA (Ma, Panda et al. 2011) show circadian rhythmicity. Diurnal fluctuations of *11 β – HSD1* mRNA expression has been observed in the hypothalamus of rats, with no circadian activity detected in the periphery (Buren, Bergstrom et al. 2007). In explant cultures of adipose tissue, derived from obese human subjects, *11 β – HSD1* and *11 β – HSD2* mRNA expression displayed circadian variation (Gomez-Santos, Gomez-Abellan et al. 2009, Garaulet, Ordovas et al. 2011). Furthermore, although rodent data suggests the absence of circadian expression of *11 β – HSD1* mRNA in the periphery, the mRNA and protein expression of hexose-6-phosphate dehydrogenase (H6PD), which generates the cofactor NADPH for *11 β – HSD1* reductase activity (Walker and Andrew 2006), exhibits diurnal rhythmicity (Janich, Arpat et al. 2015). The importance of H6PD in regulating *11 β – HSD1* reductase activity has been assessed experimentally whereby targeted inactivation of mouse H6PD impairs the ability to generate corticosterone from 11-dehydrocorticosterone (Lavery, Walker et al. 2006). Given the circadian activity of both the transcriptional factors regulating *11 β – HSD1* expression and the cofactor generating enzyme for *11 β – HSD1* activity in addition to evidence of *11 β – HSD1* and *11 β – HSD2* mRNA diurnal rhythmicity in adipose tissue, we assume circadian variation of the mRNA and protein of both enzymes.

In lieu of modeling the complex *C/EBP*-mediated mechanisms governing *11 β – HSD1* expression and activity, a semi-mechanistic approach was adopted whereby IDR models were used to capture the relevant dynamics. In Equation 28, we used an IDR to

describe the cortisol-mediated enhancement of $11\beta - HSD1$ mRNA expression (Low, Moisan et al. 1994, Voice, Seckl et al. 1996, Jamieson, Chapman et al. 1999, Morgan, McCabe et al. 2014). Dexamethasone induced upregulation of $11\beta - HSD1$ mRNA is attenuated with treatment of a glucocorticoid receptor antagonist (Sai, Esteves et al. 2008), suggesting the involvement of *GR*. We therefore modeled $11\beta - HSD1$ mRNA expression to be induced via the cortisol-receptor nuclear complex (*FGR(N)*). *CLOCK - BMAL1* was modeled to indirectly stimulate $11\beta - HSD1$ mRNA as it is known to coordinate the temporal expression of *C/EBP α* . Like GCs, pro-inflammatory cytokines (*IL-1 β* and *TNF- α*) increase activity of $11\beta - HSD1$ in the HuH-7 human hepatoma cell line (Iwasaki, Takayasu et al. 2008). *TNF- α* overexpressing mice and HepG2 cells subjected to *TNF α* treatment show increased hepatic $11\beta - HSD1$ mRNA expression and activity (Ignatova, Kostadinova et al. 2009). The stimulatory effect of pro-inflammatory cytokines on $11\beta - HSD1$ transcription was mediated by our pro-inflammatory mediator (*P*).

Experimental findings of the effects of GCs on renal $11\beta - HSD2$ are contradictory. Adrenalectomized (ADX) rats show comparable protein expression to controls but intermediate corticosterone doses increase enzyme activity while low and high doses elicit no change (Zalocchi, Matkovic et al. 2004). One study found that dexamethasone treatment in ADX rats enhanced activity but decreased mRNA expression (Li, Smith et al. 1996) whereas another reported no change in activity following dexamethasone administration (Alfaidy, Blot-Chabaud et al. 1995). Corticosterone treatment of human renal tissue inhibits $11\beta - HSD2$ activity (Diederich, Quinkler et al. 1996) while

treatment of Ishikawa (endometrial) cells (Koyama and Krozowski 2001) and bronchial epithelial cells (Suzuki, Koyama et al. 2003) with cortisol and dexamethasone increase $11\beta - HSD2$ activity, mRNA and protein expression. Dexamethasone treatment promotes mRNA expression and enhances $11\beta - HSD2$ activity via direct binding of the glucocorticoid receptor to the promoter region of $11\beta - HSD2$ in SW620 cells (human colon cell line) (Alikhani-Koupaei, Fouladkou et al. 2007). Conflicting reports of GC effects on $11\beta - HSD2$ expression and activity may be due to differences in the dosage and substrates used to measure enzyme activity. Studies quantifying the conversion of radiolabeled corticosterone typically reported no change or inhibited activity while those using dexamethasone as a substrate generally found activity to be increased with GC treatment. Corticosterone is a substrate for both $11\beta - HSD1$ and $11\beta - HSD2$ while dexamethasone is solely a $11\beta - HSD2$ substrate (Best, Nelson et al. 1997). $11\beta - HSD2$ activity findings based on corticosterone conversion rates may therefore be influenced by $11\beta - HSD1$ activity. The general consensus of the effect of GCs on $11\beta - HSD2$ expression and activity, using dexamethasone as the enzyme substrate, is stimulatory and so we modeled this influence using $FGR(N)$ (Equation 30). Treatment of LLC-PK1 cells (porcine kidney cells) with $TNF-\alpha$ suppresses $11\beta - HSD2$ mRNA expression and activity (Heiniger, Rochat et al. 2001) and $TNF-\alpha$ overexpressing transgenic mice show reduced $11\beta - HSD2$ mRNA levels and activity (Kostadinova, Nawrocki et al. 2005). The inhibitory effect of pro-inflammatory cytokines on $11\beta - HSD2$ mRNA expression was modeled using an IDR term (Equation 30). The dynamics

of E (Equation 32) is characterized by an activation and inactivation term based on $11\beta - HSD2$ and $11\beta - HSD1$ activities and a degradation term.

The enzyme kinetic parameters of $11\beta - HSD1$ and $11\beta - HSD2$ were obtained from experimental studies (Brown, Chapman et al. 1993, Shafqat, Elleby et al. 2003, Castro, Zhu et al. 2007, Gong, Morris et al. 2008). All other parameters of Equations 28 to 32 were estimated such that the relative phase between $11\beta - HSD1$ and $11\beta - HSD2$ mRNA was in accordance with experimental data (Gomez-Santos, Gomez-Abellan et al. 2009, Garault, Ordovas et al. 2011), peak $11\beta - HSD1$ mRNA expression was antiphase to cortisol's acrophase (Buren, Bergstrom et al. 2007) and that the relative phase and amplitude between cortisone and cortisol was comparable to human experimental findings (Morineau, Boudi et al. 1997, Nomura, Fujitaka et al. 1997, Weber, Lewicka et al. 2000).

$$\frac{d11\beta-HSD1_{mRNA}}{dt} = k_{8a} \left(1 + \frac{k_{8b} \cdot FGR(N)}{K_{8b} + FGR(N)}\right) \cdot \left(1 + \frac{k_{8c} \cdot CLOCK-BMAL1}{K_{8c} + CLOCK-BMAL1}\right) \cdot (1 + k_{8p} \cdot P) - k_{8d} \cdot 11\beta - HSD1_{mRNA} \quad (28)$$

$$\frac{d11\beta-HSD1}{dt} = k_{9a} \cdot 11\beta - HSD1_{mRNA} - k_{9d} \cdot 11\beta - HSD1 \quad (29)$$

$$\frac{d11\beta-HSD2_{mRNA}}{dt} = \frac{k_{10a} \cdot FGR(N)}{K_{10a} + FGR(N)} (1 - k_{10b} P) - k_{10d} \cdot 11\beta - HSD2_{mRNA} \quad (30)$$

$$\frac{d11\beta-HSD2}{dt} = k_{11a} \cdot 11\beta - HSD2_{mRNA} - k_{11d} \cdot 11\beta - HSD2 \quad (31)$$

$$\frac{dE}{dt} = \frac{k_{cat2} \cdot 11\beta-HSD2 \cdot F_{periphery}}{K_{mE} + F_{periphery}} - \frac{k_{cat1} \cdot 11\beta-HSD1 \cdot E}{K_{mF+E}} - k_{12d} \cdot E \quad (32)$$

3.3: Seasonal Changes in Circadian Dynamics

Representative circadian profiles for all seasons are depicted in Figure 12. The oscillatory amplitudes of *ACTH* (A), *F_{periphery}* (B), *E* (C), *11 β - HSD1* (E), *11 β - HSD2* (F), *P* (G) and *R_p* (H) were greatest for the winter model and lowest for the summer model. Alternatively, the amplitude of *BMAL1* (D) was heightened in the summer and diminished in the winter model. *11 β - HSD1* and *P* displayed similar acrophases (time of peak levels) near the minima of *F_{periphery}* while *11 β - HSD2* and *R_p* rhythms were at a maxima shortly after the peak of *F_{periphery}*. The acrophases of all rhythms were delayed as the seasons progressed from summer through winter, following which they were advanced.

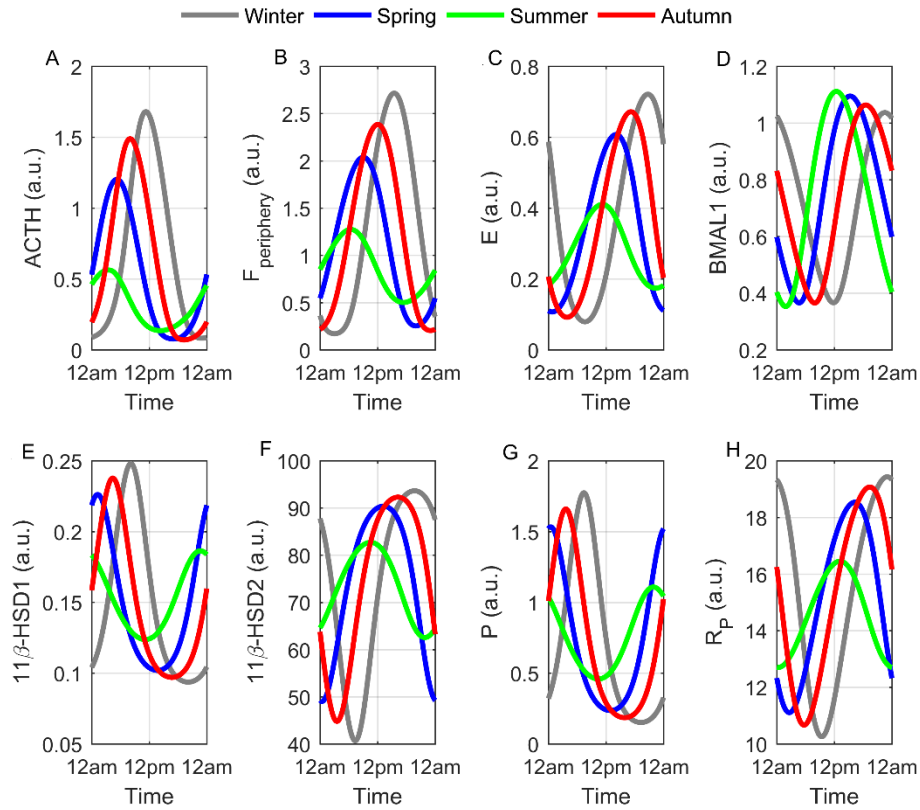


Figure 12. Seasonal circadian profiles.

Numerous seasonal profiles predicted by our model and shown in Figure 12 are in agreement with our previous work (Pierre, Schlesinger et al. 2016) and experimental findings. Cortisol levels are generally increased during the winter season (Walker, Best et al. 1997, Persson, Garde et al. 2008, Hadlow, Brown et al. 2014) with an approximate 5% increase in median cortisol concentration for each hour delay in the time of sunrise (Hadlow, Brown et al. 2014). Additionally, the phase delayed $F_{periphery}$ winter rhythm predicted by our model (12B) has been observed experimentally (Vondrasova, Hajek et al. 1997) and the amplitude increase of the pro-inflammatory mediator (P) for the winter model (12G) is in accordance with the human IL-6 seasonal study (Maes, Stevens et al. 1994). Increased expression of IL-6 mRNA and sIL-6R during the winter season and

peak expression of the *BMAL1* encoding gene, *Arntl*, during the summer season has been previously observed (Dopico, Evangelou et al. 2015) and so our seasonal circadian profiles of R_p (3H) and *BMAL1* (12D) are in agreement with these findings. Human *ACTH* (CAUTER, VIRASORO et al. 1981) and *E* (Walker, Best et al. 1997) levels are higher in winter and higher concentrations of *ACTH* have been reported in rats following SD exposure (Otsuka, Goto et al. 2012) which validates our predictions shown in Figure 12A and 12C. There have been no experimental findings pertaining to the seasonal variation of $11\beta - HSD1$ and $11\beta - HSD2$ expression but it has been theorized that enhanced $11\beta - HSD1$ activity promotes elevated cortisol levels during the winter (Walker, Best et al. 1997). Given that $11\beta - HSD2_{mRNA}$ transcription is stimulated by cortisol, the augmentation of its oscillatory amplitude during the winter season (12F) seems reasonable. The predicted elevation of $11\beta - HSD1$ (12E) levels promote increased $F_{periphery}$ which drastically reduces cortisol's nadir during the winter season via negative feedback. This attenuation diminishes the anti-inflammatory influence of $F_{periphery}$ on P and consequently results in the predicted elevated P rhythms for our winter model. Our results therefore reflect a general shift from an anti- to a pro-inflammatory state as the seasons change from summer through winter. This seasonal plasticity may play a critical role in the seasonality of diseases such as rheumatoid arthritis (RA). Both the onset of RA and aggravation of symptoms display peak occurrence during the winter season (Fleming, Crown et al. 1976, Hawley, Wolfe et al. 2001).

The underlying mechanisms governing our predicted seasonal variations of $F_{periphery}$ were then assessed. Figure 13 depicts the dynamics of $ACTH$ -, $11\beta - HSD1$ -, $11\beta - HSD2$ - and degradation enzyme-mediated rate of change of cortisol concentration for each season. $\frac{k_{p3} \cdot ACTH^{n_{season}}}{K_{p3}^{n_{season}} + ACTH^{n_{season}}}$ regulates the rate of change of adrenal production, $\frac{k_{cat.11\beta-HSD1} \cdot E}{K_{mE} + E}$ governs hepatic activation, $\frac{k_{cat2.11\beta-HSD2} \cdot F_{periphery}}{K_{mE} + F_{periphery}}$ modulates the rate of renal inactivation and $\frac{V_{d3} \cdot F_{periphery}}{K_{d3} + F_{periphery}}$ controls the rate of enzymatic degradation of $F_{periphery}$. The upper panels show the rate of change versus substrate concentrations while the lower panels depict the circadian variation of these rates. Increases in $ACTH$ and $F_{periphery}$ substrate concentrations enhances the rates of production (13A) and degradation of cortisol (13D) which eventually saturates at higher substrate concentrations. The reduced substrate concentrations for the summer model restrict the ranges of the rates of cortisol production, activation, inactivation and degradation. Seasonal disparities were observed for the rate of adrenal cortisol production whereby lower $ACTH$ concentrations resulted in higher rates of production in the summer model. At greater $ACTH$ concentrations, however, the rate of cortisol production was greater in the winter model. At comparable $F_{periphery}$ concentrations, the rate of degradation was seasonally-independent. The enzyme-mediated rates of activation and inactivation of cortisol, arbitrated by $11\beta - HSD1$ and $11\beta - HSD2$, were predicted to display hysteretic behavior (13B, 13C) with comparable substrate concentrations yielding different responses. The predicted hysteretic phenomena are attributed to the circadian variations of both the substrate and enzyme levels (Figures 14 and 15). The slower

descent of $11\beta - HSD1$ in the early morning prolongs its availability. This coupled with increasing E levels result in greater changes in $F_{periphery}$ activation rates when compared later in the day. Similarly, higher $11\beta - HSD2$ levels during the afternoon/night results in greater changes in $F_{periphery}$ deactivation rates when compared to the early morning. For all mechanisms, the circadian rate of change of cortisol concentration for the winter model displayed the greatest dynamic range (13E, 13F, 13G, 13H).

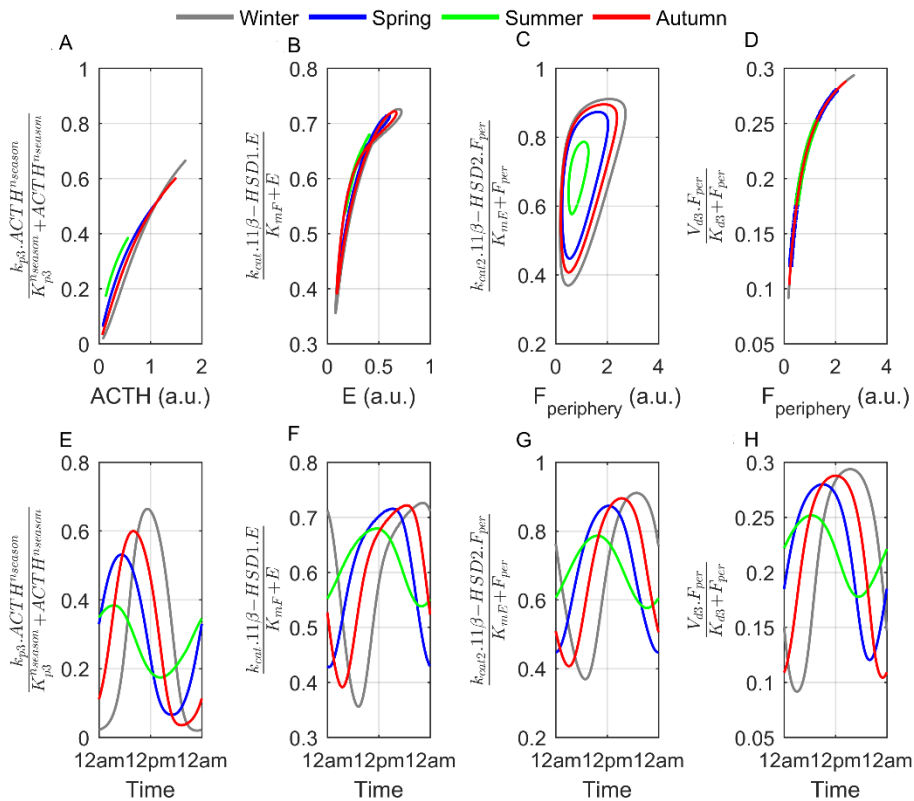


Figure 13. Seasonal and circadian variation of mechanisms regulating $F_{periphery}$ availability.

The seasonal variations of the $ACTH$ -mediated rate of cortisol production versus $ACTH$ levels are plotted in 13A. The differences amongst seasons are due to the differing adrenal sensitivities to $ACTH$ stimulation. As the seasonal Hill coefficient (n_{season})

increases, there is a more rapid change in the $F_{periphery}$ production rate with increasing substrate concentrations. At higher $ACTH$ levels, therefore, the rate of production is greatest in the winter model ($n_{season} = 1.5$). Hysteretic enzyme responses were predicted for both the metabolic enzymes. Mechanisms such as time varying concentrations of substrate, product, activator or inhibitor (Purich 2010), ligand-induced slow isomerization of an enzyme from its inactive to active conformational form and the slow displacement of an allosteric effector (N.Appaji Rao 1987) have been attributed to modulate enzyme hysteresis.

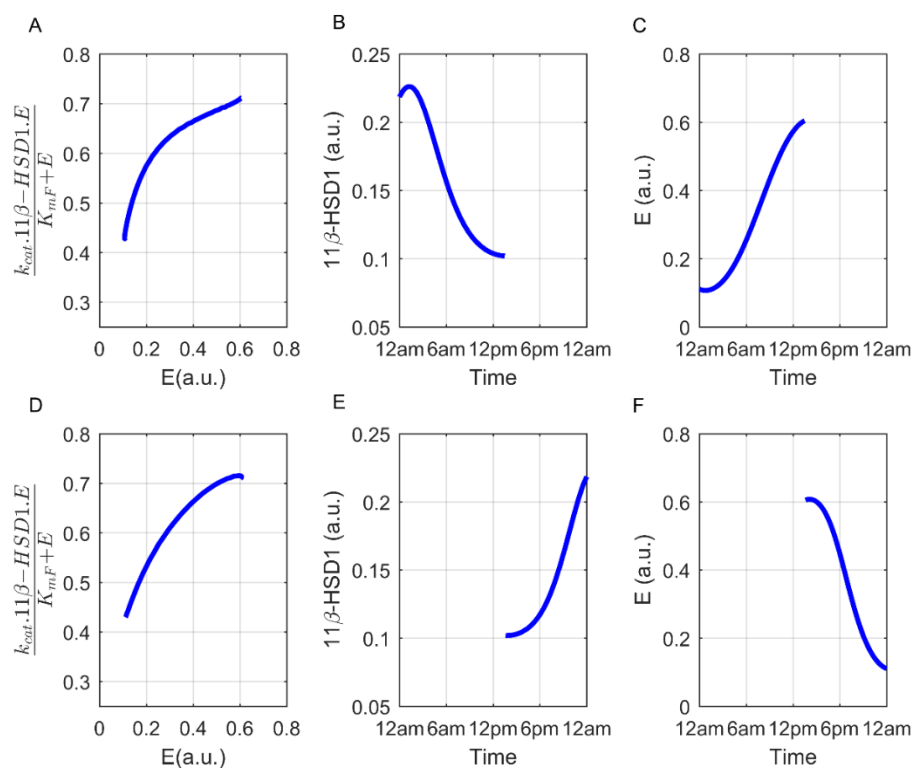


Figure 14. $F_{periphery}$ activation rate and circadian variation of 11β -HSD1 and E for the spring (baseline) model.

The activity of the phosphofructokinase enzyme is described as hysteretic as it is enhanced by the accumulation of its product, fructose diphosphate (Tornheim and

Lowenstein 1975). Recently, positive feedback loops have been shown to control enzyme hysteresis both experimentally (Kramer and Fussenegger 2005) and in silico (Novak and Tyson 2008). For our model, the circadian variation of enzyme and substrate concentrations result in the observed responses. As is evident in Figures 14 and 15, the relative phases between the substrate and the enzyme ultimately result in the predicted hysteretic phenomena. In Figures 14A and 14D, the hysteretic loop describing $11\beta - HSD1$ activity has been partitioned into two differing changes in reaction rates that depend on the time of day. The slower descent of $11\beta - HSD1$ in the early morning (14B) prolongs its availability. This coupled with increasing E levels (14C) result in greater changes in $F_{periphery}$ activation rates when compared to the later day. Similarly, higher $11\beta - HSD2$ levels during the afternoon/night (15E) results in greater changes in $F_{periphery}$ deactivation rates (15D) when compared to the early morning (15A). Apart from substrate and enzyme circadian dissimilarities, the contrasting hysteretic responses of both enzymes are also a result of binding affinity differences between the enzymes and their substrates.

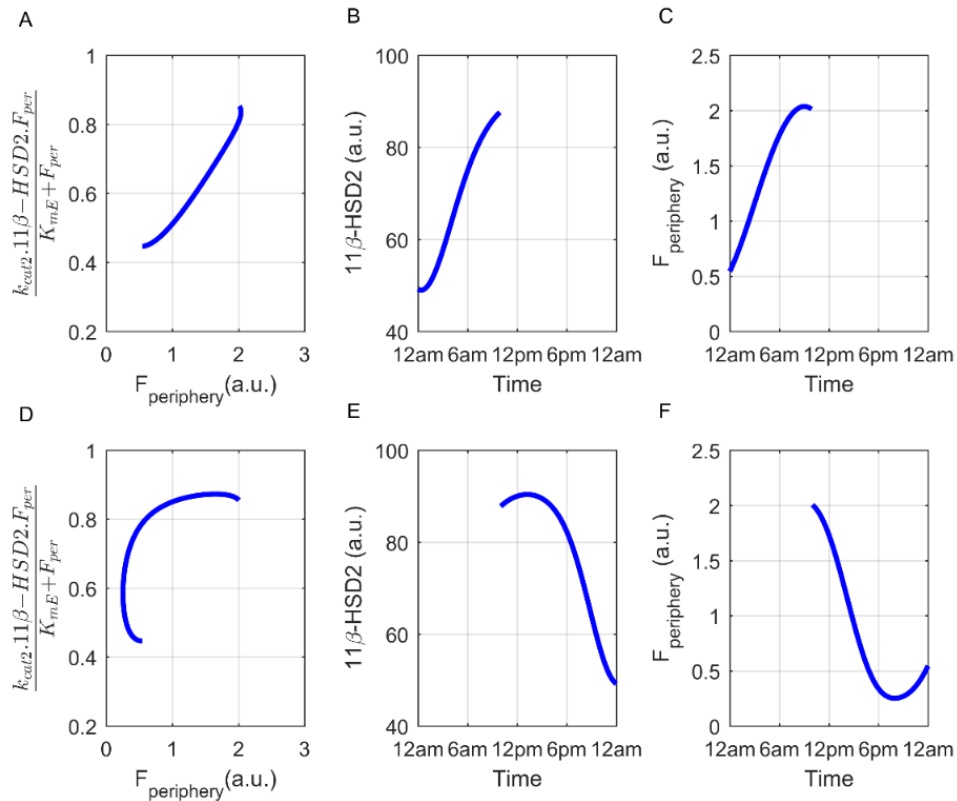


Figure 15. $F_{periphery}$ inactivation rate and circadian variation of $11\beta - HSD2$ and $F_{periphery}$ for the spring (baseline) model.

The higher affinity of $11\beta - HSD2$ for $F_{periphery}$ yields a loop that displays saturation whereas the lower affinity of $11\beta - HSD1$ for E results in activation rates that never plateau. The physiological function of enzyme hysteresis is not entirely understood but the phenomenon has been shown to control sudden metabolite fluxes (Lalanne and Henderson 1975) and modulate the amplitude of oscillations within pathways (Tornheim and Lowenstein 1975). This behavior exhibited by the $11\beta - HSD$ enzymes may therefore be critical for precisely regulating the circadian bio-availability of $F_{periphery}$.

3.4: Parameter sampling: *In silico* Population Generation, HSD11B1 KO and cluster analysis

Mice HSD11B1 knockout studies highlight the genetic influences of 11β – *HSD1* on HPA axis activity. 11β – *HSD1* deficient 129/MF1 mice display elevated basal corticosterone and *ACTH* levels with an exacerbated and prolonged stress response (Harris, Kotelevtsev et al. 2001) while *HSD1* $-/-$ mice congenic on a C57BL/6J background exhibit normal basal corticosterone and *ACTH* levels which return to baseline concentrations in a similar manner as control following exposure to restraint stress (Carter, Paterson et al. 2009). Contrarily, high basal corticosterone levels with an attenuated maxima are observed in 11β – *HSD1* deficient mice on a novel genetic background (96% C57BL/6J and 4% CBA/C³H)(Paterson, Holmes et al. 2007). Most mutations in the human gene encoding for 11β – *HSD2* (HSD11B2) impair enzymatic activity and result in AME (Nunez, Rogerson et al. 1999) with targeted disruption of mice HSD11B2 producing characteristic AME symptoms such as hypertension and hypokalemia (Kotelevtsev, Brown et al. 1999). Although 11 – *HSD2* deficiency results in defective conversion of cortisol to cortisone, normal cortisol and *ACTH* levels are maintained; purportedly due to an extended cortisol half-life which suppresses enhanced *ACTH* secretion via negative feedback (Stewart, Corrie et al. 1988).

Under basal conditions, differences in 11β – *HSD* dynamics may still yield normal cortisol (and corticosterone) profiles and urinary ratios of cortisol to cortisone metabolites due to the opposing effects of the 11β – *HSD1* and 11β – *HSD2* enzymes

on cortisol's bioavailability (Gambineri, Tomassoni et al. 2011). Mutations in HSD11B1 and HSD11B2 are assumed to regulate enzyme activity by impacting enzyme transcription (Draper, Walker et al. 2003), translation efficiency and/or stability (Nunez, Rogerson et al. 1999, Malavasi, Kelly et al. 2010). We assume therefore that the experimentally determined kinetic parameters for both enzymes (k_{cat} , k_{cat2} , K_{mF} , K_{mE}) (Brown, Chapman et al. 1993, Shafqat, Elleby et al. 2003, Castro, Zhu et al. 2007, Gong, Morris et al. 2008) are constant and modeled inter-subject variability in cortisol metabolism dynamics by sampling ($\pm 50\%$) the 16 estimated parameters of Equations 28 to 32. Latin hypercube sampling ($n = 2^{16} = 65536$) was employed to ensure an even coverage of individual parameter ranges (McKay, Beckman et al. 1979). The generation of "virtual patients" by sampling physiological parameters is commonly used to generate a virtual population that matches the diversity observed in clinical cohorts (Klinke 2008, Allen, Rieger et al. 2016). Virtual patients are usually weighted such that the simulated population depicts baseline characteristics of the observed population-level data. For our model, we implemented a filtering criteria such that a population of simulated subjects with "normal" cortisol levels were retained. Normalcy was assessed based on the *in silico* subject's similarity to our spring model's profile which was normalized to experimental data. Numerical integration of Equations 1 through 32 was implemented for each of the 65536 unique parameter sets and solutions were only retained if they satisfied the $F_{periphery}$ "criteria of normality". This filtering criteria specifies that the spring model's (baseline) $F_{periphery}$ profile must have an amplitude within $\pm 5\%$ and an acrophase within ± 1 hour of our original model (Pierre, Schlesinger et al. 2016), the period of all

seasonal $F_{periphery}$ oscillations should be 24 ± 0.25 hours and the winter model's $F_{periphery}$ amplitude of oscillation should be the highest. Using the parameter sets that yielded the aforementioned accepted $F_{periphery}$ solutions, a second stage of numerical integration was conducted using an *in silico* HSD11B1 knockout model whereby the transcription rate of $11 - HSD1_{mRNA}$ (k_{8a}) was set to zero. The subsequently generated solutions were only accepted if all the seasonal $F_{periphery}$ and *ACTH* oscillations were 24 ± 0.25 hours.

Of the 65536 solution sets obtained, 828 solutions satisfied our baseline $F_{periphery}$ "criteria of normality" as well as the *ACTH* and $F_{periphery}$ oscillatory period specification of 24 ± 0.25 hours following *in silico* HSD11B1 knockout ($k_{8a} = 0$). The $11\beta - HSD1$ and $11\beta - HSD2$ profiles of these 828 *in silico* subjects, with unique cortisol metabolism kinetic parameters, were subject to clustering analysis to identify sub-populations within our dataset. Due to differing scales, the amplitude of both $11\beta - HSD1$ and $11\beta - HSD2$ rhythms were first z-score normalized. Data mining was conducted separately for each season using k-means clustering with the optimum number of cluster centers (k=4) estimated using the gap-statistic (Tibshirani, Walther et al. 2001). Of the 828 subjects, 741 were assigned to identical clusters, independent of season, and so we only considered these for the seasonal circadian dynamics and *in silico* HSD11B1 knockout analyses.

Statistical Analysis

After identifying the unique parameter sets for each subject of each cluster, the Kruskal-Wallis test was performed to compare parameter distributions between clusters. This nonparametric version of ANOVA was used to test the null hypothesis that parameters came from populations with the same distribution. The Tukey's Honestly Significant Difference Procedure was used to conduct post-hoc pairwise mean rank comparisons between groups (clusters) of significantly different parameter distributions. The Kruskal-Wallis test followed by the Tukey's Honestly Significant Difference Procedure was also employed to determine if any significant differences existed between seasons for cortisol added/removed by each mechanism.

A multivariate multiple linear model was developed to assess the relationship between the 11 parameters and the observed $11\beta - HSD1$ and $11\beta - HSD2$ amplitudes within each cluster. Similar to the rescaling done for cluster analysis, the predictors (parameters) and the responses ($11\beta - HSD1$ and $11\beta - HSD2$ amplitudes) were z-score normalized prior to model development. The general form of the regression equation is shown in Equation 33 whereby Y represents the bivariate amplitudes, β_i the regression weights that represent the amplitude change(s) (in standard deviations) associated with a one standard deviation change of the predictors and ε is a matrix of residuals.

$$Y = \beta_1 k_{8a} + \beta_2 k_{8p} + \beta_3 k_{8d} + \beta_4 k_{9a} + \beta_5 k_{9d} + \beta_6 k_{10a} + \beta_7 k_{10d} + \beta_8 k_{10d} + \beta_9 k_{11a} + \beta_{10} k_{11d} + \beta_{11} k_{12d} + \varepsilon \quad (33)$$

3.5: Population seasonal changes in circadian dynamics

Expanding our assessment to account for subject variability, we used our *in silico* 741 subject dataset (see the aforementioned Parameter sampling section for details on dataset generation) to analyze seasonal variations in the mechanisms regulating $F_{periphery}$ availability at a population level. The *ACTH*-, $11\beta - HSD1$ -, $11\beta - HSD2$ -mediated and degradation terms regulating cortisol's rate of change were numerically integrated (from $t = 0$ to $t = 24$ hours) to estimate the contribution of each on cortisol's daily levels. The ratio of cortisol activated by $11\beta - HSD1$ to cortisol inactivated by $11\beta - HSD2$ was also determined. Figure 16 illustrates the seasonal whisker plots for total daily cortisol regulated by each mechanism with the exclusion of $11\beta - HSD2$ -inactivated cortisol which displayed no significant differences between seasons. *ACTH*-induced cortisol (16A) was highest in the winter and autumn and lowest during the summer. Pairwise comparison (see the aforementioned Statistical Analysis section) revealed that no significant difference existed between the winter and autumn values. $11\beta - HSD1$ -activated cortisol in the summer (16B) was predicted to be significantly higher than winter and autumn values with the ratio of activated to inactivated cortisol also highest in the summer season (16C). Enzymatic degradation of cortisol was the most pronounced in the spring season (16D). Furthermore, as is shown in Figure 16E, our model predicted the greatest $F_{periphery}$ to E ratio for the winter (Win) model followed by autumn (Aut), spring (Spr) and summer (Sum).

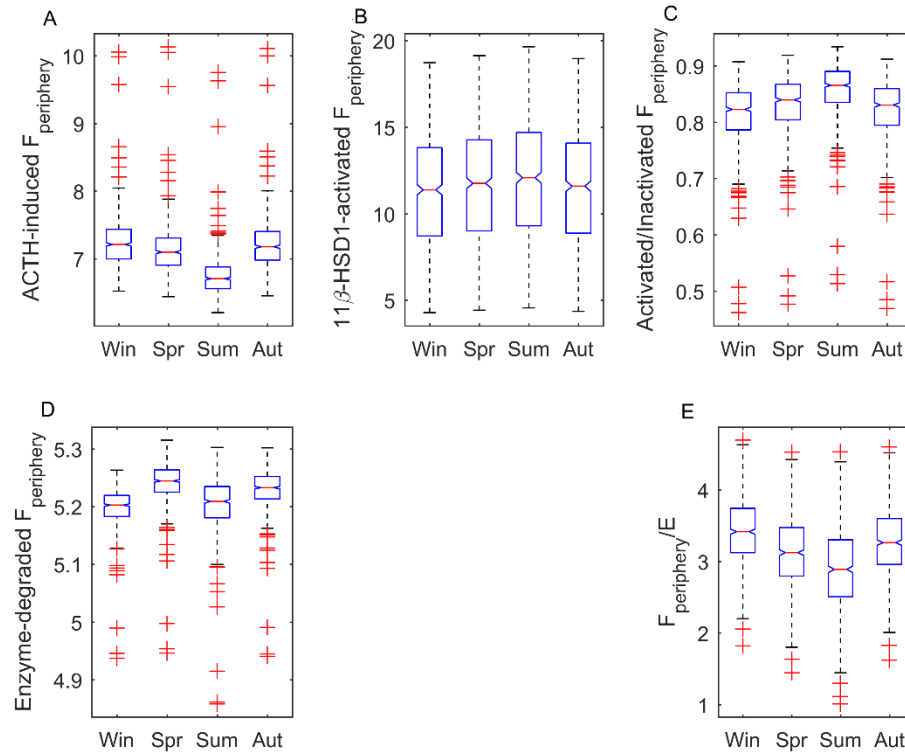


Figure 16. Seasonal whisker plots for $F_{periphery}$ added or removed from the system by various mechanisms and the ratio of $F_{periphery}$ to E .

It has been previously hypothesized that the seasonal increase in cortisol during the winter season is a consequence of elevated $11\beta - HSD1$ activity and a paradoxical reduction in cortisol secretion rate (Walker, Best et al. 1997). In this study by Walker et al., the tetrahydrocortisol/tetrahydrocortisone (THF/THE) ratio was used to quantify $11\beta - HSD1$ activity and the total excretion of cortisol metabolites was used as an index of cortisol's secretion rate. Our model predicted slightly lower cortisol clearance (16D) but greater adrenal secretion of cortisol in the winter versus the summer (16A). Despite the prediction of higher amplitude $11\beta - HSD1$ oscillations in the winter model, $11\beta - HSD1$ activation of $F_{periphery}$ was elevated in the summer (16B, 16C). For our model,

this increase in $11\beta - HSD1$ activity for the summer compensates for the reduced sensitivity to *ACTH* stimulation. The differences between our model's predictions and the seasonal experimental study may be due to confounding enzymatic mechanisms. While urinary analysis of cortisol metabolites may provide insight into adrenal function and peripheral metabolism, it is important to note that cortisol metabolites are also regulated by other enzymes such as 20β -oxoreductase, 5β -reductase and 5α -reductase which may lead to conflicting findings. A recent study found no relationships between HSD11B1 genotypes and urinary cortisol/cortisone metabolite ratios in a cohort of women that expressed higher HSD11B1 mRNA levels and exhibited elevated $11\beta - HSD1$ activity (Gambineri, Tomassoni et al. 2011). Walker et al. found no seasonal differences in urinary cortisol to cortisone ratios whereas our model predicted an elevation of this ratio for the winter model (Figure 16). While this ratio is frequently used to characterize $11\beta - HSD1$ activity, we again emphasize the involvement of other mechanisms, such as adrenal production, which also regulate $F_{periphery}$ levels. These ratios, as metrics for $11\beta - HSD1$ activity, should therefore be interpreted with caution.

3.6: Sub-population classification and in-silico 11β -HSD1 knockout

HPA axis activity is characterized by pronounced inter-individual variability under both basal and stressed conditions. Differences in HPA axis responses underlie differential vulnerability to a variety of disorders however the bases of these variations are poorly understood (Federenko, Nagamine et al. 2004). Polymorphisms in the human

gene encoding for $11\beta - HSD1$ (HSD11B1) have direct functional effects on $11\beta - HSD1$ enzyme activity (Draper, Walker et al. 2003, Malavasi, Kelly et al. 2010) and are associated with increased nadir cortisol levels and depression (Dekker, Tiemeier et al. 2012), diabetes, and metabolic syndrome (Gambineri, Tomassoni et al. 2011). In select ethnic groups, conflicting associations have been reported between HSD11B1 single nucleotide polymorphisms (SNPs) and diseases such as metabolic syndrome and type 2 diabetes (Devang, M et al. 2016). Furthermore, the A allele of rs13306421, an allelic variation known to enhance expression and activity of $11\beta - HSD1$, is found in African American and Japanese populations but not in Chinese, European or Nigerian (Malavasi, Kelly et al. 2010). The observance of strain dependent HPA axis responses in mice HSD11B1 knockout studies (Harris, Kotelevtsev et al. 2001) (Paterson, Holmes et al. 2007, Carter, Paterson et al. 2009) as well as varying sub-population incidence of HSD11B1 SNPs with ethnic group-dependent associations of these SNPs with disease, however, suggest that these metabolic variations could render select cohorts more susceptible to HPA axis dysfunction following perturbation; potentially leading to the development of a diseased state. In line with the mice $11\beta - HSD1$ knockout studies, we consider the effect of *in silico* suppression of $11\beta - HSD1_{mRNA}$ expression in modulating HPA axis activity (see the Parameter sampling section for more details on modeling subject variability, *in silico* knockout and cluster analysis).

Figure 17 illustrates the scatter plots of $11\beta - HSD2$ (y) versus $11\beta - HSD1$ (x) with each subject color coded by cluster for the spring season. Four sub-populations are clearly identified: those with low $11\beta - HSD1$ and $11\beta - HSD2$ (Cluster 1, $\bar{x} =$

0.0646, $\bar{y} = 28.0250$), intermediate $11\beta - HSD1$ and low $11\beta - HSD2$ (Cluster 2, $\bar{x} = 0.1216$, $\bar{y} = 34.3723$), low $11\beta - HSD1$ and high $11\beta - HSD2$ (Cluster 3, $\bar{x} = 0.0920$, $\bar{y} = 45.7049$) and high $11\beta - HSD1$ and $11\beta - HSD2$ (Cluster 4, $\bar{x} = 0.1702$, $\bar{y} = 47.5001$) amplitudes. Of the 16 parameters sampled, the distributions of 11 were determined to be significantly different (see *statistical analysis* section). These parameters as well as their median values are shown in Table 1 with representative distributions of $11\beta - HSD1$ transcription rate (k_{8a}), $11\beta - HSD2$ transcription rate (k_{10a}) and the degradation rate of E (k_{12d}), arranged by cluster illustrated in Figure 18. Lower transcription and translation rates for $11\beta - HSD1$ and $11\beta - HSD2$ (k_{8a} , k_{9a} , k_{10a} , k_{11a}) were observed in the subjects of cluster 1; a group characterized by low amplitude $11\beta - HSD1$ and $11\beta - HSD2$ oscillations.

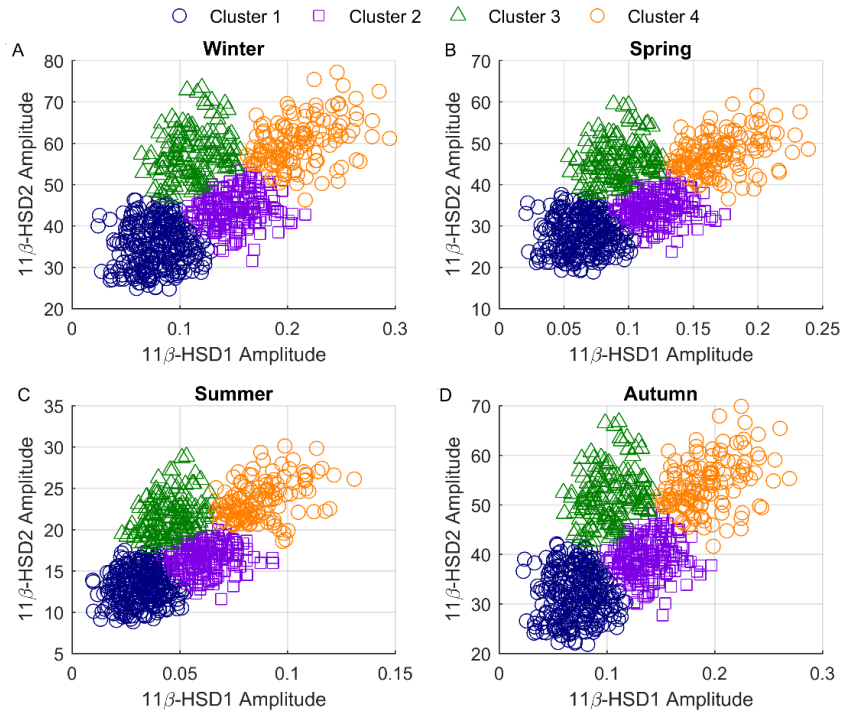


Figure 17. Scatter plots of 741 subjects' $11\beta - HSD2$ versus $11\beta - HSD1$ amplitudes for all four seasons with each point color-coded by cluster association.

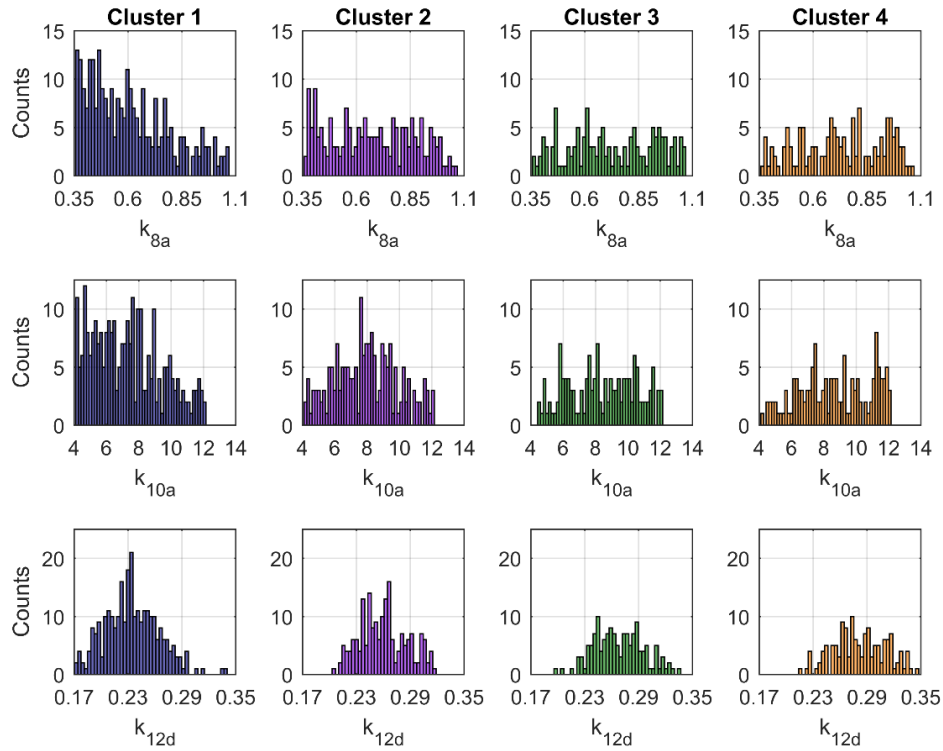


Figure 18. Cluster variation of spring parameter distributions for k_{8a} , k_{10a} and k_{12d} .

The highest production rates (transcription and translation) are associated with clusters 3 and 4. Alternatively, degradation rate constants were maximal in cluster 1 when compared to the other three clusters, with the exception of the degradation rate of cortisone (k_{12d}) which was elevated in cluster 4. Table 2 shows the coefficient estimates of the multivariate multiple linear regression model of both responses for the spring model. Across all seasons, the intra- and inter-cluster relations of all coefficients remained consistent; only differing by magnitude. Each row represents the coefficient values corresponding to the response of that column. β_1 to β_5 are regression coefficients of $11\beta - HSD1_{mRNA}$ and $11\beta - HSD1$ related parameters, β_6 to β_{10} are regression coefficients of $11\beta - HSD2_{mRNA}$ and $11\beta - HSD2$ related parameters and β_{11} is

multiplied by cortisone's degradation constant. The higher coefficient values of β_1 to β_5 in the left column of cluster 4 in comparison to that in cluster 1 indicates that a change of the associated parameters would produce a larger change in the amplitude of $11\beta - HSD1$ oscillations. A one standard deviation increase in k_{9a} , for instance, would produce a 0.369 versus a 0.607 increase (in standard deviations) in the amplitude of $11\beta - HSD1$ in cluster 1 versus cluster 4. Similarly, β_6 through β_{10} are greatest in the right column of cluster 4; emphasizing the considerable impact of $11\beta - HSD2$ related parameter changes on its amplitude.

Parameters	Cluster 1	Cluster 2	Cluster 3	Cluster 4
$k_{8a}/\mu M \cdot h^{-1}$	0.582	0.673 ^{§¶}	0.712 ^{§Ω}	0.727 ^{¶Ω}
$k_{8p}/\mu M^{-1}$	1.269	1.762 [§]	1.010	1.776 [§]
k_{8d}/h^{-1}	2.818	2.610 ^{§Ω}	2.478 ^{§¶}	2.600 ^{Ω¶}
k_{9a}/h^{-1}	1.072	1.239	1.418 [§]	1.415 [§]
k_{9d}/h^{-1}	7.219 [§]	6.905 ^{§Ω}	6.704 ^Ω	5.900
$k_{10a}/\mu M \cdot h^{-1}$	7.117	7.936 [§]	8.345 ^{§Ω}	8.588 ^Ω
$K_{10a}/\mu M$	0.324 [§]	0.295 [§]	0.409 [¶]	0.410 [¶]
k_{10d}/h^{-1}	1.627 [§]	1.520 ^{§¶Ω}	1.429 ^{¶‡}	1.434 ^{Ω‡}
k_{11a}/h^{-1}	12.320 [§]	13.678 ^{§Ω}	14.902 [‡]	14.363 ^{Ω‡}
k_{11d}/h^{-1}	0.896 ^{§¶}	0.861 ^{§Ω‡}	0.872 ^{¶Ω‡}	0.818 ^{‡‡}
k_{12d}/h^{-1}	0.233	0.260 [§]	0.266 [§]	0.280

Table 1. Median values of each parameter arranged by cluster for the spring (baseline) model. ^{§¶Ω‡} Same symbol indicates no significant difference between clusters.

Coef	Cluster 1		Cluster 2		Cluster 3		Cluster 4	
	$11\beta - HSD1$ amp	$11\beta - HSD2$ amp						
β_1	0.375	0.207	0.420	0.131	0.350	0.132	0.652	0.219
β_2	0.503	-0.103	0.532	-0.231	0.722	-0.193	0.767	-0.066
β_3	- 0.313	-0.223	-0.368	-0.149	-0.340	-0.195	-0.573	-0.227
β_4	0.369	0.191	0.420	0.151	0.341	0.153	0.607	0.211
β_5	- 0.331	-0.198	-0.363	-0.137	-0.319	-0.166	-0.603	-0.227
β_6	0.285	0.526	0.246	0.456	0.200	0.656	0.155	0.686
β_7	- 0.004	0.217	-0.068	0.272	-0.051	0.257	-0.109	0.302
β_8	- 0.243	-0.457	-0.242	-0.415	-0.205	-0.638	-0.208	-0.727
β_9	0.278	0.519	0.252	0.435	0.202	0.665	0.181	0.718
β_{10}	- 0.243	-0.411	-0.229	-0.356	-0.210	-0.643	-0.224	-0.627
β_{11}	0.086	0.333	0.054	0.270	0.094	0.331	0.109	0.230

Table 2. Cluster regression coefficients for the spring model.

Increasing k_{12d} results in the greatest $11\beta - HSD1$ and $11\beta - HSD2$ amplitude increases in clusters 4 and 1 respectively. The higher amplitude oscillations of both enzymes during the winter (17A) agree with the representative profiles shown in Figure 12. As shown in Figure 18 and Table 1, transcriptional and translational rate constants governing enzyme dynamics were varying among the sub-populations. Despite the possession of equivalent phenotypes (comparable circadian $F_{periphery}$ profiles), the parameters regulating enzyme dynamics were substantially different. The lower production and higher enzyme degradation rate constants of cluster 1 promote lower amplitude $11\beta - HSD1$ and $11\beta - HSD2$ oscillations while those of cluster 4 result in elevated amplitudes. Normal $F_{periphery}$ circadian rhythms are maintained as low enzyme

levels and activity (cluster 1) are countered by lower cortisone degradation rates (k_{12d}) and high enzyme oscillations with higher degradation rates (cluster 4). In the case of cluster 1 for instance, a lower degradation rate prolongs the availability of cortisone which allow lower levels of $11\beta - HSD1$ to significantly contribute to cortisol's profile. Our multivariate multiple linear regression model (Table 2) indicated that the relationships between the predictor variables (rate constants) and the enzyme's amplitudes were cluster dependent with changes in the transcription and translation rate of $11\beta - HSD1$ predicted to have a greater impact on the amplitude of $11\beta - HSD1$ oscillations in cluster 4 versus cluster 1. The differing regression models generated for each cluster underscores the fact that similar phenotypic representations under baseline (unperturbed) conditions are possible despite the variability in parameters regulating enzyme dynamics.

Cortisol's ($F_{periphery}$) zenith (maxima) and nadir (minima) values following *in silico* HSD11B1 knockout (KO) were compared to their control levels. Figure 19 illustrates scatter plots of the zenith and nadir fold changes of cortisol. Fold change distributions for each cluster are shown in Figures 20 and 21. Fold change was computed as shown below as the ratio of cortisol's maxima or minima following knockout to the control case.

$$Fold\ Change = \frac{F_{peripheryZenith\ (or\ Nadir)HSD11B1KO}}{F_{peripheryZenith\ (or\ Nadir)Control}} \quad (34)$$

The maxima levels of *in silico* subjects in cluster 1 were generally unaffected by knockout with fold changes (x-axis) close to 1. Alternatively, the maxima of profiles in

clusters 2, 3 and 4 were diminished and exhibited fold change values less than 1. Augmented minima values following HSD11B1 KO were observed in clusters 2, 3 and 4 whereas diminished levels were predicted for the simulated subjects of cluster 1. Overall, the winter model (Figures 19A, 20A and 21A) displayed the most marked changes while the summer model (Figures 19C, 20C and 21C) exhibited the least. Figure 22 depicts the mean circadian profiles of $F_{periphery}$ under control (solid lines) and *in silico* HSD11B1 knockout conditions (dashed lines) for the spring model. Simulated subjects of cluster 1 (22A) were less affected by $11\beta - HSD1_{mRNA}$ knockout versus the other clusters as the amplitude of the rhythms were only slightly decreased. Despite comparable baseline $F_{periphery}$ oscillations among clusters, the activation of $F_{periphery}$ by $11\beta - HSD1$ is lowest in cluster 1 (23A); highlighting a lower dependency on $11\beta - HSD1$ activity for the maintenance of normal $F_{periphery}$ circadian rhythms.

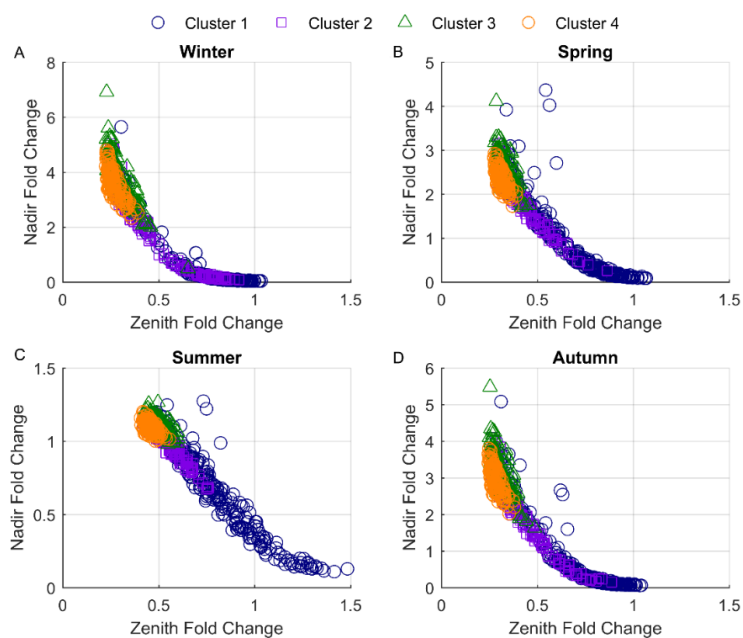


Figure 19. Cortisol fold change scatter plots.

Our *in silico* HSD11B1 knockout study yielded differing $F_{periphery}$ responses that varied by cluster association and season (Figure 19, 20 and 21). $11\beta - HSD1_{mRNA}$ transcription suppression resulted in the general elevation of cortisol's minima (nadir fold change > 1) and attenuation of its maxima (zenith fold change < 1) for simulated subjects of clusters 2, 3 and 4 while cluster 1 exhibited slight decreases in minima and maxima. The simulated knockout of HSD11B1 resulted in a loss of cortisol regeneration that reduced negative feedback to the central compartment. *ACTH* production subsequently increased as a compensatory response (Figure S23) which promoted elevation of cortisol's minima. This response was greatest for the simulated subjects of cluster 4. The greater fold change predicted for the winter model is due to seasonal augmentation of adrenal sensitivity to *ACTH*. Figure 22 depicts the mean $F_{periphery}$ profiles for both the control and HSD11B1 KO case for the spring model. These profiles further echo our previous observations whereby cortisol's circadian rhythm is only mildly affected for *in silico* subjects of cluster 1 (22A) and vastly attenuated in the others.

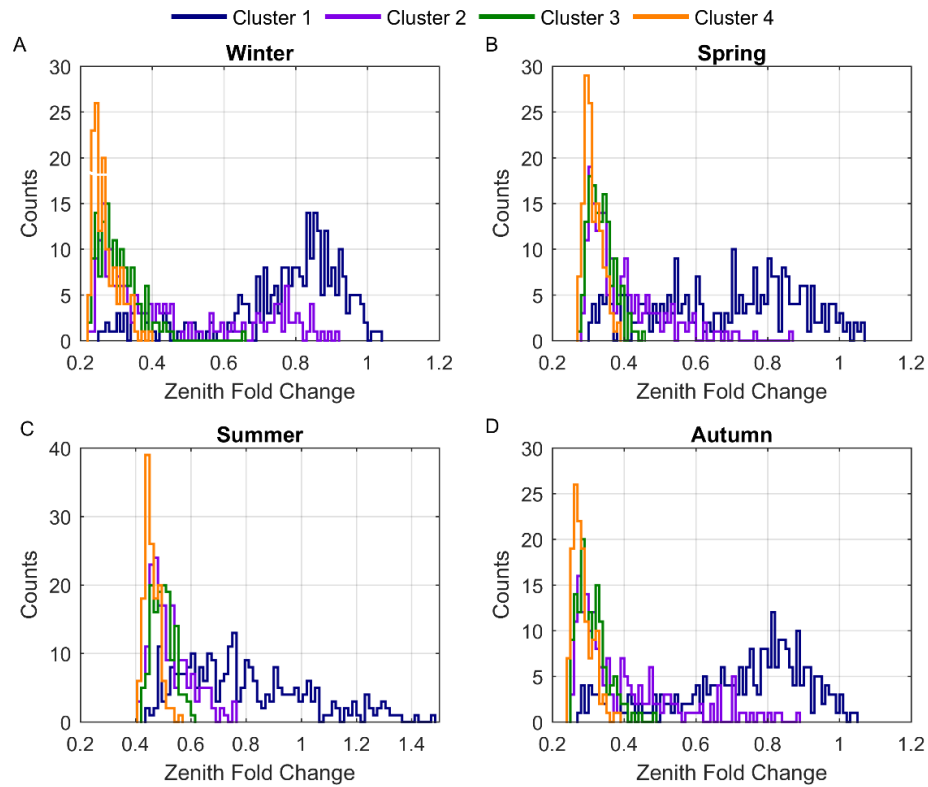


Figure 20. Distributions of zenith fold changes for each season and cluster.

Those of cluster 1 are less responsive to the loss of $11\beta - HSD1$ as their $F_{periphery}$ dynamics are less dependent on peripheral cortisol activation (Figure 23) and so the loss of HSD11B1 resulted in minimal change. Differing strain-dependent responses following HSD11B1 KO have been observed with reports of no change (Carter, Paterson et al. 2009), elevated basal corticosterone and *ACTH* levels (Harris, Kotelevtsev et al. 2001) as well as attenuated corticosterone levels (Paterson, Holmes et al. 2007).

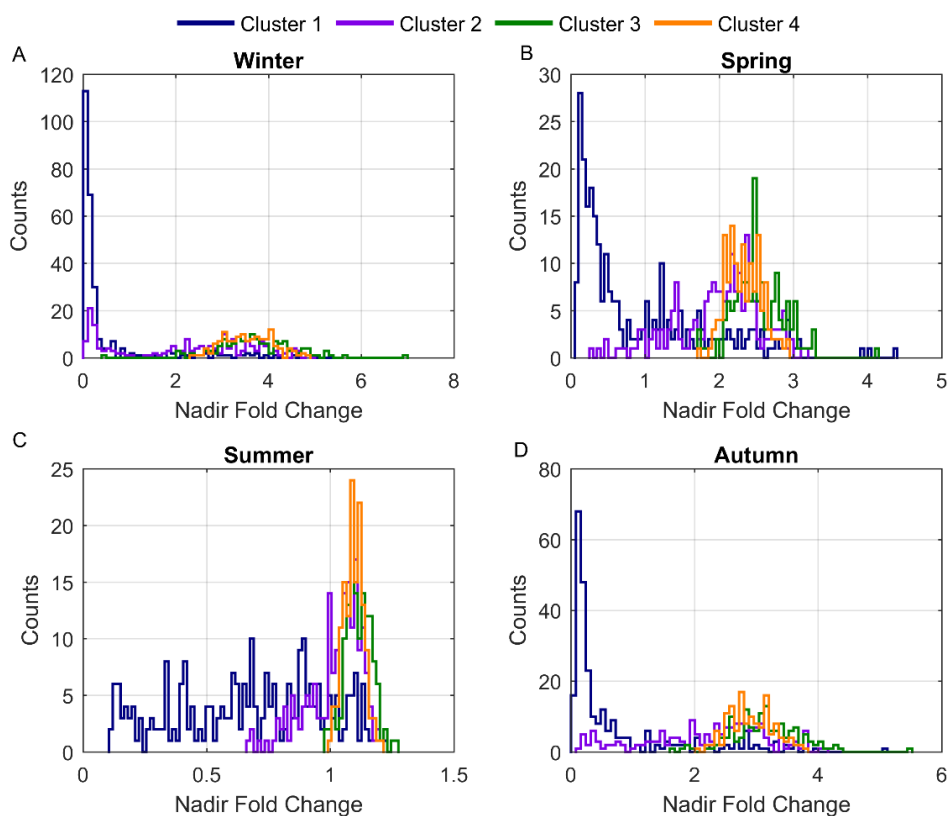


Figure 21. Distributions of nadir fold changes for each season and cluster.

Given our model's predictions, these differences in HPA axis responsiveness may be a result of genetic variations which may alter transcription, translation and degradation rates of enzyme transcripts and proteins. Additionally, these genetic variations may account for select groups of individuals being more susceptible to diseases as a result of differential HPA axis regulation, the ethnic specific incidence of HSD11B1 SNPs (Malavasi, Kelly et al. 2010) and also the contradictory associations between HSD11B1 SNPs and disease (Devang, M et al. 2016).

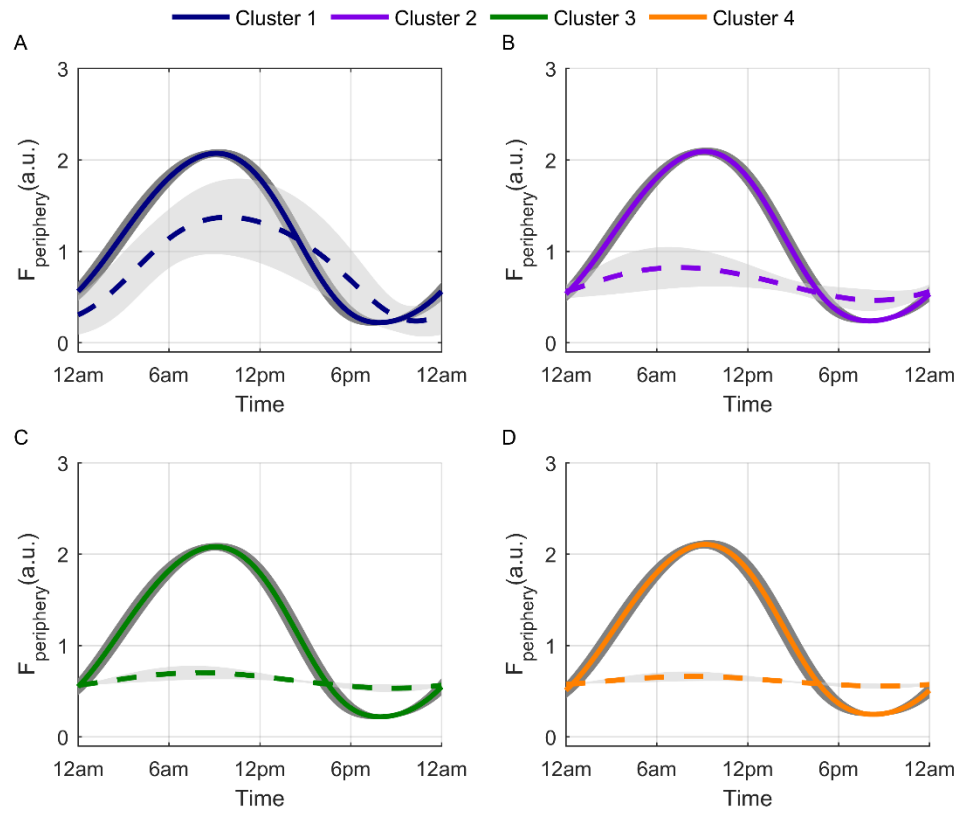


Figure 22. Comparison of $F_{\text{periphery}}$ circadian profiles of each cluster for the spring model.

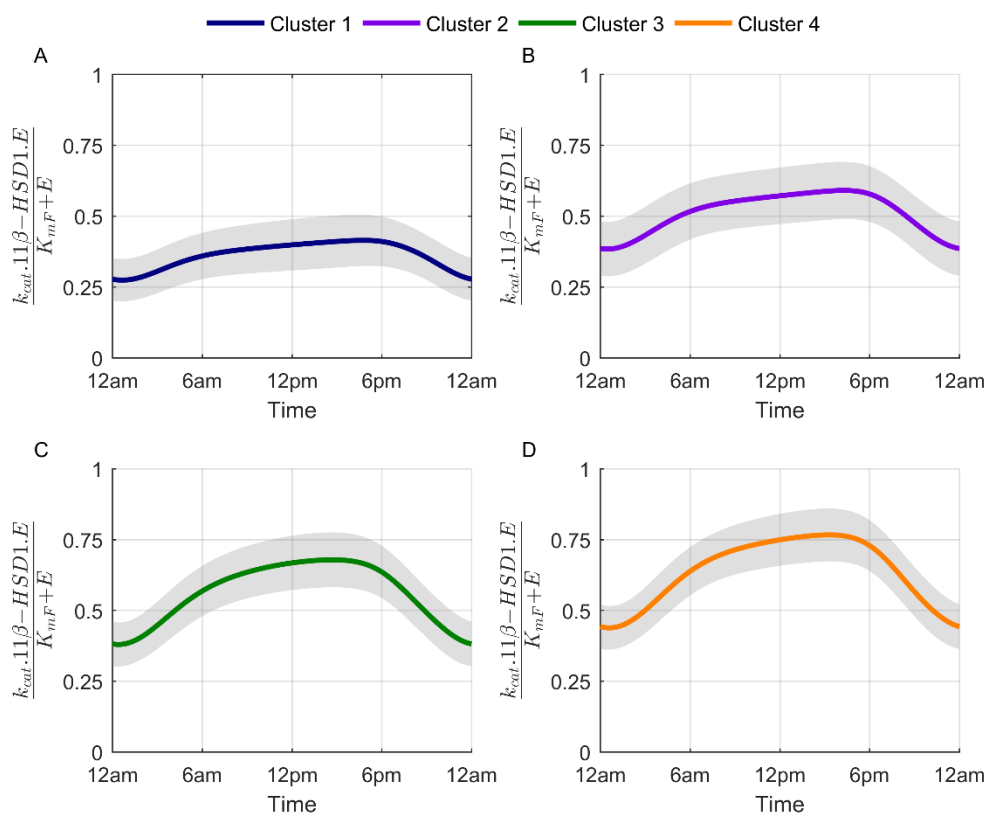


Figure 23. Cluster variation in $F_{periphery}$ activation for the spring (baseline) model under normal conditions.

As identified in Tables 1 and 2, the *in silico* subjects of cluster 4 exhibit the highest $11\beta - HSD1$ transcription and translation rates, are stimulated the strongest by the pro-inflammatory mediator and respond the greatest to changes in production rates and pro-inflammatory stimulation. These simulated subjects also display the greatest decrease in cortisol maxima following HSD11B1 KO. Based on our analyses, subjects with a cluster-4 type physiology would be more susceptible to systemic perturbation following the presentation of inflammatory triggers but may also be more responsive to therapeutic, $11\beta - HSD1$ inhibitory agents. These agents are currently being developed for the treatment of metabolic syndrome and obesity-related disorders (Anagnostis, Katsiki et al. 2013).

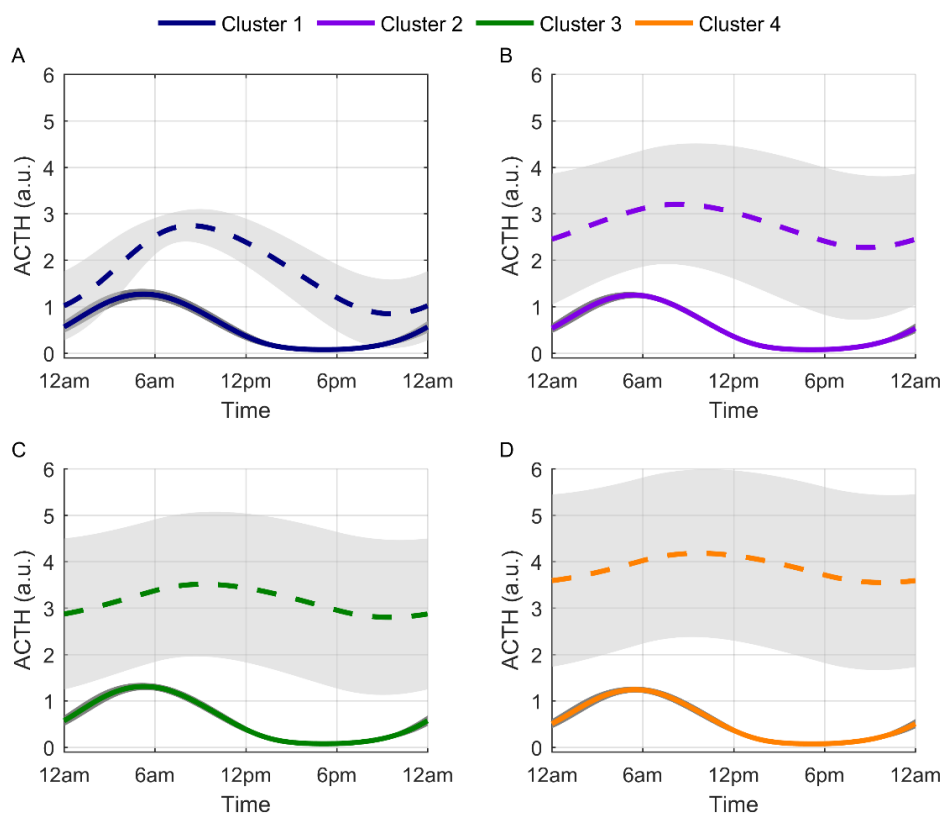


Figure S23. Comparison of ACTH circadian profiles of each cluster for the spring model.

3.7: Sensitivity Analysis

Both local and global sensitivity analysis approaches were employed to assess the impact of variations of the newly introduced, estimated parameters of Equations 28 to 32 on our model's representative output; cortisone (E). The impact of small parameter perturbations on our model's output was evaluated via local sensitivity analysis (Zi 2011). Using this approach, relative sensitivity indices (SI_{rel}) for a parameter (p_j) was determined as the ratio of the relative change of the state variable (y_i) to the relative change of the parameter value (Equation 35, (Scheff, Calvano et al. 2010, Rodriguez-Fernandez, Banga et al. 2012)). Using the amplitude and phase of cortisone (E) as our model's

representative output, parameters were varied by $\pm 10\%$ and SI_{rel} was computed as the average of the indices following an increase and decrease of a given parameter. A similar approach was employed by (Ihekweba, Broomhead et al. 2004).

$$SI_{rel}(p_j) = \frac{\text{Relative Change } y_i}{\text{Relative Change } p_j} = \frac{\partial y_i / y_i}{\partial p_j / p_j} = \frac{p_j}{y_i} \left(\frac{\partial y_i}{\partial p_j} \right) \quad (35)$$

In conjunction with the local sensitivity analysis technique, which analyzes the effect of each parameter individually while the others remained fixed, a global sensitivity analysis approach was pursued to evaluate the impact of each parameter while all others were simultaneously varied. A multi-parametric sensitivity analysis (MPSA) method (Choi, Hulseapple et al. 1998, Cho, Shin et al. 2003, Zi, Cho et al. 2005, Zi 2011, Tiemann, Vanlier et al. 2013) was employed with 65536 parameter sets generated via Latin hypercube sampling. Each parameter set was input into our system and numerical solutions were only retained if the periods of all the seasonal $F_{periphery}$ and $ACTH$ oscillations were 24 ± 0.25 hours. Using the filtered 20606 solutions, parameter sets were then classified by comparing its objective function value to a threshold numerically equal to the average of all the objective function values. The objective function for a varied parameter set (p_{set}) is the squared error between the observed (y_{obs}) and perturbed (y_{per}) output (Equation 36). Just as before, we considered the amplitude and phase of E to be our representative output with the observed values corresponding to those predicted using our nominal parameter values. For each season, a parameter set was classified as “acceptable” if its objective function value was less than the threshold and “unacceptable” otherwise. For a given parameter set (p_{set}), sensitivity was statistically

evaluated using the Kolmogorov-Smirnov statistic (SI_{KS}) which quantified the vertical distance between its two cumulative distributions that generated acceptable and unacceptable results. Just as for the local sensitivity analysis, the nominal parameters of Equations 28 to 32 were sampled but within a range of $\pm 50\%$ (versus the $\pm 10\%$ used for computation of SI_{rel}).

$$f_{obj}(p_{set}) = (y_{obs} - y_{per}(p_{set}))^2 \quad (36)$$

The numbered labels on the x -axis for Figures 24 through 27 correspond to the parameters of Table 3.

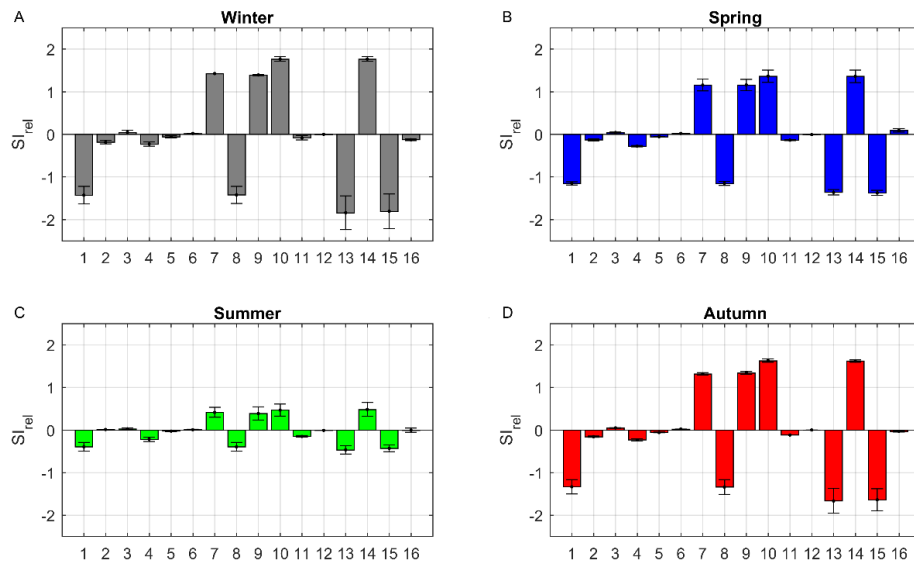


Figure 24. Local sensitivity indices with respect to the amplitude of E .

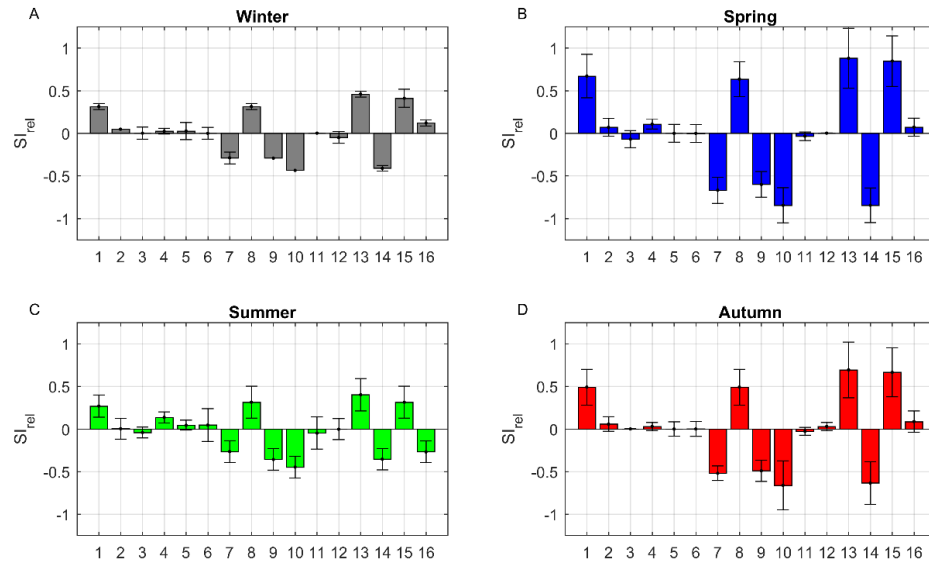


Figure 25. Local sensitivity indices with respect to the phase of *E*.

#	Parameters
1	k_{8a}
2	k_{8b}
3	K_{8b}
4	k_{8p}
5	k_{8c}
6	K_{8c}
7	k_{8d}
8	k_{9a}
9	k_{9d}
10	k_{10a}
11	K_{10a}
12	k_{10b}
13	k_{10d}
14	k_{11a}
15	k_{11d}
16	k_{12d}

Table 3. Reference numbers and their corresponding parameter names for sensitivity analysis bar graph plots.

For the local sensitivity analysis, the parameters with the highest sensitivity indices (SI_{rel}) were those directly regulating the production and degradation of the transcript and

protein levels of the enzymes which are k_{8a} (#1), k_{8d} (#7), k_{9a} (#8), k_{9d} (#9), k_{10a} (#10), k_{10d} (#13), k_{11a} (#14), and k_{11d} (#15). Increasing the transcription and translation rate constants (k_{8a}, k_{9a}) or decreasing the degradation constants (k_{8d}, k_{9d}) result in an elevation of $11\beta - HSD1_{mRNA}$ and $11\beta - HSD1$ which subsequently decreases the amplitude of E (Figure 24) which will peak later in the day due to a delay in the ascent of E production (Figure 25). Alternatively, increasing k_{10a} and k_{11a} or decreasing k_{10d} and k_{11d} will increase $11\beta - HSD2$ levels as well as its product E . This will therefore result in an increase in the amplitude of E (Figure 24) which will also be phase advanced due to rapid production (Figure 25). From a seasonal perspective, we predicted that the cortisone's winter amplitude (24A) and spring's phase (25B) were the most sensitive to local parameter changes. These differences are a consequence of the differing seasonal sensitivities to *ACTH* stimulation. Perturbations in the periphery ultimately regulate negative feedback to the central compartment and alter $F_{periphery}$ dynamics which subsequently impact dynamics in the periphery. The higher seasonal coefficient (n_{season}) for the winter model results in more pronounced amplitude changes. Typically, increases in production are accompanied by amplified but phase delayed oscillations. Due to the elevated winter sensitivity, however, an increase in secretion, for instance, results in a much steeper ascending phase that peaks earlier when compared to the spring and autumn models. The low summer adrenal sensitivity ($n_{season} = 0.75$) results in minimally altered outputs following local parameter perturbations.

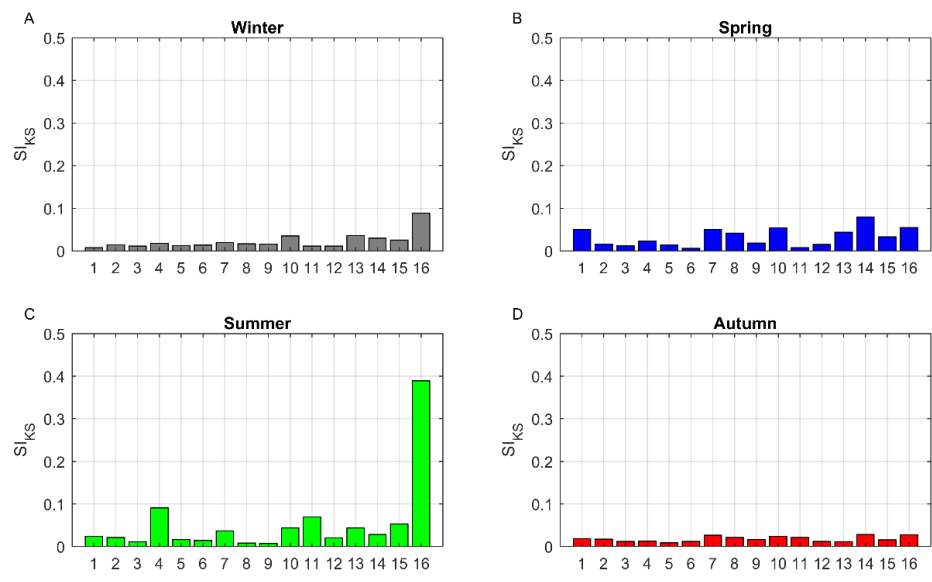


Figure 26. Global sensitivity indices with respect to the amplitude of E.

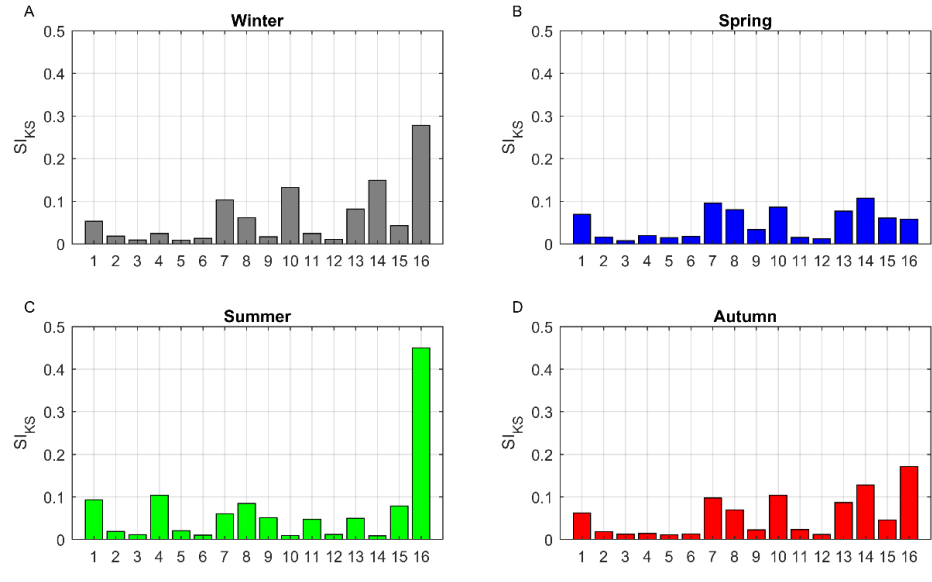


Figure 27. Global sensitivity indices with respect to the phase of E.

In contrast to the previous findings, the MPSA global sensitivity analysis revealed that our system’s output was only slightly sensitive to those identified as sensitive via the

local approach with a heightened summer sensitivity (26C, 27C) to k_{12d} (#16) variations. The contradictory sensitivity findings between the local and global sensitivity analysis approaches is quite commonly observed (Rodriguez-Fernandez, Banga et al. 2012, Kent, Neumann et al. 2013). Unlike local sensitivity analysis, the global approach evaluates the relative contributions of each parameter as well as the interactions between parameters (Zhang, Trame et al. 2015). This discrepancy between approaches may also be the result of a larger exploration of the parameter space i.e. $\pm 50\%$ for the global analysis and $\pm 10\%$ for the local approach. Global sensitivity analysis approaches provide insight of a model's robustness to parameter perturbations with robustness considered as an inverse measure of sensitivity (Kent, Neumann et al. 2013). The results indicate that our model is generally robust with higher sensitivities to transcription, translation and degradation rate constants. Overall, large changes in the cortisone's degradation rate constant would ultimately affect the amplitude and phase of its oscillations. The heightened sensitivity to k_{12d} perturbations in the summer model may be a consequence of its reduced adrenal sensitivity and greater dependency on $F_{periphery}$ activation and inactivation in the periphery for maintenance of baseline circadian $F_{periphery}$ and E rhythms. Although there has been a recent surge in development of $11\beta - HSD1$ inhibitors, sufficient knowledge of the inhibitors' impact on the HPA axis is lacking (Harno and White 2010). Based on our sensitivity analysis as well as our in silico knockout study, it is apparent that inhibition of $11\beta - HSD1$ would indubitably impact the HPA axis which may vary in a subject dependent manner. In the context of our model, subjects of cluster 1, with reduced sensitivity to changes in $11\beta - HSD1$ transcription rates (Table 2), may be the

least responsive to therapeutic treatment and HPA axis changes following $11\beta - HSD1$ inhibitor treatment.

3.8: Time scale Analysis

A time scale (or time constant) measures the time span over which significant changes occur in a given system, generally during relaxation following system perturbation. Within a biological network, it is possible that numerous reactions occur on vastly different time scales. Time dependent systems can be decomposed into processes that move in the time scale of interest, are so slow that they can be neglected or are fast and contribute to system equilibria (Heinrich and Schuster 1996). In simplifying a system, one can formally reduce a model's complexity by lumping variables that react in similar pathways and share comparable time scales into surrogate species (Whitehouse, Tomlin et al. 2004). The time scales of our model were approximated by computing the inverse of the eigenvalues of the Jacobian of the right hand side of Equations 1 to 32 as shown below in Equation 37. i corresponds to the i th system variable, λ_i the eigenvalue of the Jacobian and $|x|$ the modulus of x . A similar approach was employed by (Goussis and Najm 2006) to assess the core processes driving circadian oscillations. Instead of re-describing our system in a reduced form, we speculate on a means of model simplification based on the time varying time scales.

$$\tau_i = \frac{1}{|\lambda_i|}, \quad i = 1, \dots, 32 \quad (37)$$

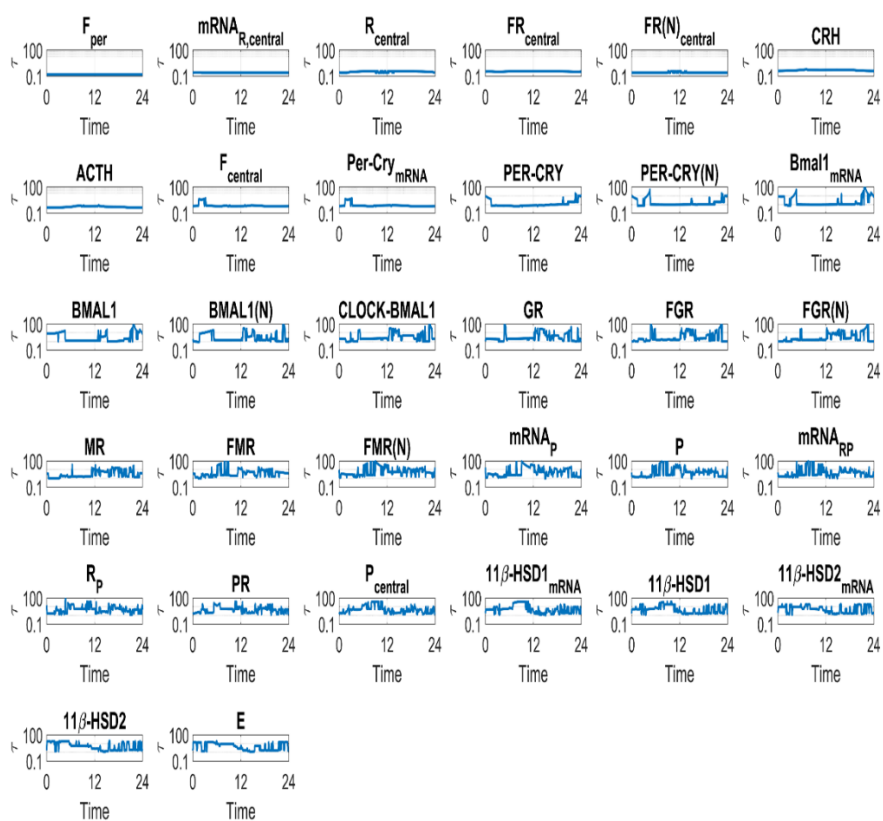


Figure 28. Diurnal variation of time-scales for the spring model.

Our detailed model in this chapter explores the emergent properties that arise out of complex interactions between the central and peripheral compartments. It is possible, however, to describe our model in a simplified form. Time-scale analysis revealed that numerous variables, that shared similar reaction pathways, evolved with comparable time scales (Figure 28). Groups of species acting through the same pathways with comparable time-scales share similar dynamics and so can be lumped together without compromising

the system's description (Whitehouse, Tomlin et al. 2004). While the implementation of a formal model reduction technique is outside the scope of this manuscript, our system can potentially be described using a central compartment consisting of three core variables: *ACTH*, *CRH* and $F_{periphery}$. The nuclear *PER* – *CRY* complex, *BMAL1* and *CLOCK* – *BMAL1* variables could characterize the peripheral clock dynamics and only the activated *FMR(N)* and *FGR(N)* complexes are needed to mediate cortisol signaling in the periphery. Pro-inflammatory dynamics can be described primarily with *P* while the active enzymes 11β – *HSD1* and 11β – *HSD2* with *E* (in conjunction with $F_{periphery}$) would be sufficient to describe the bioavailability of cortisol in the periphery.

The model presented integrates the effects of photoperiod, HPA axis regulation and 11β – *HSD* activity to predict how these influences interact to modulate cortisol dynamics. The photoperiod-induced seasonal predictions were qualitatively similar to experimental data. By sampling parameters regulating 11β – *HSD* dynamics, we were able to predict and hypothesize about the underlying mechanisms contributing to the experimentally observed, differential HPA axis responses following 11β – *HSD1* knockout in mice. Human sub-population differences in the regulation of 11β – *HSD* enzymes may alter enzyme functionality and render select groups more susceptible to HPA axis dysfunction following system perturbation. This may lead to the irreparable transition from normal to abnormal state. Our future work will involve the investigation of how these multi-tiered regulatory influences of cortisol dynamics respond to, and are affected by, chronic inflammatory triggers.

CHAPTER 4: Seasonal Entrainment of Physiological Oscillators

4.1: Entrainment of the peripheral molecular clock by a seasonally varying cortisol signal

4.1.1: Background

In our investigation of the putative role of cortisol in regulating the dynamics of downstream, physiological processes, we have considered synchronization primarily in the context of cortisol's ability to align the rhythm(s) of a representative unit subsystem (comparable to a single functional cell) to that of the external photoperiod. Cortisol secretion, entrained to the seasonally varying light-dark cycle, synchronized peripheral processes such as pro-inflammatory cytokine production via activation of the cortisol-glucocorticoid or cortisol-mineralocorticoid complexes ($FGR(N)$, $FMR(N)$) which subsequently induced or inhibited the expression of transcripts. Systemically, however, optimum physiological functionality is not contingent solely on the action of a single cell but is a consequence of the concerted interactions among a population of cells that respond to external inputs (Glass 2001). The output rhythm from the multicellular SCN, for instance, relies upon mutual synchronization among neuronal cells. Activity phase-shifting between individual SCN neurons consequentially affects the amplitude of the SCN's electrical activity and the strength of its entraining signal (Ramkisoensing and Meijer 2015). In wound repair, excessive formation of fibrotic connective tissue and

failed regeneration has been associated with asynchronous tissue remodeling following injury (Dadgar, Wang et al. 2014). This pathological molecular phenotype can be diminished with GC treatment.

It is well established that the peripheral molecular clock synchronizes various biological activities such as immune function (Keller, Mazuch et al. 2009), glucose homeostasis (Marcheva, Moynihan Ramsey et al. 2010) and steroidogenesis (Son, Chung et al. 2008). Despite the intrinsic ability to oscillate autonomously, the expression of the clock components are regulated by humoral signals such as glucocorticoids (Mohawk, Green et al. 2012). Administration of dexamethasone promotes the oscillation of *Bmal1*, *Cry1 – 2*, *Dbp*, *Npas2*, *Per1 – 3* and *Rev – Erba* in mesenchymal stem cells (MSCs) while oral administration of Cortef, a synthetic GC, induces phase shifts of *Per2 – 3* and *Bmal1* expression in peripheral blood mononuclear cells (PBMCs) (Cuesta, Cermakian et al. 2015). *In vitro* analysis of circadian gene expression in mouse fibroblast cells indicate that while these individual clock components oscillate robustly and independently in culture, a loss of synchrony among cells results in the dampening of the ensemble rhythm over time (Welsh, Yoo et al. 2004). Restoration of synchronous clock gene expression can be induced via pulsed dexamethasone treatment (Nagoshi, Saini et al. 2004). The systemic increase in *Per1* mRNA levels in the peripheral organs of mice subjected to acute restraint stress is believed to occur as a result of elevated stress-induced corticosterone levels which stimulate upregulation of the clock component via the glucocorticoid response element (GRE) (Yamamoto, Nakahata et al. 2005).

The dynamics of an array of central and peripheral processes are regulated by glucocorticoids and so homeostatic regulation of both the amplitude and rhythmicity of endogenous circulating glucocorticoids is critical for the maintenance of a healthy state (Chung, Son et al. 2011). Abnormal cortisol dynamics is associated with chronic conditions such as RA (Straub, Paimela et al. 2002, Perry, Kirwan et al. 2009), advanced stages of breast cancer (Sephton, Sapolsky et al. 2000), type 2 diabetes (Lederbogen, Hummel et al. 2011), cardiovascular disease mortality (Kumari, Shipley et al. 2011) and behavioral disorders such as post-traumatic stress disorder and depression (Sriram, Rodriguez-Fernandez et al. 2012). These diseased states are typically characterized by dampened, low-amplitude cortisol circadian profiles with high trough and low peak levels. The circadian sensitivity of peripheral clocks to glucocorticoid signaling in peripheral organs such as the heart, liver and kidney in mice (Balsalobre, Brown et al. 2000) suggests that variation in cortisol's rhythmic properties may alter its influence in regulating dynamics of the molecular clock as well as inter-connecting component processes. Blunted cortisol circadian profiles have been associated with circadian misalignment whereby endogenous circadian rhythms were not adequately synchronized with the 24-hour environmental/behavioral cycle (Morris, Purvis et al. 2016). In response to *in vivo* acute endotoxin administration, the uncoupling of circadian clock gene expression from the centrally entrained cortisol has been observed in peripheral blood leukocytes of human subjects following (Haimovich, Calvano et al. 2010). In the controlled laboratory by Morris et al., it was determined that short-term circadian misalignment resulted in increased blood pressure and inflammatory markers such as IL-

6, TNF- α and CRP. These experimental findings potentially explain why shift workers, with behavioral patterns uncoupled from the environment, are typically afflicted with hypertension (Ohlander, Keskin et al. 2015), cardiovascular disease risk (Mosendane, Mosendane et al. 2008) and inflammation (Puttonen, Viitasalo et al. 2011).

Synchronization of the internal circadian dynamics with external, environmental signals is therefore critical for health and fitness with misalignment leading to detrimental health outcomes (Harrington 2010). It has been theorized that the robustness of entrainment of an intrinsic oscillator increases with increasing zeitgeber strength (entraining signal) (Bordyugov, Abraham et al. 2015). Despite assuming a seasonally invariant intensity light profile, our seasonal model predicts significant changes in the circadian properties of cortisol. Given that cortisol acts as our putative entrainer, we investigated the role of a seasonally varying cortisol profile in synchronizing dynamics in the periphery.

4.1.2: Approach

Simulation of a population of cells was conducted by sampling the parameters of Equations 9 through 32 which describes the majority of the peripheral processes. Using Latin Hypercube Sampling (LHS) and a population of $n = 1000$ cells, intercellular variability was introduced by varying the aforementioned parameters by $\pm 10\%$ of their nominal values. The dynamics of $F_{periphery}$ (Equation 3), E (Equation 32) and the central compartment components (Equations 1, 4-8), the core systemic drivers, were assumed to be homogenous and regulated by the ensemble average of the peripheral

signals. As such, Equations 2, 3, and 32 were adjusted as shown below in Equations 2a, 3a and 32a. The coupling constant (k_c) of Equation 16 was also kept constant. For a given cell, the stimulatory influence of P on $Per - Cry_{mRNA}$ (Equation 16) and $11\beta - HSD1_{mRNA}$ (Equation 28) transcription was modeled to be autocatalytic and not the result of paracrine or endocrine signaling. Modulation of $11\beta - HSD1_{mRNA}$ expression and activity by pro-inflammatory cytokines occur via autocrine mechanisms (Cooper, Bujalska et al. 2001, Hardy, Filer et al. 2006) while CEBP- β , whose expression, localization and activity is controlled by autocrine signaling (Baer, Williams et al. 1998), is believed to mediate the induction of $Per1$ gene expression by IL-6 (Motzkus, Albrecht et al. 2002).

Modified equations accounting for cell population influence

$$\frac{dACTH}{dt} = \frac{k_{p2} \cdot CRH}{K_{p2} + FR(N)_{central}} (1 + k_{fp1} \cdot mean(P_{central})) - \frac{V_{d2} \cdot ACTH}{K_{d2} + ACTH} \quad (2a)$$

$$\begin{aligned} \frac{dF_{periphery}}{dt} = & \frac{k_{p3} \cdot ACTH^{n_{season}}}{K_{p3}^{n_{season}} + ACTH^{n_{season}}} (1 + k_{fp2} \cdot mean(P)) + \frac{k_{cat1} \cdot mean(11\beta - HSD1) \cdot E}{K_{mF+E}} - \\ & \frac{k_{cat2} \cdot mean(11\beta - HSD2) \cdot F_{periphery}}{K_{mE} + F_{periphery}} - \frac{V_{d3} \cdot F_{periphery}}{K_{d3} + F_{periphery}} \end{aligned} \quad (3a)$$

$$\frac{dE}{dt} = \frac{k_{cat2} \cdot mean(11\beta - HSD2) \cdot F_{periphery}}{K_{mE} + F_{periphery}} - \frac{k_{cat1} \cdot mean(11\beta - HSD1) \cdot E}{K_{mF+E}} - k_{12d} \cdot E \quad (32a)$$

Quantifying cell synchrony

Two metrics were used to quantify synchronization among the cellular component oscillations. Temporal profile synchronization was computed using R_{syn} (Equation 38) which compares the ratio of the variance of the mean oscillations to the mean variance of

each oscillator (Gonze, Bernard et al. 2005). F is the average profile of all oscillators, V_i represents the i th oscillator and n is the number of oscillators. ρ , the other synchronization index, is based on Shannon entropy and compares the distribution of the circadian metrics to a uniform distribution (Tass, Rosenblum et al. 1998). This metric is computed using Equation 39. N is the number of bins, S_{max} represents maximum entropy given by $S_{max} = \ln N$ and the distribution's entropy, S , is measured by $S = -\sum_{k=1}^N p_k \ln(p_k)$. p_k represents the proportion of cells in a given bin. For both metrics, a value of 1 indicates synchronization whereas 0 is indicative of the most asynchronous state.

$$R_{syn} = \frac{\langle F^2 \rangle - \langle F \rangle^2}{\frac{1}{n} \sum_1^n (\langle V_i^2 \rangle - \langle V_i \rangle^2)} \quad (38)$$

$$\rho = \frac{S_{max} - S}{S_{max}} \quad (39)$$

4.1.3: Seasonality of Entrainment and Intercellular Synchronization

Entrainment signals from P and cortisol ($FGR(N)$) converge on $Per - Cry_{mRNA}$ transcription regulation and so we use this clock component as our representative variable for our synchronization assessment. Figures 29 and 30 below depict the distributions of the periods (T) and phases (ϕ) of $Per - Cry_{mRNA}$ for the unentrained oscillators with both k_f and k_c , which describe the entrainment strength of P and $FGR(N)$ respectively (Equation 16), set to 0 for all cells. As is evident, the unentrained oscillators display a broad distribution of periods and phases with very low synchronization indices (ρ).

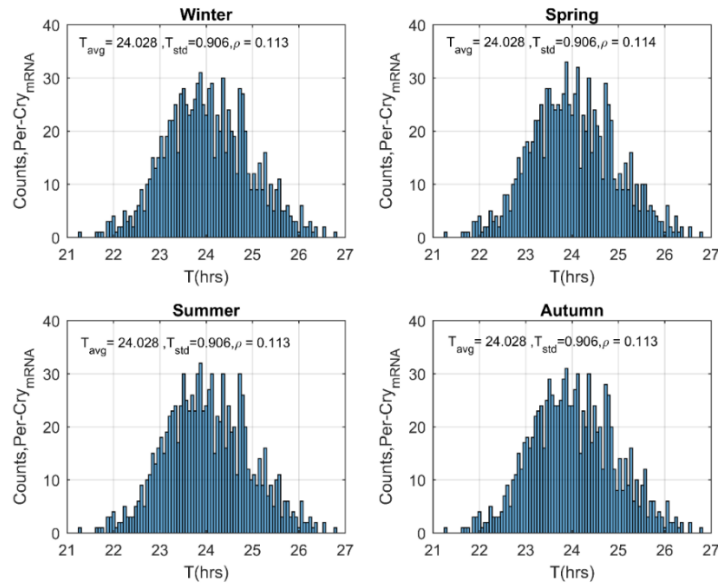


Figure 29. Seasonal distributions of $Per - Cry_{mRNA}$ periods for the unentrained oscillators.

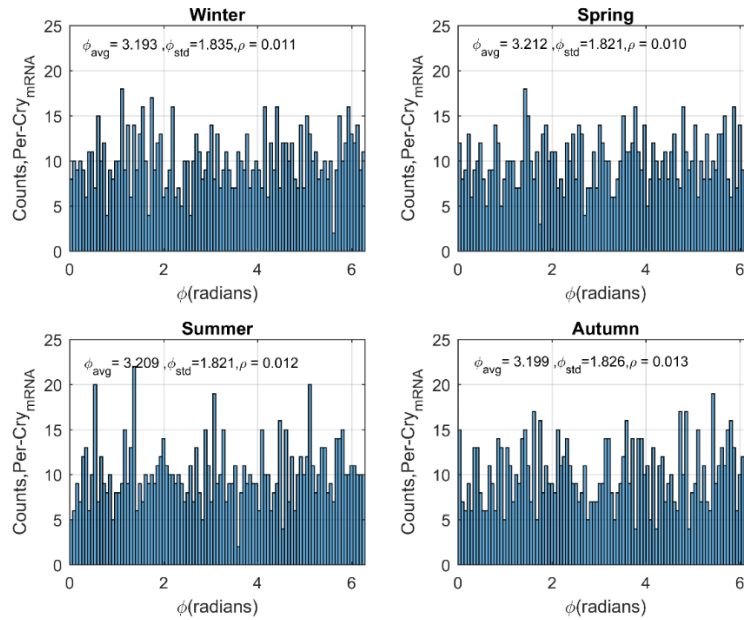


Figure 30. Seasonal distributions of $Per - Cry_{mRNA}$ for the unentrained oscillators.

In Figure 31, the circadian profiles of the unentrained $Per - Cry_{mRNA}$ for the population of 1000 cells are shown. The R_{syn} metric provides a similar quantification of

synchronization, indicating little to no synchrony among the $Per - Cry_{mRNA}$ oscillations of the cell population. As a consequence of the asynchrony, a dampened, low-amplitude ensemble average profile is observed (black plot). In contrast to the molecular clock, the population's oscillations of the pro-inflammatory mediator P are synchronized (Figure 32) with comparably large R_{syn} values for all seasons. The ensemble average amplitude of P is the most elevated in winter ($Amp_{<ens>} = 1.689$) while that of summer is the lowest with an $Amp_{<ens>}$ value of 0.671.

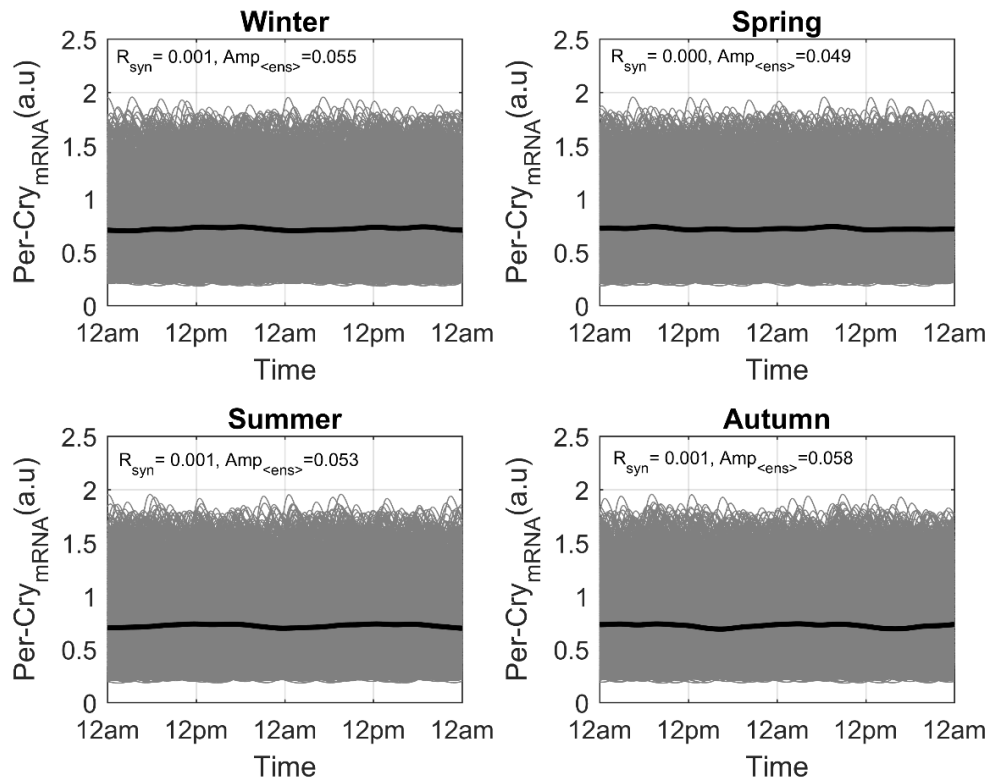


Figure 31. Seasonal circadian profiles of the unentrained $Per - Cry_{mRNA}$ oscillators.

Setting k_c to its non-zero nominal value and using the sampled parameter values for Equations 9 through 32 (including k_f) as previously described, simulations were reran to

explore the impact of entrainment on $Per - Cry_{mRNA}$ oscillations. Figure 33 reflects the distribution of periods of $Per - Cry_{mRNA}$ following entrainment. With coupling to $FGR(N)$ and P , entrainment is significantly augmented with the molecular clock adopting a period (~ 24 hours) equivalent to the external photoperiod. The summer season displayed the weakest entrainment to the systemic signal. The phase distributions of the entrained $Per - Cry_{mRNA}$ oscillations (Figure 34) is much broader than that of the period distributions with relatively low synchronization index, ρ . The spring, autumn and winter seasons are more synchronized than the summer season.

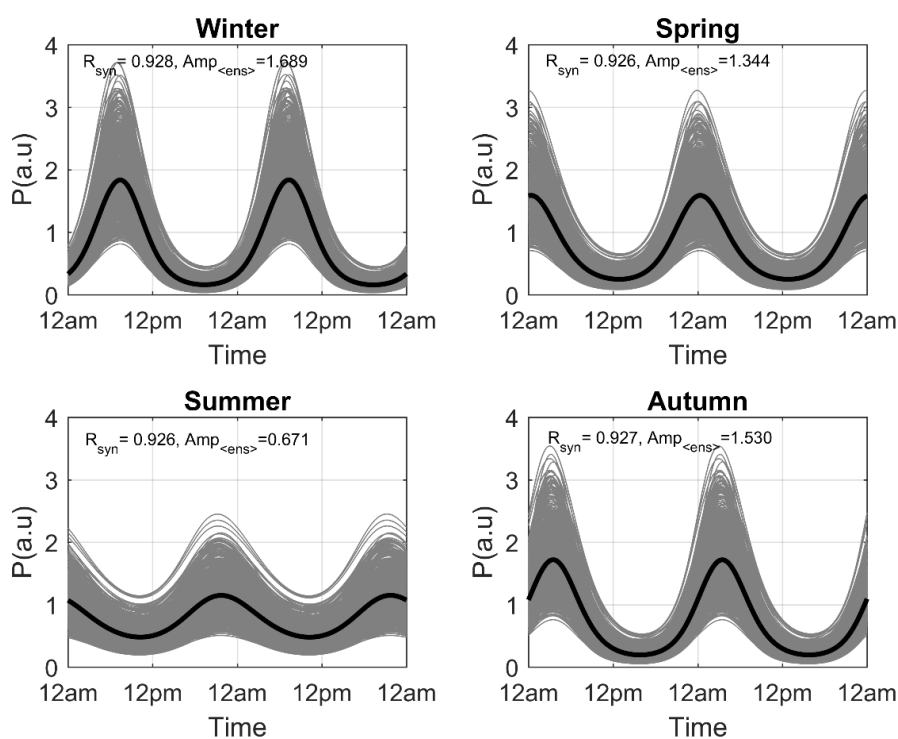


Figure 32. Seasonal circadian profiles of the pro-inflammatory mediator P with the unentrained molecular clock.

The distinct bimodal phase distribution (Figure 34) disappears as one progresses through autumn, spring and summer. With the exception of summer, a distinct sub-population of

phase delayed, low-amplitude $Per - Cry_{mRNA}$ oscillations among the cell populace is observed which is also evident in the oscillations of Figure 35. In line with the ρ parameter, the R_{syn} metric further testifies to the seasonal differences in synchrony with spring exhibiting the most synchronous oscillations and summer the most asynchronous. The synchronization among the temporal profiles of P is similar for the unentrained (Figure 32) and entrained (Figure 36) molecular clock simulations. No significant changes in the ensemble averaged amplitude of P was observed for the entrained and unentrained cases.

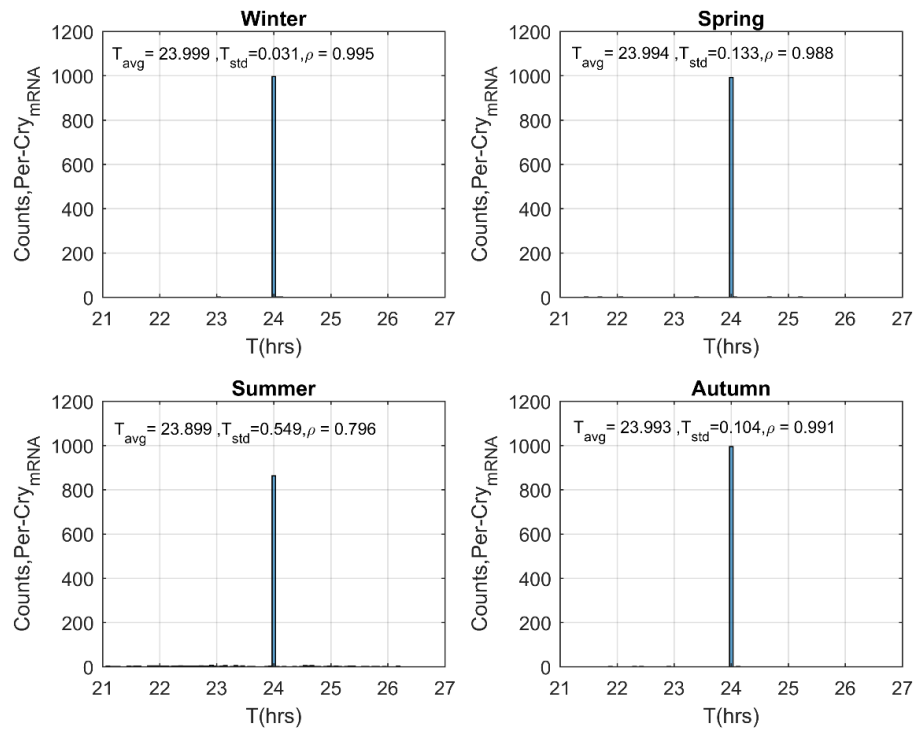


Figure 33. Seasonal distributions of $Per - Cry_{mRNA}$ periods for the entrained oscillators.

In the absence of systemic entraining signals, the $Per - Cry_{mRNA}$ components oscillate with an average period of 24 ± 0.9 hours (\pm SD) between 21 and 27 hours (Figure 29).

The approximate 24-hour mean, broad range of unentrained cell periods, and the prediction of damped ensemble oscillations as a consequence of individual oscillator asynchrony (Figures 30 and 31) are in agreement with experimental data (Nagoshi, Saini et al. 2004, Welsh, Yoo et al. 2004). With the implementation of entrainment, arbitrated by both the pro-inflammatory mediator P and activated cortisol-glucocorticoid receptor complex $FGR(N)$, $Per - Cry_{mRNA}$ oscillations for cells of all seasons adopted periods of oscillations identical or extremely close to the entraining signal's 24 hour period. As was observed in Figure 33, period distributions were much narrower distributed with smaller ranges and standard distributions following entrainment. Assessing the period, phase and temporal profiles of $Per - Cry_{mRNA}$, the ρ and R_{syn} metrics consistently identified summer as the season of greatest asynchrony (Figures 33 through 35). In contrast to the ρ indices found using the period of $Per - Cry_{mRNA}$ oscillations, the phases and circadian profiles of the spring season was predicted to be slightly more synchronized than the other seasons. Thus far, the terms entrainment and synchronization have been used interchangeably, however they differ subtly. Oftentimes, entrainment is described as the synchronization of endogenous oscillators to the external cycle (Glass 2001) (Golombek and Rosenstein 2010). As defined in (Hirschie Johnson, Elliott et al. 2003), entrainment quantifies the degree to which the free-running period of the peripheral clock conforms to the 24h period of the environment whereas synchrony measures how well rhythms coincide. Our definition can thus be refined to describe entrainment as a 1:1 synchronization of the circadian oscillator with the entraining signal i.e. for every cycle of cortisol (or photoperiod), the clock component also oscillates once. In this regard, all

our seasonal profiles were sufficiently entrained and synchronized to the environmental cycle despite displaying moderate inter-cellular synchronicity; quantified on the bases of their phase distributions and circadian profiles. We establish, therefore, that although entrainment is necessary, it is not sufficient for synchrony.

The *Per* – *Cry*_{mRNA} oscillations were strongly entrained to the environmental signal with the winter and summer models displaying the strongest and weakest entrainments to the environmental photoperiod (Figure 33). Both photoperiod and amplitude characterize the strength of a zeitgeber and its ability to robustly entrain (Bordyugov, Abraham et al. 2015). It has been hypothesized that the entraining power of a zeitgeber weakens when the fractions of light and dark deviate from a 1:1 ratio (Aschoff and Pohl 1978). The spring model, therefore, with a light profile described with equal hours of light and darkness (12L:12D) represents the optimum entraining photoperiod. Conceptually, one can consider light profiles with extended periods of light or darkness as approximate constant environmental signals and so would expect them to be weaker entrainers of circadian dynamics. Using a generic amplitude-phase-oscillator and square-wave entrainment signal, the greatest range of entrainment was predicted for a photoperiod parameter (κ) of 0.5 (Schmal, Myung et al. 2015). This parameter was calculated as the ratio of the duration of the light signal to total hours of the light/dark cycle. Experimentally, however, the identification of an optimum entraining photoperiod remains elusive. The activity of the southern flying squirrel can be entrained to light schedules ranging from 1 second to 18 hours a day (DeCoursey 1972) while intermittent light exposure is capable of entraining the human biological clock (Duffy and Wright Jr

2005). As discussed in (Schmal, Myung et al. 2015), while the strength of the zeitgeber may be photoperiod-dependent, the effective entraining intensity relies on the organism's sensitivity to the zeitgeber; an emergent property of the systemic network. Within the framework of our developed model, the effective intensity of the zeitgeber signal is manifested in the circadian characteristics of cortisol which is regulated by the seasonally varying photoperiod and adrenal sensitivity (modeled with seasonal coefficient: n_{season}). This seasonal coefficient simulates the documented increase in adrenal sensitivity to *ACTH* stimulation in the winter season (Amirat and Brudieux 1993) which is hypothesized to be effected via the autonomous nervous pathway (Otsuka, Goto et al. 2012).

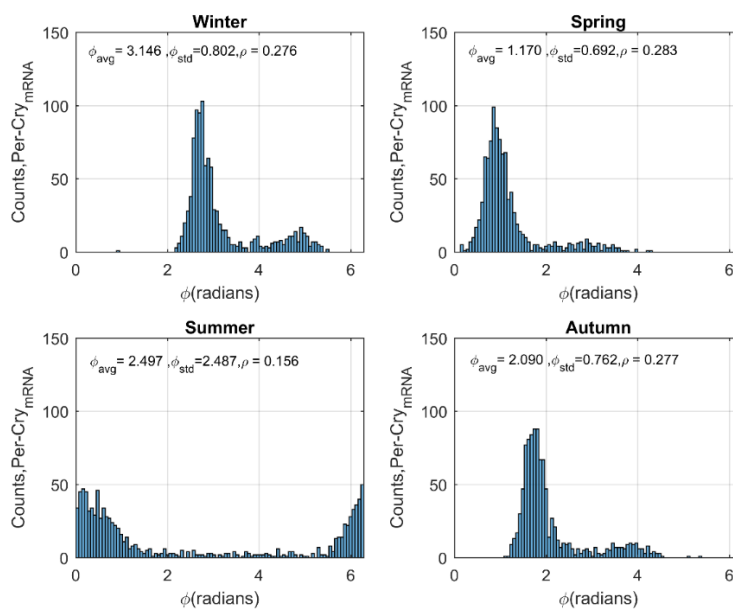


Figure 34. Seasonal distributions of *Per* – *Cry*_{mRNA} phases for the entrained oscillators.

Given the pivotal role of the SCN-sympathetic nervous system in regulating steroid synthesis (Ishida, Mutoh et al. 2005), the influence of SCN in regulating the time-of-day

variation of *ACTH*-induced corticosterone secretion (Sage, Maurel et al. 2002) and that the ensemble amplitude of SCN neuronal activity is augmented in shorter days (Schaap, Albus et al. 2003, Rohling, Wolters et al. 2006, VanderLeest, Houben et al. 2007, Meijer, Michel et al. 2010), this coefficient was the most elevated in the winter season.

Consequentially, the higher amplitude cortisol oscillations during the winter season (Figure 12) resulted in greater entrainment of *Per – Cry_{mRNA}* oscillations in the winter versus the summer. In conjunction with reduced entrainment, the *Per – Cry_{mRNA}* oscillations of the cells in the summer model were the least synchronous (Figure 35).

Unlike the extensively investigated SCN, documented findings on the effects of photoperiod in modulating entrainment and synchrony of peripheral oscillators are lacking. The transition from long to short days was reported to resynchronize mice SCN clock gene expression rhythms due to a phase advancement of the decline of clock gene expression (Sosniyenko, Parkanová et al. 2010). Liver *Per2* was reported to adjust in a similar manner to the SCN whereas *Rev – Erba* adjusted by lengthening its expression and activity with no discussion on changes in peripheral clock synchrony. In Siberian hamsters, photoperiod differentially regulated the expression of *Per1* in central and peripheral tissues with body temperature rhythms and feeding identified as additional pathways of peripheral clock regulation (Carr, Johnston et al. 2003). Due to high neuronal connectivity of the SCN and the ability of light to entrain peripheral clocks in an SCN perturbed system, it is speculated that alternative routes of entrainment may involve other hypothalamic and extra-hypothalamic nuclei (Husse, Eichele et al. 2015). Apart from the aforementioned, environmental factors such as light intensity and temperature

regulate circadian clock dynamics (Devlin 2002). It is expected that seasonal changes in these cues would also modulate synchronization of the molecular clock with the environment (Wikelski, Martin et al. 2008). While our developed model does not capture all the complexities associated with seasonal entrainment of peripheral clocks, it does underscore the shortcomings of a dampened cortisol profile in regulation dynamics in the periphery. Weaker entrainment of the peripheral circadian clock resulted in select cells exhibiting $Per - Cry_{mRNA}$ with periods greater and less than 24 hours for the summer season (Figure 33). This misalignment between the internal clock and external stimuli is a recently identified risk factor for metabolic disease (Li, Li et al. 2012) and can exacerbate cardiovascular disease progression (Takeda and Maemura 2011).

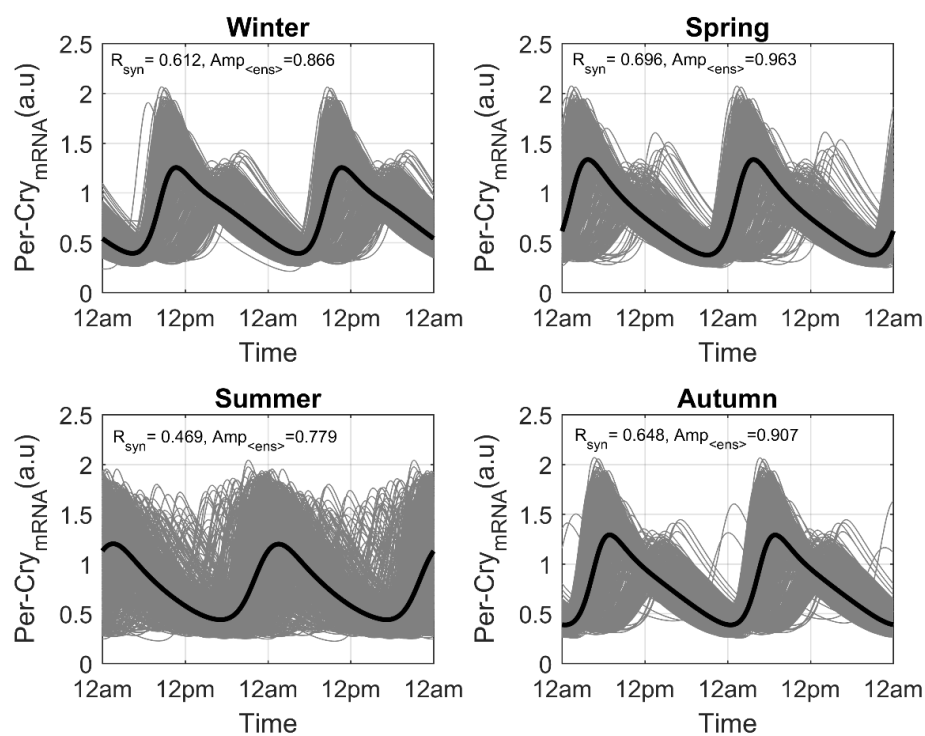


Figure 35. Seasonal circadian profiles of the entrained $Per - Cry_{mRNA}$ oscillators.

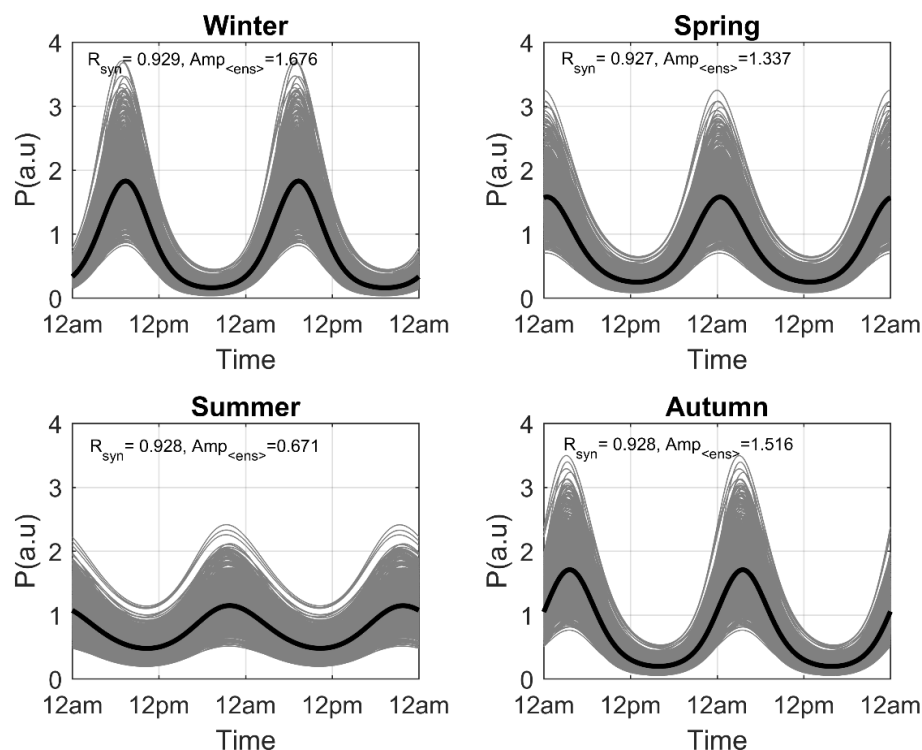


Figure 36. Seasonal circadian profiles of the pro-inflammatory mediator P with the entrained molecular clock.

Interestingly, the bimodal distributions of $Per - Cry_{mRNA}$ expression predicted for the winter, spring and autumn seasons have been observed experimentally. Following 6 days of oral administration of Cortef, a cortisol analogue, a significant bimodal rhythm of $PER3$ expression in PBMCs was found in a subset of cohorts (Cuesta, Cermakian et al. 2015). $PER3$ expression displayed two peaks; one in the morning and another in the early evening. In the experimental study, it was assumed that this bimodal response to GC treatment was the result of different cell populations present within the PBMCs (lymphocytes, monocytes and dendritic cells). Alternatively, it was speculated that 1 peak was a result of central clock control whereas the shifted peak was in response to GC administration. For our model, existence of the lower amplitude, phase-delayed

oscillations were a result of variability in the dynamics of *CLOCK* – *BMAL1*. Lower amplitude *CLOCK* – *BMAL1* oscillations, which predominate in the winter season, result in diminished inhibition of the *FGR(N)* entrainment term (Equation 16). As a consequence of this, the stronger entrainment resulted in a phase delay of *Per* – *Cry_{mRNA}* oscillations which then become aligned with the minima (and not the maxima) of the second entrainer, *P*. This diminished entrainment signal from *P* caused these delayed oscillations to exhibit attenuated amplitudes. Summer's flattened *FGR(N)* and *P* profiles precludes the occurrence of this phenomenon in the cell population. The similarity between the seasonal ensemble *P* profiles in the unentrained and entrained cases reflect the overwhelming influence of $F_{periphery}$ in entraining the pro-inflammatory mediator's dynamics.

4.2: Seasonal Entrainment of the Cell Cycle Oscillator

4.2.1: Background

Apart from the molecular clock, the cell cycle is another oscillator in the periphery that exhibits circadian rhythmicity. The cell cycle refers to the process leading to cell division and consists of four phases: The S phase, when DNA replication occurs, the mitotic (M) phase, and the G1 and G2 growth phases. Non-dividing cells exist in a quiescent state (G0) (Feillet, van der Horst et al. 2015). Cell cycle progression is regulated by a family of cyclin-dependent kinases (CDKs) that are activated following binding to cyclin proteins (Sherr 1994). The periodic production and degradation of

cyclins at specific times throughout the cell cycle result in oscillations of CDK activities; forming the basis for temporally coordinated cell cycle progression (Giacinti and Giordano 2006). Transition from G1 through the S phase is regulated by cyclins D, E, A and their associated kinases while cyclin B1 (with its allied kinases) facilitate the G2/M transition. The duration of the mammalian cell cycle lasts approximately one day (Hahn, Jones et al. 2009) and circadian variation in the expression of cyclins E, A, B, tumor suppressor protein p53, a mediator of G1 arrest, and the cellular marker for proliferation, Ki-67, has been documented (Bjarnason, Jordan et al. 1999). The progression of cell cycle phases at select times during the course of the day is believed to confer an evolutionary advantage. For instance, DNA replication at a time when metabolic or UV stressors are lowest could mitigate the risk for DNA damage (Destici, Oklejewicz et al. 2011).

It is believed that cell cycle timing is regulated in peripheral tissues by the molecular clock. Synchronization between the cell cycle and molecular clock has been determined experimentally in mouse fibroblast NIH3T3 cells. Cell division occurs approximately 5 hours before *Rev – Erba* peak expression (Bieler, Cannavo et al. 2014) with a robust 1:1 phase-locking between the two oscillators (Feillet, van der Horst et al. 2015). The *CLOCK – BMAL1* clock component has been implicated as a primary circadian entrainer of the cell cycle as it promotes transcription of the *wee1* gene which encodes for *Wee1* kinase; an inhibitor of the cyclin B/CDK-1 complex (Cardone and Sassone-Corsi 2003).

In conjunction with the molecular clock, glucocorticoids (GCs) can also regulate cell cycle dynamics by a diversity of mechanisms. Dexamethasone, a cortisol analog, can induce cell cycle arrest by repressing the expression of E2F-1 and c-Myc, transcription factors involved in the G2/S transition (Rogatsky, Trowbridge et al. 1997). Contrarily, dexamethasone can also rescue aberrant cell cycle rhythms (Dickmeis, Lahiri et al. 2007) and stimulate tumor cell proliferation (Zibera, Gibelli et al. 1991, Langeveld, Van Waas et al. 1992, Kawamura, Tamaki et al. 1998). The contradictory effects of GCs on cell cycle progression and growth displays a dose dependence whereby high doses of dexamethasone generally inhibits growth while lower concentrations stimulate it (Mattern, Büchler et al. 2007). These responses may be mediated by different receptors with the proliferative inductive effect arbitrated by the mineralocorticoid receptor (*MR*) and the inhibitory effect by the glucocorticoid receptor (*GR*) (Feng, Reini et al. 2013). The potency of GCs as an entrainer has been identified experimentally with pulsed dexamethasone treatment augmenting cell cycle synchrony and regeneration while suppressing inflammatory cytokine production of asthmatic epithelial cells following mechanical scrape-wounding (Freishtat, Watson et al. 2011). The increase in secretion of *TGF* – β as a result of mitotic asynchrony in epithelial cells (Alcala, Benton et al. 2014) is reduced with GC treatment.

The regulatory influences of GCs and the molecular clock on cell cycle dynamics provide a multitude of channels via which a population of heterogeneous cells could be synchronized. Variations in these entraining signals could result in mitotic asynchrony and subsequent exacerbated inflammatory responses. Expanding on our assessment of

cortisol's entrainment capabilities, we consider the direct and indirect (by way of the molecular clock) effects of seasonally varying cortisol profiles in coordinating cell cycle synchrony. Our aim is to identify the putative mechanisms that modulate cell cycle progression and to determine the circadian and seasonal influences that mediate the shift between synchronous and asynchronous states in a population of cells.

4.2.2: Approach

The model structure was updated to incorporate the cell cycle component. The modified schematic is indicated in Figure 37. Equations 40 through 45 below characterize the dynamics of the cell cycle regulatory components. These equations are a modified form of the skeletal model cell cycle developed by (Gérard and Goldbeter 2011) that now incorporates entrainment facilitated by cortisol and the molecular clock. It is assumed that the cyclin/Cdk complexes are already in an inducible state with the transcription, translation, translocation and complex formation processes neglected. The activated cyclin D/Cdk4-6 complex (*CYCD*, Equation 40) promotes G1 progression and subsequently activates the E2F transcription factor (*E2F*, Equation 41). *E2F* promotes the activation of cyclin E/Cdk2 (*CYCE*, Equation 42) and cyclin A/Cdk2 (*CYCA*, Equation 43). *CYCE*, which facilitates the G1/S transition, further reinforces *E2F* activation (Equation 41). The S phase, whose progression is moderated by *CYCA*, is exited following the *CYCA* mediated inhibition of *E2F* and stimulation of cyclin B/Cdk1 (*CYCB*, Equation 44) activity. *CYCB* which promotes the G2/M phase transition activates the cell-division cycle protein 20 (*CDC20*, Equation 45). With the accumulation of

CDC20, the activity of *CYCA* and *CYCB* is inhibited via phosphorylation and the cell exits the mitotic phase.

$$\frac{dCYCD}{dt} = v_{sd} \left(1 + \frac{k_{fd} \cdot FMR(N)}{K_{fd} + FMR(N)} \right) - V_{dd} \left(\frac{CYCD}{K_{dd} + CYCD} \right) \quad (40)$$

$$\begin{aligned} \frac{dE2F}{dt} = & V_{1e2f} \left(\frac{E2F_{tot} - E2F}{K_{1e2f} + (E2F_{tot} - E2F)} \right) \cdot (CYCD + CYCE) \left(1 - \frac{k_{fe2f} \cdot FGR(N)}{K_{fe2f} + FGR(N)} \right) - \\ & V_{2e2f} \left(\frac{E2F}{K_{2e2f} + E2F} \right) CYCA \end{aligned} \quad (41)$$

$$\frac{dCYCE}{dt} = v_{se} E2F - V_{de} CYCA \left(\frac{CYCE}{K_{de} + CYCE} \right) \quad (42)$$

$$\frac{dCYCA}{dt} = v_{sa} E2F - V_{da} Cdc20 \left(\frac{CYCA}{K_{da} + CYCA} \right) \quad (43)$$

$$\frac{dCYCB}{dt} = v_{sb} CYCA \cdot \left(1 - \frac{k_{cb} \cdot CLOCK - BMAL1}{K_{cb} + CLOCK - BMAL1} \right) - V_{db} Cdc20 \left(\frac{CYCB}{K_{db} + CYCB} \right) \quad (44)$$

$$\begin{aligned} \frac{dCDC20}{dt} = & V_{1cdc20} CYCB \left(\frac{Cdc20_{tot} - Cdc20}{K_{1cdc20} + (Cdc20_{tot} - Cdc20)} \right) - V_{2cdc20} \left(\frac{Cdc20}{K_{2cdc20} + Cdc20} \right) \\ & \quad (45) \end{aligned}$$

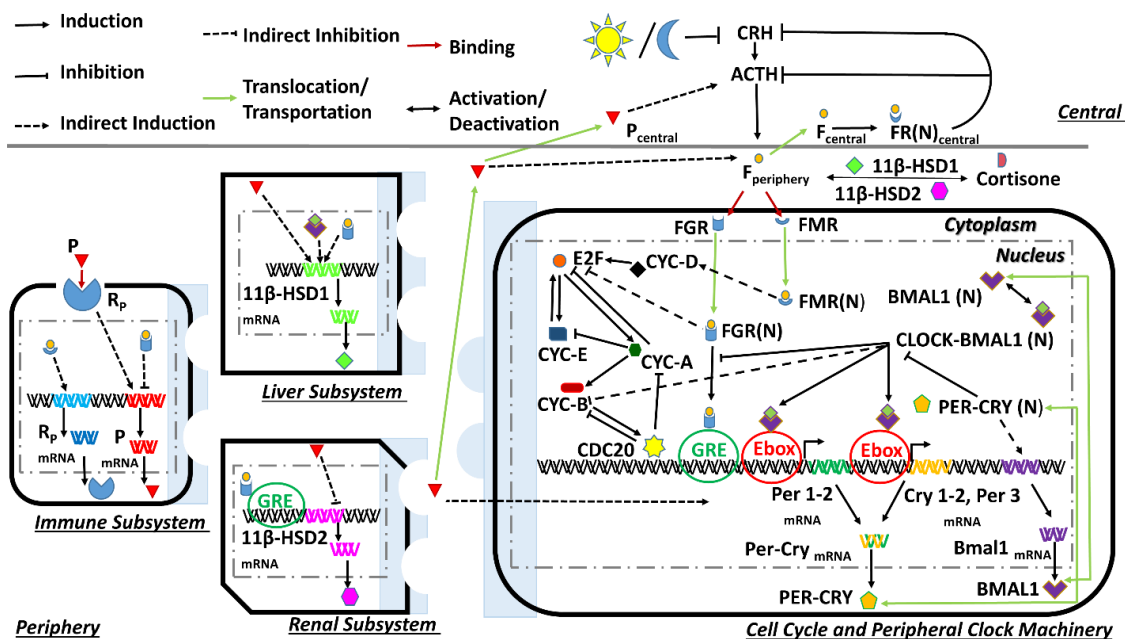


Figure 37. Modified model schematic incorporating the cell cycle component.

In assessing the response of fetal heart development to cortisol treatment, the mineralocorticoid receptor (*MR*) was found to promote proliferation whereas the glucocorticoid receptor induced apoptosis (Feng, Reini et al. 2013). Additionally, promotion of cell proliferation in rat mesangial cells via aldosterone treatment occur via *MR*-mediated activation of cyclin D and A (Terada, Kobayashi et al. 2005). Given that GC induces cell cycle arrest by inhibiting *E2F* (Rogatsky, Trowbridge et al. 1997), *FGR(N)* was modeled to inhibit *E2F* (Equation 41) and *FMR(N)* to stimulate cyclin D (Equation 40). The inductive effect of *CLOCK – BMAL1* on transcription of the *wee1* gene, which encodes for the inhibitor of the cyclin B/CDK-1 complex, was modeled by adding a *CLOCK – BMAL1*-mediated inhibitory term in Equation 44. In contrast to the original model, the growth factor variable (*GF*) which activates the transition from the quiescent (G0) to the G1 phase was omitted. This variable rapidly reaches a steady state

and so its contribution is assumed to be incorporated into the v_{sd} parameter which represents the basal activation rate of *CYCD*.

4.2.3: Model Construction and Validation

With the inclusion of the three entrainment terms (Equations 40, 41 and 44) and the removal of the activating influence of the GF variable, 7 new parameters were added to the cell cycle model (v_{sd} , k_{fd} , K_{fd} , k_{fe2f} , K_{fe2f} , k_{cb} and K_{cb}). Using the experimentally data from (Bjarnason, Jordan et al. 1999), these newly introduced parameters were optimized to decrease the sum of squared errors between the acrophases of the experimental and simulated spring model profiles for cyclins E, A and B. The optimized profiles are shown in Figure 38. The resultant simulated spring acrophases for the cyclin E/Cdk2, cyclin A/Cdk2, cyclin B/Cdk1 complexes were 14:12, 17:36 and 22:00 hours which is similar to the experimentally determined acrophases of 14:59, 16:09 and 21:13 hours for cyclins E, A and B respectively. Sustained oscillations should occur in the presence of sufficient growth factor (Gérard and Goldbeter 2011). As mentioned previously, the influence of GF is assumed to be inherent to the v_{sd} parameter which should be high enough to ensure the existence of oscillations in the absence of the entraining signals. To assess this, the entrainment inducing parameters (k_{fd} , k_{fe2f} and k_{cb}) were set to zero. As is evident in Figure 39, lower amplitude oscillations for all cyclin complexes are observed. The occurrence of high amplitude cell cycle rhythms in the presence of GCs in zebrafish (Dickmeis, Lahiri et al. 2007) renders

our cortisol entrained model qualitatively comparable to experimental findings.

Parameter values and their descriptions are included in Table A3 of the Appendix.

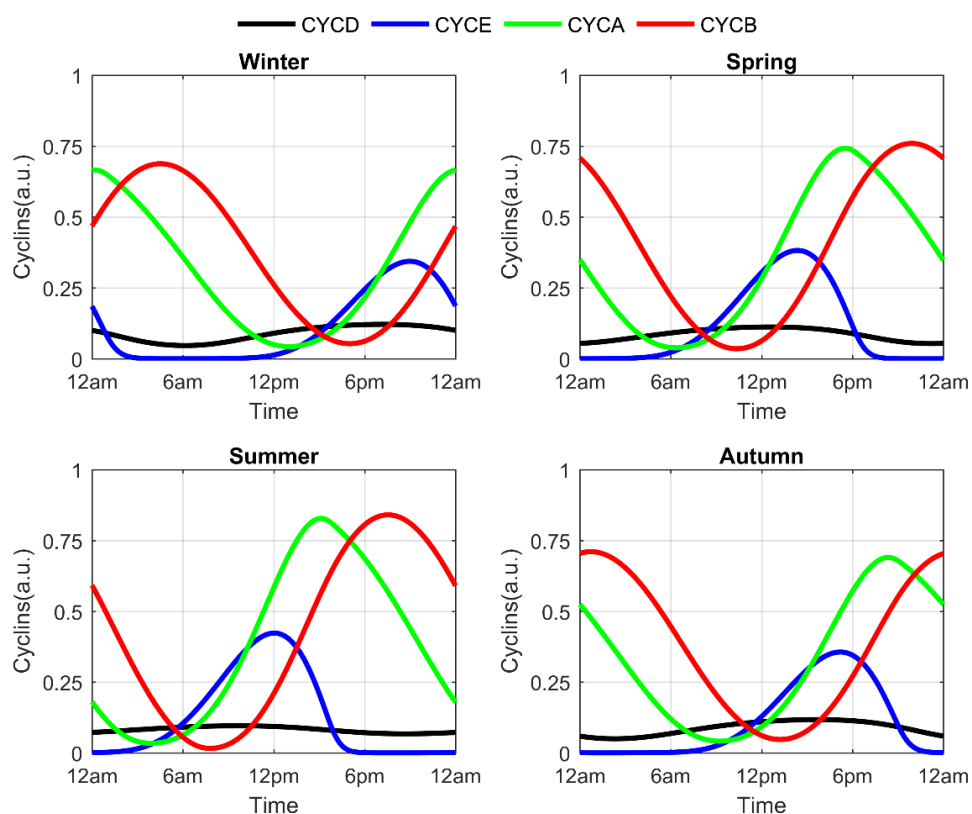


Figure 38. Seasonal circadian profiles for cyclin/Cdk complexes.

Following the attainment of optimized cyclin/Cdk circadian profiles, we again simulated a population of cells by sampling the parameters of Equations 9 through 32. This was done just as with the previous molecular clock simulations using Latin Hypercube Sampling with a population of $n = 1000$ cells and by sampling the parameters by $\pm 10\%$. Given that the phase of the molecular clock is inherited by daughter cells upon division (Nagoshi, Saini et al. 2004) and that the duration of the mammalian cell cycle is correlated within a lineage, it is hypothesized that cell cycle variability is due to

molecular clock variability (Pearl Mizrahi, Sandler et al. 2016). Given such, parameters characterizing cell cycle dynamics (Equations 40 through 45) were kept constant across the simulated cell population.

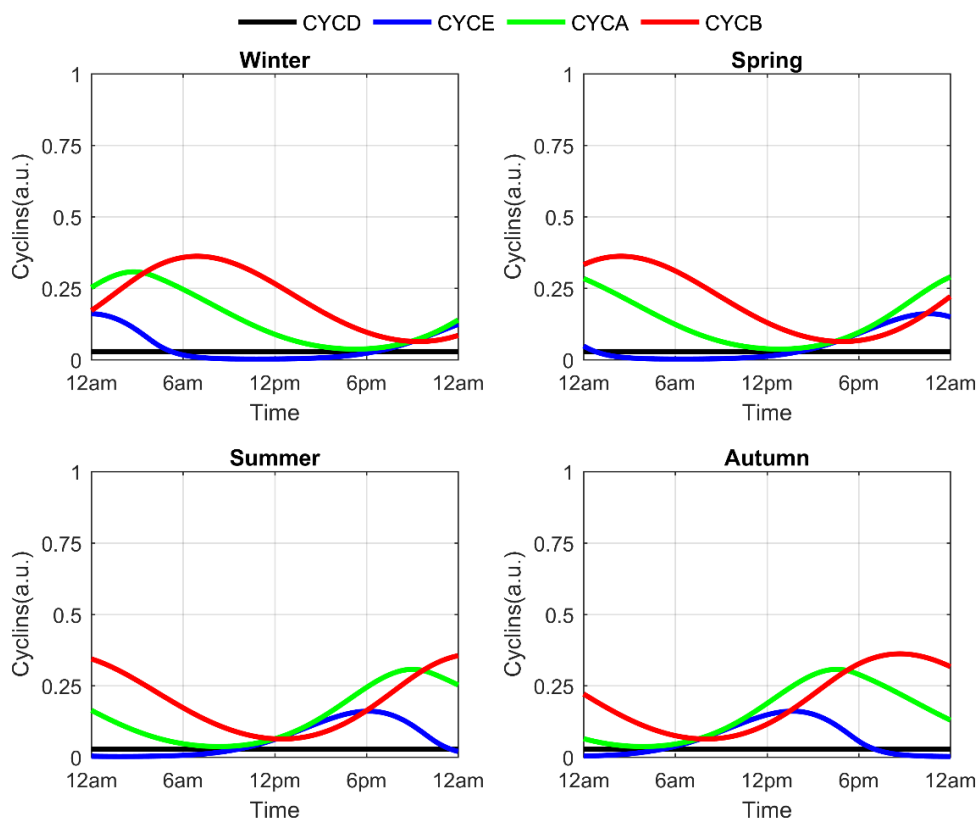


Figure 39. Seasonal circadian profiles for cyclin/Cdk complexes following the removal of the entraining signals.

4.2.4: Cell population cyclin oscillations and cell cycle mapping

Figure 40 below shows the circadian profiles of *CYCD*, *CYCE*, *CYCA* and *CYCE* for the spring season as well as the representative molecular clock components *Per* – *Cry_{mRNA}* and *CLOCK* – *BMAL1*. Despite the introduction of intercellular variability, the

cell cycle components oscillated robustly with a period approximating 24 hours for all seasons. Amplitude and phase differences were predicted for all seasons with phase advanced cyclin profiles in the summer and delayed profiles in the winter. Figure 41 shows seasonal *CYCD* oscillations for the cell population. Due to the stimulatory influence of cortisol (arbitrated by the $FMR(N)$ variable), low amplitude oscillations of *CYCD* were predicted for the summer model with its dampened cortisol profile. Alternatively, higher *CYCD* oscillations were predicted for the winter model with an amplitude fluctuation that parallels its cortisol profile.

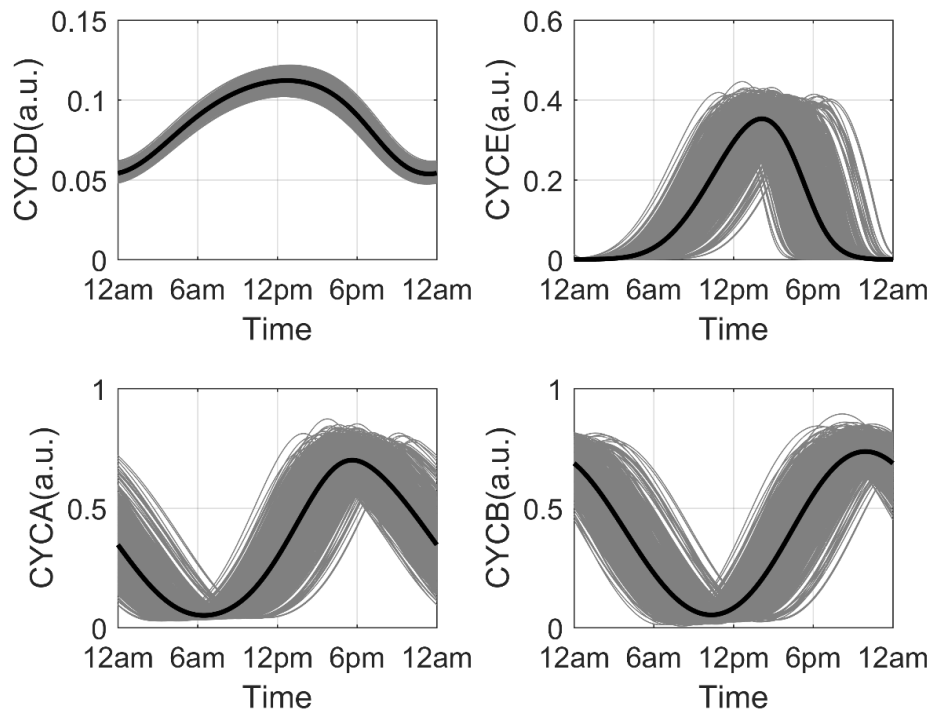


Figure 40. Representative circadian profiles of the molecular clock and cell cycle.

The transition between cell cycle phases are a result of adequate accumulation of cyclins (Neganova and Lako 2008). In the context of mathematical modelling, the relative

amplitude of cyclin oscillations has been used to predict transitions from one phase to another with large amplitude cyclin B oscillations used to estimate proliferating cells (Gérard and Goldbeter 2011). Due to seasonal and intercellular variability, the amplitude of the cyclin/Cdk complexes are diverse. Biologically, steady state concentrations of the cell cycle components result in quiescence. As is the case with our model, it becomes challenging to characterize this quiescent state in the presence of persistent oscillations. There exists, therefore, no one objective threshold that can be used to globally indicate the transition from one phase to another. In line with the methodology employed by (Toettcher, Loewer et al. 2009), it was assumed that all cells would progress through the cell cycle but that transition into a subsequent phase occurred when the corresponding cyclin/Cdk complex, for a given cell, exceeded a 90% threshold. With such an implementation, we ensure that all cells oscillate through the cell cycle for all seasons.

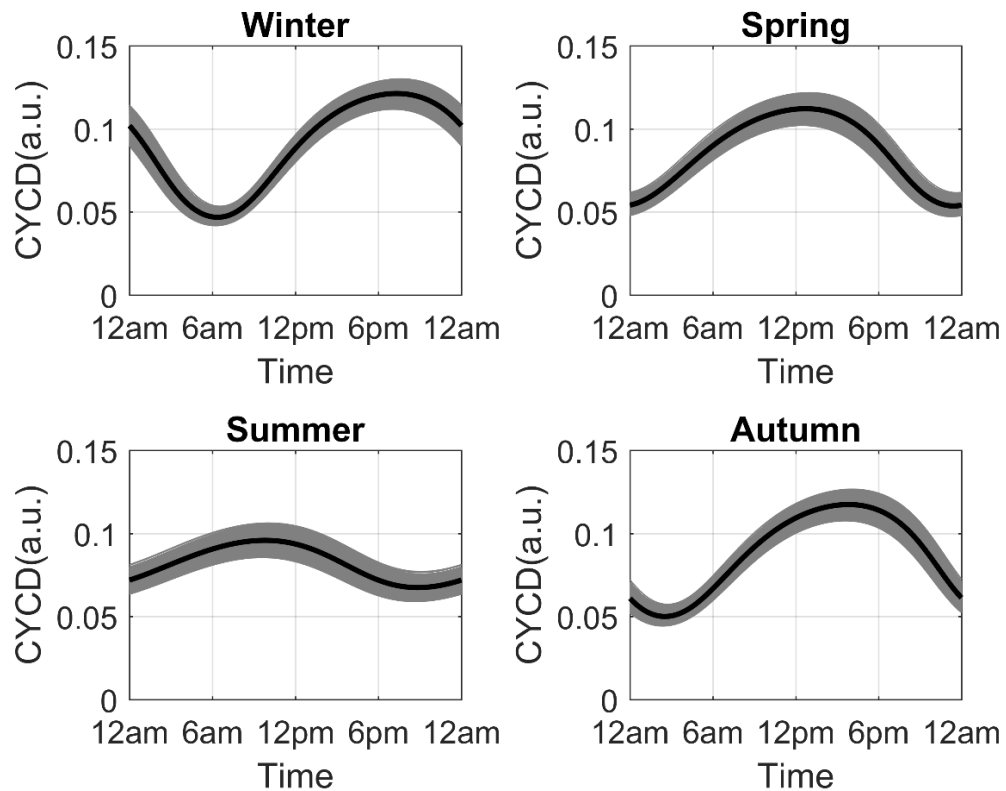


Figure 41. Seasonal circadian profiles of *CYCD*.

Intervals between successive cyclin/Cdk complex peak thresholds were used to determine the cell cycle phase of a given cell. Figure 42 summarizes the approach used to assign cell cycle phases. The late G1 phase (G1b) is initiated with increasing levels of *CYCD* and ends when levels exceed 90% of the maxima of *CYCD*. At this time, the cell enters the G1/S phase with transition into the S phase occurring above 90% of *CYCE* max levels. Termination of the S phase and initiation of the G2/M phase occurs at 90% of peak *CYCA* levels with the cell entering the G1 phase when the threshold of 90% of *CYCB* is surpassed. For some cells, there exists a dormant phase before *CYCD* levels begin ascending. This time window is assigned the G1a phase.

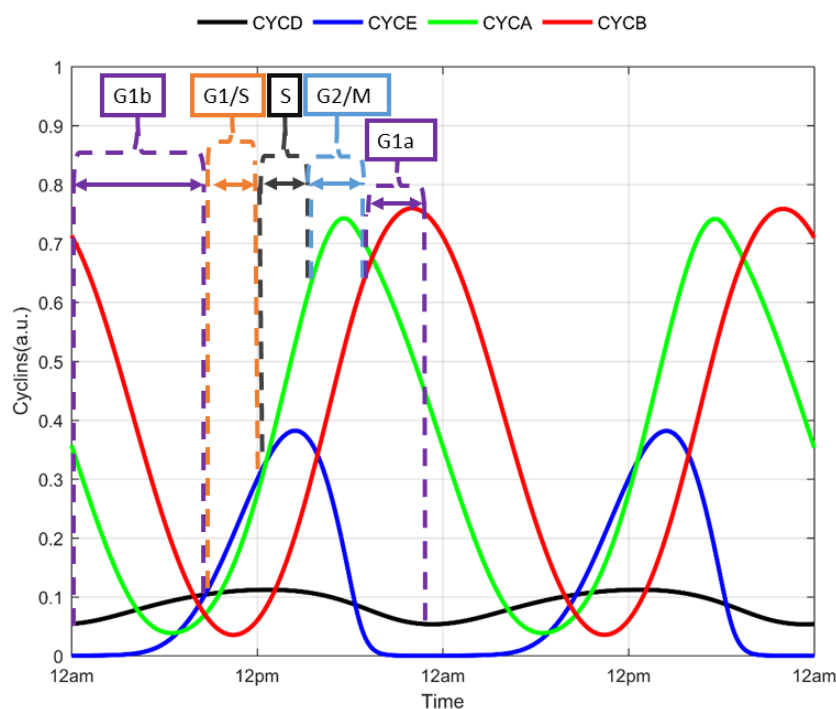


Figure 42. Cell cycle phase determination

Figure 43 shows the time duration distributions of cell cycle phases for the spring model. For all seasons, the total duration of the cell cycle was on the order of 20 hours which is consistent with the findings by (Hahn, Jones et al. 2009). Although the total duration of the cell cycle was seasonally invariant, there were seasonal differences in the time spent in select phases. In the summer model, for instance, the average duration of the G1 phase was 7.624 hours while the average duration of the G1/S phase was 6.270 hours. The shorter duration G1 phase was compensated with a prolonged G1/S phase. Compensatory changes in cell cycle phases has been observed in rat-1 fibroblasts induced to overexpress cyclin D1 and E (Resnitzky, Gossen et al. 1994). In this study, a shorter duration G1 phase was followed by a compensatory lengthening of the S phase. Similarly, PC12 cells

treated with NGF (nerve growth factor) spend a prolonged time in the G1 phase but with a parallel reduction of time spent in the S phase (Hahn, Jones et al. 2009).

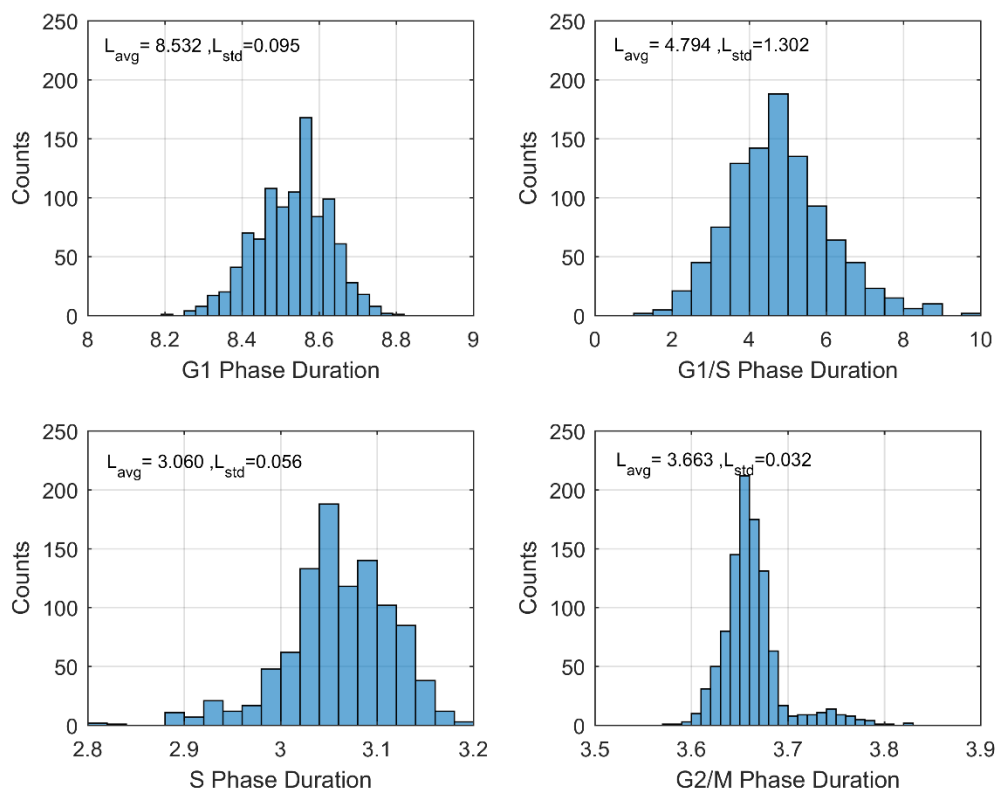


Figure 43. Spring distribution for duration of cell cycle phases.

To assess the circadian and seasonal changes in cell cycle synchrony, the fraction of cells occupying each phase of the cell cycle at each hour of the simulated day was determined. The bar plots in Figure 44 depict these variations in cell cycle phase occupancy. The plots indicate a time-of-day and seasonal variation in the cell cycle oscillations of the population. For the spring model, the G1b phase is predominantly occupied in the early hours of the morning with transition into the subsequent phases as the day progresses.

This G1b phase is later in the day for the winter model indicating an acrophase shift. This phase shift was a consequence of the seasonal variation in cortisol profiles.

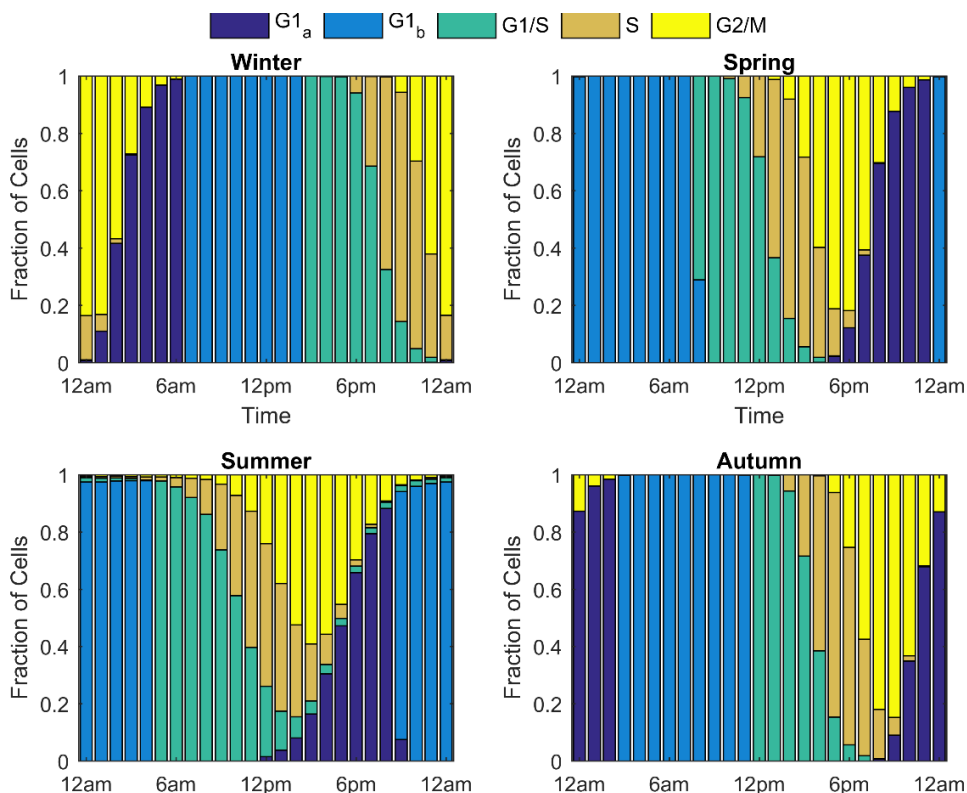


Figure 44. Bar graph depicting circadian and seasonal variations in cell cycle progression.

Circannual variations in the acrophases of cell cycle phases have been observed in mouse bone marrow (Laerum, Sletvold et al. 1988) as well as in the bone marrow and rectal mucosa of humans (Sothorn, Smaaland et al. 1995). The documented shift of the acrophases of the S and G2 phases from late night/early morning to later in the day is analogous to our model's predictions. The later initiation of these cell cycle processes as the seasons progress through winter is a consequence of the phase delayed cortisol rhythms. To quantify the degree of synchrony throughout the course of the day for each

of the modeled seasons, we again employed the synchronization metric previously used in the molecular clock entrainment simulations. The index has been modified to quantify synchrony at each hour of the day (Equation 46). $p_k(t)$ represents the proportion of cells in a given cell cycle phase at a select time point.

$$\rho(t) = \frac{S_{max}(t) - S(t)}{S_{max}(t)} \quad (46)$$

$$S(t) = -\sum_{k=1}^n p_k(t) \ln(p_k(t)), \quad n = 1, \dots, 1000, \quad t = 0:1:24 \text{ hours}$$

In Figure 45 below we superimpose plots of $\rho(t)$ and the $F_{periphery}$ versus the time of day for each season. The dashed line represents the circadian variation in cortisol's profile while the beaded plot represents the synchronization metric. The circadian variation of $\rho(t)$ is congruent with the cell cycle phase progression depicted in the bar plots of Figure 44. In the early morning of the winter model, for instance, there is trough in cell cycle synchrony at 2 am corresponding to more cells occupying the G1a phase at this time. The sharp decrease in synchrony at 8 am in the spring model is a consequence of an increase in the transition of cells into the G1/S phase. Overall, the winter model displayed the greatest consistency in cell cycle synchrony throughout the day with summer exhibiting the lowest. Figure 45 reflects the cortisol-dependence of the circadian rhythm of cell cycle synchrony. Lower levels of cortisol were associated with cell cycle asynchrony with cells being most synchronized with increasing levels of cortisol. Reports of circadian and seasonal oscillations, as well as the associated mediators of such variations, in cell cycle synchrony are limited. Variations in light exposure has, however, been found to modify the circadian rhythms of cell division in the esophagus of

melatonin-deficient ICR mice (Bogoeva, Mileva et al. 2004). In this study, the mitotic index (MI), or the ratio between the number of cells undergoing mitosis to those that were not, was assessed over the course of 24 hours. Mice exposed to constant darkness exhibited a pronounced diurnal MI variation versus those in constant light. The phase delayed MI rhythm observed for those in constant light was advanced with the exogenous administration of melatonin.

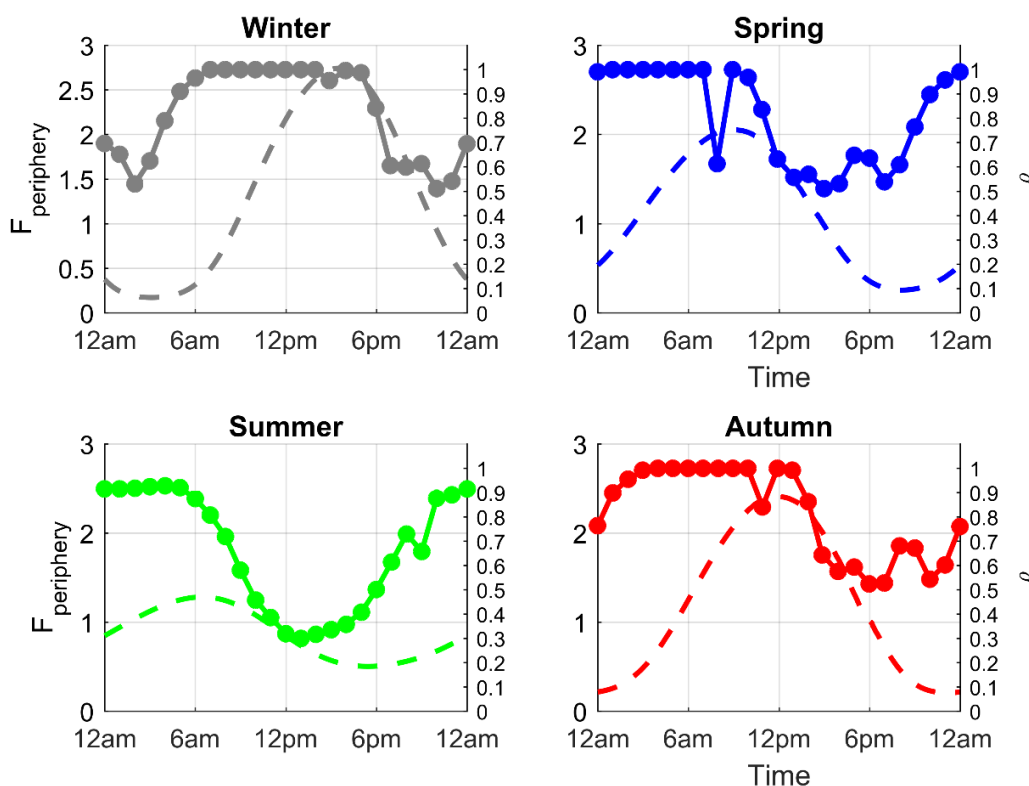


Figure 45. Seasonal and circadian variation in cell cycle synchronization and cortisol levels.

Assuming similar cellular proliferative potential for all conditions, the MI can be considered as a crude measure for cell synchrony. The acrophase shift in MI with melatonin injection implies that systemic signals can mediate *in vivo* synchronization of

the cell cycle. Pulsed glucocorticoid treatment has been found to restore regenerative synchrony and alleviate the inflamed state of asynchronous and proinflammatory asthmatic cells (Freishtat, Watson et al. 2011, Alcala, Benton et al. 2014). As discussed in (Freishtat, Watson et al. 2011), the pulsed GC signal is somewhat analogous to the circadian rhythm of cortisol's profile. The high-amplitude rhythm of the winter model, therefore, acts as a dominant entrainer to synchronize the cell cycle phase.

4.2.5: Seasonal Populations, Perturbations and Future Considerations

The seasonal variations explored thus far indicate a general augmentation of cell cycle synchronization in the winter season with the concomitant increase in the amplitude of cortisol's circadian rhythm. For the developed model, population dynamics were ignored with no consideration of the expansion or inhibition of a population size. Cell communication by means of the GJIC (Gap Junction Intercellular Coupling) is commonly considered when describing and modeling cell growth (Loewenstein 1979). It is believed that the transfer of signaling molecules such as Ca^{2+} , $cAMP$ and K^+ which traverse intercellular channels are integral in cell population regulation. Representing the intrinsic cell cycle oscillator of each cell in a population by a sinusoid with a unique frequency, it was predicted that coupling between biochemical oscillators promotes contact inhibition between cells with unregulated growth being a consequence of excessive intrinsic oscillation, synchronization and lack of communication between cells (Burton and Canham 1973). Seasonal variations in blood composition has been found in recent human studies (Dopico, Evangelou et al. 2015, Liu and Taioli 2015) with general increases in the

number of white blood cells and neutrophils in the winter-spring season.

Synchronization increases the number of cells representing a certain cell cycle phase (Juan, Hernando et al. 2002). The extended durations of enhanced cell cycle synchronization for a simulated day in winter season could potentially be translated to increase in cell numbers. The merit of this claim needs to be assessed in future works.

Our assessment of the seasonal variation in cell cycle synchronization focused primarily on baseline, non-stressed conditions. In this regard, the winter system was found to be the most synchronous with the summer model reflecting the opposite. With SD exposure, Siberian hamsters exhibit increases in GC secretion, the absolute number of circulating blood leukocytes, lymphocytes, T cells and natural killer cells (Bilbo, Dhabhar et al. 2002). Following exposure to restraint stress, the hamsters housed under short-day conditions exhibited an increase in delayed type-hypersensitive responses with a rapid redistribution of leukocytes. Simulating stress conditions, a cortisol dose of 10 nM was found to increase IL-6 expression as well as cell proliferation (at a later time point) of oral squamous cell carcinoma cell lines (OSCC) cells (Bernabé, Tamae et al. 2011). As a preliminary step, we simulated acute stress at every hour of the day for each season by instantaneously increasing cortisol levels by 0.25 au. The effect of this perturbation on the cell cycle was then investigated. Figure 46 shows the circadian variation in cell cycle synchrony following our acute stress simulation at the times of cortisol maxima for each season. The system was therefore perturbed at 4pm in winter, 9am in spring, 7 am in summer and 12 pm in spring. As a consequence of negative feedback, an increase in the maxima of cortisol results in the diminution of the minima

that follows. All seasons but summer showed prolonged disruptions in cell cycle synchrony following this perturbation. Due to the lower cortisol maxima, the negative feedback response was less pronounced than the other seasons and, as a result, the response (as compared to baseline) was minimal. This induced asynchrony may result in the pro-inflammatory molecular phenotype found in the asthmatic epithelial cell studies (Freishtat, Watson et al. 2011, Alcalá, Benton et al. 2014) and contribute to the stress induced inflammatory responses previously discussed.

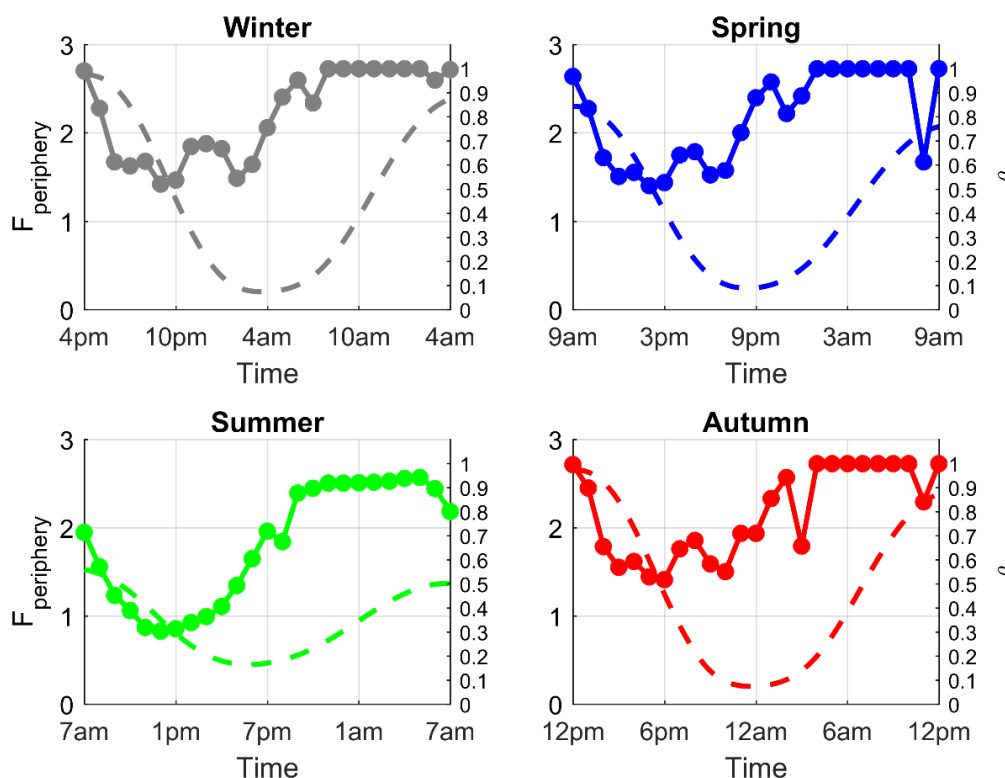


Figure 46. Seasonal differences in cell cycle synchrony following cortisol perturbation.

The model developed provides a preliminary structure that can be used to assess the cross-communication among numerous interacting sub-systems. With the developed

network, it is possible to incorporate coupling between the cell cycle and circadian oscillator. This can be accounted for with either the direct or indirect modeling of the influence of the tumor suppressor protein, p53, which regulates *Per2* expression (Miki, Matsumoto et al. 2013) and is regulated by *Per2* (Gotoh, Vila-Caballer et al. 2014). Additionally, the dynamical influence of the pro-inflammatory mediator, *P*, could be incorporated as NF- κ B, the mediator of pro-inflammatory signaling, modulates and is itself regulated by cell cycle (Ankers, Awais et al. 2016). With the inclusion of a few of these influences, more experimentally profound circadian and seasonal predictions are expected.

CHAPTER 5: Conclusions

The existence of seasonal immunological plasticity is extensively reported in literature with most animal studies focusing on the assessment of the role of melatonin in conferring the photoperiod-induced changes in immune function. Very few functional studies investigate the role of cortisol in regulating immune function seasonality. The semi-mechanistic mathematical model developed in this body of work provides a powerfully predictive platform and provides simulated results that are qualitatively comparable to a diversity of experimentally observed phenomena. The prediction of the predominant pro-inflammatory state in the winter with augmented levels of cortisol, $11\beta - HSD1$, P and exacerbated sensitivity to inflammatory triggers is in accordance with reported findings. Heightened expression of $11\beta - HSD1$ has been associated with numerous diseases and cortisol seasonality however experimental validation of its influence is inherently challenging. Our model suggests a prominent involvement of this enzyme in impairing HPA axis function and its potential to contribute to disease seasonality. The preliminary findings of the cell cycle synchronization module imply an increased synchrony of cell cycle progression in the winter season. This is a direct consequence of the higher amplitude entraining cortisol signal in the winter. The increased synchrony and prolonged perturbation following simulated stress could potentially be related to the observed increased leukocyte numbers and delayed inflammatory responses in winter. Future modeling efforts will incorporate the bidirectional coupling of the molecular clock with the cell cycle, consider the role of pro-inflammatory cytokines in regulating the cell cycle and also investigate the effect of cell-

cell communication. The work discussed within this thesis provides the framework from which new and exciting trajectories in immune function dynamics can be explored. It is anticipated that the knowledge gained herein could be used to predict the seasonality of disease as well as the diurnal and seasonal variations of core components associated with inflammatory disease. Furthermore, this understanding could ultimately be applied in the development of efficacious chronotherapeutic interventions for numerous inflammatory diseases.

REFERENCES

- Abasolo, L., A. Tobias, L. Leon, L. Carmona, J. L. Fernandez-Rueda, A. B. Rodriguez, B. Fernandez-Gutierrez and J. A. Jover (2013). "Weather conditions may worsen symptoms in rheumatoid arthritis patients: the possible effect of temperature." Reumatol Clin **9**(4): 226-228.
- Alam, T., M. R. An and J. Papaconstantinou (1992). "Differential expression of three C/EBP isoforms in multiple tissues during the acute phase response." J Biol Chem **267**(8): 5021-5024.
- Alcala, S. E., A. S. Benton, A. M. Watson, S. Kureshi, E. M. Reeves, J. Damsker, Z. Wang, K. Nagaraju, J. Anderson and A. M. Williams (2014). "Mitotic asynchrony induces transforming growth factor- β 1 secretion from airway epithelium." American journal of respiratory cell and molecular biology **51**(3): 363-369.
- Alfaidy, N., M. Blot-Chabaud, D. Robic, S. Kenouch, R. Bourbouze, J. P. Bonvalet and N. Farman (1995). "Characteristics and regulation of 11 beta-hydroxysteroid dehydrogenase of proximal and distal nephron." Biochim Biophys Acta **1243**(3): 461-468.
- Alikhani-Koupaei, R., F. Fouladkou, P. Fustier, B. Cenni, A. M. Sharma, H. C. Deter, B. M. Frey and F. J. Frey (2007). "Identification of polymorphisms in the human 11beta-hydroxysteroid dehydrogenase type 2 gene promoter: functional characterization and relevance for salt sensitivity." FASEB J **21**(13): 3618-3628.
- Allen, R., T. R. Rieger and C. J. Musante (2016). "Efficient Generation and Selection of Virtual Populations in Quantitative Systems Pharmacology Models." CPT: pharmacometrics & systems pharmacology **5**(3): 140-146.
- Almerighi, C., A. Sinistro, A. Cavazza, C. Ciaprin, G. Rocchi and A. Bergamini (2009). "1 α ,25-dihydroxyvitamin D₃ inhibits CD40L-induced pro-inflammatory and immunomodulatory activity in human monocytes." Cytokine **45**(3): 190-197.
- Amirat, Z. and R. Brudieus (1993). "Seasonal changes in in vivo cortisol response to ACTH and in plasma and pituitary concentrations of ACTH in a desert rodent, the sand rat (*Psammomys obesus*)." Comp Biochem Physiol Comp Physiol **104**(1): 29-34.
- Anagnostis, P., N. Katsiki, F. Adamidou, V. G. Athyros, A. Karagiannis, M. Kita and D. P. Mikhailidis (2013). "11beta-Hydroxysteroid dehydrogenase type 1 inhibitors: novel agents for the treatment of metabolic syndrome and obesity-related disorders?" Metabolism **62**(1): 21-33.

- Andrew, R., K. Smith, G. C. Jones and B. R. Walker (2002). "Distinguishing the activities of 11beta-hydroxysteroid dehydrogenases in vivo using isotopically labeled cortisol." J Clin Endocrinol Metab **87**(1): 277-285.
- Ankers, J. M., R. Awais, N. A. Jones, J. Boyd, S. Ryan, A. D. Adamson, C. V. Harper, L. Bridge, D. G. Spiller, D. A. Jackson, P. Paszek, V. Sée and M. R. H. White (2016). "Dynamic NF- κ B and E2F interactions control the priority and timing of inflammatory signalling and cell proliferation." eLife **5**: e10473.
- Aranow, C. (2011). "Vitamin D and the immune system." J Investig Med **59**(6): 881-886.
- Aschoff, J. and H. Pohl (1978). "Phase relations between a circadian rhythm and its zeitgeber within the range of entrainment." Naturwissenschaften **65**(2): 80-84.
- Baer, M., S. C. Williams, A. Dillner, R. C. Schwartz and P. F. Johnson (1998). "Autocrine signals control CCAAT/enhancer binding protein β expression, localization, and activity in macrophages." Blood **92**(11): 4353-4365.
- Balsalobre, A., S. A. Brown, L. Marcacci, F. Tronche, C. Kellendonk, H. M. Reichardt, G. Schütz and U. Schibler (2000). "Resetting of circadian time in peripheral tissues by glucocorticoid signaling." Science **289**(5488): 2344-2347.
- Barnes, P. J. (1998). "Anti-inflammatory actions of glucocorticoids: molecular mechanisms." Clin Sci (Lond) **94**(6): 557-572.
- Basu, R., R. J. Singh, A. Basu, E. G. Chittilapilly, C. M. Johnson, G. Toffolo, C. Cobelli and R. A. Rizza (2004). "Splanchnic cortisol production occurs in humans: evidence for conversion of cortisone to cortisol via the 11-beta hydroxysteroid dehydrogenase (11beta-hsd) type 1 pathway." Diabetes **53**(8): 2051-2059.
- Becker-Weimann, S., J. Wolf, H. Herzel and A. Kramer (2004). "Modeling feedback loops of the Mammalian circadian oscillator." Biophys J **87**(5): 3023-3034.
- Becker-Weimann, S., J. Wolf, A. Kramer and H. Herzel (2004). "A model of the mammalian circadian oscillator including the REV-ERB α module." Genome Inform **15**(1): 3-12.
- Bernabé, D. G., A. C. Tamae, É. R. Biasoli and S. H. P. Oliveira (2011). "Stress hormones increase cell proliferation and regulates interleukin-6 secretion in human oral squamous cell carcinoma cells." Brain, Behavior, and Immunity **25**(3): 574-583.
- Berson, D. M., F. A. Dunn and M. Takao (2002). "Phototransduction by Retinal Ganglion Cells That Set the Circadian Clock." Science **295**(5557): 1070-1073.

- Best, R., S. Nelson and B. Walker (1997). "Dexamethasone and 11-dehydrodexamethasone as tools to investigate the isozymes of 11 β -hydroxysteroid dehydrogenase in vitro and in vivo." Journal of Endocrinology **153**(1): 41-48.
- Bhat, G. K., M. L. Hamm, J. U. Igietseme and D. R. Mann (2003). "Does leptin mediate the effect of photoperiod on immune function in mice?" Biol Reprod **69**(1): 30-36.
- Bieler, J., R. Cannavo, K. Gustafson, C. Gobet, D. Gatfield and F. Naef (2014). "Robust synchronization of coupled circadian and cell cycle oscillators in single mammalian cells." Molecular systems biology **10**(7): 739.
- Bilbo, S. D., F. S. Dhabhar, K. Viswanathan, A. Saul, S. M. Yellon and R. J. Nelson (2002). "Short day lengths augment stress-induced leukocyte trafficking and stress-induced enhancement of skin immune function." Proc Natl Acad Sci U S A **99**(6): 4067-4072.
- Bilbo, S. D. and R. J. Nelson (2002). "Melatonin regulates energy balance and attenuates fever in Siberian hamsters." Endocrinology **143**(7): 2527-2533.
- Bjarnason, G. A., R. C. Jordan and R. B. Sothorn (1999). "Circadian variation in the expression of cell-cycle proteins in human oral epithelium." The American journal of pathology **154**(2): 613-622.
- Blackhurst, G., P. K. McElroy, R. Fraser, R. L. Swan and J. M. Connell (2001). "Seasonal variation in glucocorticoid receptor binding characteristics in human mononuclear leucocytes." Clin Endocrinol (Oxf) **55**(5): 683-688.
- Bodenstein, C., M. Gosak, S. Schuster, M. Marhl and M. Perc (2012). "Modeling the seasonal adaptation of circadian clocks by changes in the network structure of the suprachiasmatic nucleus." PLoS Comput Biol **8**(9): e1002697.
- Bogoeva, M., M. Mileva, K. Tsanova and E. Gabev (2004). "Circadian variations of cell division in mouse esophagus at LL and DD conditions and effects of daily melatonin treatment." Comptes Rendus de l'Academie Bulgare des Sciences **57**(1): 1: 97.
- Bolland, M. J., A. B. Grey, R. W. Ames, B. H. Mason, A. M. Horne, G. D. Gamble and I. R. Reid (2007). "The effects of seasonal variation of 25-hydroxyvitamin D and fat mass on a diagnosis of vitamin D sufficiency." Am J Clin Nutr **86**(4): 959-964.
- Bordyugov, G., U. Abraham, A. Granada, P. Rose, K. Imkeller, A. Kramer and H. Herzog (2015). "Tuning the phase of circadian entrainment." Journal of the Royal Society Interface **12**(108): 20150282.
- Bousquet-Melou, A., E. Formentini, N. Picard-Hagen, L. Delage, V. Laroute and P. L. Toutain (2006). "The adrenocorticotropin stimulation test: contribution of a

physiologically based model developed in horse for its interpretation in different pathophysiological situations encountered in man." Endocrinology **147**(9): 4281-4291.

Brown, R. W., K. E. Chapman, C. R. Edwards and J. R. Seckl (1993). "Human placental 11 beta-hydroxysteroid dehydrogenase: evidence for and partial purification of a distinct NAD-dependent isoform." Endocrinology **132**(6): 2614-2621.

Buren, J., S. A. Bergstrom, E. Loh, I. Soderstrom, T. Olsson and C. Mattsson (2007). "Hippocampal 11beta-hydroxysteroid dehydrogenase type 1 messenger ribonucleic acid expression has a diurnal variability that is lost in the obese Zucker rat." Endocrinology **148**(6): 2716-2722.

Burton, A. and P. Canham (1973). "The behaviour of coupled biochemical oscillators as a model of contact inhibition of cellular division." Journal of theoretical biology **39**(3): 555-580.

Cardone, L. and P. Sassone-Corsi (2003). "Timing the cell cycle." Nature cell biology **5**(10): 859-861.

Carr, A.-J. F., J. D. Johnston, A. G. Semikhodskii, T. Nolan, F. R. Cagampang, J. A. Stirland and A. S. Loudon (2003). "Photoperiod differentially regulates circadian oscillators in central and peripheral tissues of the Syrian hamster." Current Biology **13**(17): 1543-1548.

Carrillo-Vico, A., R. J. Reiter, P. J. Lardone, J. L. Herrera, R. Fernandez-Montesinos, J. M. Guerrero and D. Pozo (2006). "The modulatory role of melatonin on immune responsiveness." Curr Opin Investig Drugs **7**(5): 423-431.

Carter, R. N., J. M. Paterson, U. Tworowska, D. J. Stenvers, J. J. Mullins, J. R. Seckl and M. C. Holmes (2009). "Hypothalamic-pituitary-adrenal axis abnormalities in response to deletion of 11beta-HSD1 is strain-dependent." J Neuroendocrinol **21**(11): 879-887.

Castro, A., J. X. Zhu, G. R. Alton, P. Rejto and J. Ermolieff (2007). "Assay optimization and kinetic profile of the human and the rabbit isoforms of 11beta-HSD1." Biochem Biophys Res Commun **357**(2): 561-566.

CAUTER, E. W. V., E. VIRASORO, R. Leclercq and G. Copinschi (1981). "SEASONAL, CIRCADIAN AND EPISODIC VARIATIONS OF HUMAN IMMUNOREACTIVE β -MSH, ACTH AND CORTISOL." International journal of peptide and protein research **17**(1): 3-13.

Chapman, K., M. Holmes and J. Seckl (2013). "11beta-hydroxysteroid dehydrogenases: intracellular gate-keepers of tissue glucocorticoid action." Physiol Rev **93**(3): 1139-1206.

- Charmandari, E., G. P. Chrousos, G. I. Lambrou, A. Pavlaki, H. Koide, S. S. Ng and T. Kino (2011). "Peripheral CLOCK regulates target-tissue glucocorticoid receptor transcriptional activity in a circadian fashion in man." PLoS One **6**(9): e25612.
- Cho, K.-H., S.-Y. Shin, W. Kolch and O. Wolkenhauer (2003). "Experimental design in systems biology, based on parameter sensitivity analysis using a monte carlo method: A case study for the $\text{tnf}\alpha$ -mediated $\text{nf-}\kappa\text{b}$ signal transduction pathway." Simulation **79**(12): 726-739.
- Choi, J., S. Hulseapple, M. Conklin and J. Harvey (1998). "Modeling CO₂ degassing and pH in a stream-aquifer system." Journal of Hydrology **209**(1): 297-310.
- Chung, S., G. H. Son and K. Kim (2011). "Circadian rhythm of adrenal glucocorticoid: Its regulation and clinical implications." Biochimica et Biophysica Acta (BBA) - Molecular Basis of Disease **1812**(5): 581-591.
- Cooper, M. S., I. Bujalska, E. Rabbitt, E. A. Walker, R. Bland, M. C. Sheppard, M. Hewison and P. M. Stewart (2001). "Modulation of 11 β -Hydroxysteroid Dehydrogenase Isozymes by Proinflammatory Cytokines in Osteoblasts: An Autocrine Switch from Glucocorticoid Inactivation to Activation." Journal of Bone and Mineral Research **16**(6): 1037-1044.
- Cuesta, M., N. Cermakian and D. B. Boivin (2015). "Glucocorticoids entrain molecular clock components in human peripheral cells." FASEB J **29**(4): 1360-1370.
- Curtis, A. M., C. T. Fagundes, G. Yang, E. M. Palsson-McDermott, P. Wochal, A. F. McGettrick, N. H. Foley, J. O. Early, L. Chen, H. Zhang, C. Xue, S. S. Geiger, K. Hokamp, M. P. Reilly, A. N. Coogan, E. Vigorito, G. A. FitzGerald and L. A. O'Neill (2015). "Circadian control of innate immunity in macrophages by miR-155 targeting Bmal1." Proc Natl Acad Sci U S A **112**(23): 7231-7236.
- Cutolo, M. and R. H. Straub (2008). "Circadian rhythms in arthritis: hormonal effects on the immune/inflammatory reaction." Autoimmun Rev **7**(3): 223-228.
- Dadgar, S., Z. Wang, H. Johnston, A. Kesari, K. Nagaraju, Y.-W. Chen, D. A. Hill, T. A. Partridge, M. Giri and R. J. Freishtat (2014). "Asynchronous remodeling is a driver of failed regeneration in Duchenne muscular dystrophy." J Cell Biol **207**(1): 139-158.
- DeCoursey, P. J. (1972). "LD ratios and the entrainment of circadian activity in a nocturnal and a diurnal rodent." Journal of comparative physiology **78**(3): 221-235.
- Dedovic, K., A. Duchesne, J. Andrews, V. Engert and J. C. Pruessner (2009). "The brain and the stress axis: The neural correlates of cortisol regulation in response to stress." NeuroImage **47**(3): 864-871.

Dekker, M. J. H. J., H. Tiemeier, H. J. Luijendijk, M. Kuningas, A. Hofman, F. H. d. Jong, P. M. Stewart, J. W. Koper and S. W. J. Lamberts (2012). "The Effect of Common Genetic Variation in 11 β -Hydroxysteroid Dehydrogenase Type 1 on Hypothalamic-Pituitary-Adrenal Axis Activity and Incident Depression." The Journal of Clinical Endocrinology & Metabolism **97**(2): E233-E237.

Demas, G. E., D. L. Drazen, A. M. Jasnow, T. J. Bartness and R. J. Nelson (2002). "Sympathoadrenal system differentially affects photoperiodic changes in humoral immunity of Siberian hamsters (*Phodopus sungorus*)." J Neuroendocrinol **14**(1): 29-35.

Demas, G. E. and R. J. Nelson (2012). Ecoimmunology. Oxford; New York, Oxford University Press.

Demitrack, M. A., J. K. Dale, S. E. Straus, L. Laue, S. J. Listwak, M. J. Kruesi, G. P. Chrousos and P. W. Gold (1991). "Evidence for impaired activation of the hypothalamic-pituitary-adrenal axis in patients with chronic fatigue syndrome." J Clin Endocrinol Metab **73**(6): 1224-1234.

Destici, E., M. Oklejewicz, S. Saito and G. T. van der Horst (2011). "Mammalian cryptochromes impinge on cell cycle progression in a circadian clock-independent manner." Cell cycle **10**(21): 3788-3797.

Devang, N., N. M, S. Rao and P. Adhikari (2016). "HSD11B1 gene polymorphisms in type 2 diabetes and metabolic syndrome—Do we have evidence for the association?" International Journal of Diabetes in Developing Countries **36**(1): 95-102.

Devlin, P. F. (2002). "Signs of the time: environmental input to the circadian clock." Journal of Experimental Botany **53**(374): 1535-1550.

Dickmeis, T., K. Lahiri, G. Nica, D. Vallone, C. Santoriello, C. J. Neumann, M. Hammerschmidt and N. S. Foulkes (2007). "Glucocorticoids play a key role in circadian cell cycle rhythms." PLoS Biol **5**(4): e78.

Diederich, S., M. Quinkler, K. Miller, P. Heilmann, M. Schoneshofer and W. Oelkers (1996). "Human kidney 11 beta-hydroxysteroid dehydrogenase: regulation by adrenocorticotropin?" Eur J Endocrinol **134**(3): 301-307.

Doganci, A., T. Eigenbrod, N. Krug, G. T. De Sanctis, M. Hausding, V. J. Erpenbeck, B. Haddad el, H. A. Lehr, E. Schmitt, T. Bopp, K. J. Kallen, U. Herz, S. Schmitt, C. Luft, O. Hecht, J. M. Hohlfeld, H. Ito, N. Nishimoto, K. Yoshizaki, T. Kishimoto, S. Rose-John, H. Renz, M. F. Neurath, P. R. Galle and S. Finotto (2005). "The IL-6R alpha chain controls lung CD4+CD25+ Treg development and function during allergic airway inflammation in vivo." J Clin Invest **115**(2): 313-325.

Dopico, X. C., M. Evangelou, R. C. Ferreira, H. Guo, M. L. Pekalski, D. J. Smyth, N. Cooper, O. S. Burren, A. J. Fulford, B. J. Hennig, A. M. Prentice, A. G. Ziegler, E. Bonifacio, C. Wallace and J. A. Todd (2015). "Widespread seasonal gene expression reveals annual differences in human immunity and physiology." Nat Commun **6**: 7000.

Douglas, A. S., M. G. Dunnigan, T. M. Allan and J. M. Rawles (1995). "Seasonal variation in coronary heart disease in Scotland." J Epidemiol Community Health **49**(6): 575-582.

Draper, N., E. A. Walker, I. J. Bujalska, J. W. Tomlinson, S. M. Chalder, W. Arlt, G. G. Lavery, O. Bedendo, D. W. Ray, I. Laing, E. Malunowicz, P. C. White, M. Hewison, P. J. Mason, J. M. Connell, C. H. L. Shackleton and P. M. Stewart (2003). "Mutations in the genes encoding 11[beta]-hydroxysteroid dehydrogenase type 1 and hexose-6-phosphate dehydrogenase interact to cause cortisone reductase deficiency." Nat Genet **34**(4): 434-439.

Duffy, J. F. and K. P. Wright Jr (2005). "Entrainment of the human circadian system by light." Journal of biological rhythms **20**(4): 326-338.

Eccles, R. (2002). "An explanation for the seasonality of acute upper respiratory tract viral infections." Acta Otolaryngol **122**(2): 183-191.

Edwards, C. (2012). "Sixty years after Hench--corticosteroids and chronic inflammatory disease." J Clin Endocrinol Metab **97**(5): 1443-1451.

Esteves, C. L., V. Kelly, A. Breton, A. I. Taylor, C. C. West, F. X. Donadeu, B. Peault, J. R. Seckl and K. E. Chapman (2014). "Proinflammatory cytokine induction of 11beta-hydroxysteroid dehydrogenase type 1 (11beta-HSD1) in human adipocytes is mediated by MEK, C/EBPbeta, and NF-kappaB/RelA." J Clin Endocrinol Metab **99**(1): E160-168.

Federenko, I. S., M. Nagamine, D. H. Hellhammer, P. D. Wadhwa and S. Wüst (2004). "The Heritability of Hypothalamus Pituitary Adrenal Axis Responses to Psychosocial Stress Is Context Dependent." The Journal of Clinical Endocrinology & Metabolism **89**(12): 6244-6250.

Feillet, C., G. T. J. van der Horst, F. Levi, D. A. Rand and F. Delaunay (2015). "Coupling between the Circadian Clock and Cell Cycle Oscillators: Implication for Healthy Cells and Malignant Growth." Frontiers in Neurology **6**: 96.

Feng, X., S. A. Reini, E. Richards, C. E. Wood and M. Keller-Wood (2013). "Cortisol stimulates proliferation and apoptosis in the late gestation fetal heart: differential effects of mineralocorticoid and glucocorticoid receptors." American Journal of Physiology-Regulatory, Integrative and Comparative Physiology **305**(4): R343-R350.

Fleming, A., J. M. Crown and M. Corbett (1976). "Early rheumatoid disease. I. Onset." Ann Rheum Dis **35**(4): 357-360.

Forsling, M. L., H. Montgomery, D. Halpin, R. J. Windle and D. F. Treacher (1998). "Daily patterns of secretion of neurohypophysial hormones in man: effect of age." Exp Physiol **83**(3): 409-418.

Foteinou, P. T., S. E. Calvano, S. F. Lowry and I. P. Androulakis (2009). "Modeling endotoxin-induced systemic inflammation using an indirect response approach." Math Biosci **217**(1): 27-42.

Foteinou, P. T., S. E. Calvano, S. F. Lowry and I. P. Androulakis (2010). "Multiscale model for the assessment of autonomic dysfunction in human endotoxemia." Physiol Genomics **42**(1): 5-19.

Freishtat, R. J., A. M. Watson, A. S. Benton, S. F. Iqbal, D. K. Pillai, M. C. Rose and E. P. Hoffman (2011). "Asthmatic airway epithelium is intrinsically inflammatory and mitotically dyssynchronous." American journal of respiratory cell and molecular biology **44**(6): 863-869.

Galon, J., D. Franchimont, N. Hiroi, G. Frey, A. Boettner, M. Ehrhart-Bornstein, J. J. O'Shea, G. P. Chrousos and S. R. Bornstein (2002). "Gene profiling reveals unknown enhancing and suppressive actions of glucocorticoids on immune cells." FASEB J **16**(1): 61-71.

Gambineri, A., F. Tomassoni, A. Munarini, R. H. Stimson, R. Mioni, U. Pagotto, K. E. Chapman, R. Andrew, V. Mantovani and R. Pasquali (2011). "A combination of polymorphisms in HSD11B1 associates with in vivo 11 β -HSD1 activity and metabolic syndrome in women with and without polycystic ovary syndrome." European Journal of Endocrinology **165**(2): 283-292.

Garaulet, M., J. M. Ordovas, P. Gomez-Abellan, J. A. Martinez and J. A. Madrid (2011). "An approximation to the temporal order in endogenous circadian rhythms of genes implicated in human adipose tissue metabolism." J Cell Physiol **226**(8): 2075-2080.

Gathercole, L. L., G. G. Lavery, S. A. Morgan, M. S. Cooper, A. J. Sinclair, J. W. Tomlinson and P. M. Stewart (2013). "11beta-Hydroxysteroid dehydrogenase 1: translational and therapeutic aspects." Endocr Rev **34**(4): 525-555.

Gérard, C. and A. Goldbeter (2011). "A skeleton model for the network of cyclin-dependent kinases driving the mammalian cell cycle." Interface Focus **1**(1): 24-35.

Giacinti, C. and A. Giordano (2006). "RB and cell cycle progression." Oncogene **25**(38): 5220-5227.

Gibbs, J., L. Ince, L. Matthews, J. Mei, T. Bell, N. Yang, B. Saer, N. Begley, T. Poolman, M. Pariollaud, S. Farrow, F. DeMayo, T. Hussell, G. S. Worthen, D. Ray and A. Loudon (2014). "An epithelial circadian clock controls pulmonary inflammation and glucocorticoid action." Nat Med **20**(8): 919-926.

Gibbs, J. E., J. Blaikley, S. Beesley, L. Matthews, K. D. Simpson, S. H. Boyce, S. N. Farrow, K. J. Else, D. Singh, D. W. Ray and A. S. Loudon (2012). "The nuclear receptor REV-ERB α mediates circadian regulation of innate immunity through selective regulation of inflammatory cytokines." Proc Natl Acad Sci U S A **109**(2): 582-587.

Glass, L. (2001). "Synchronization and rhythmic processes in physiology." Nature **410**(6825): 277-284.

Golombek, D. A. and R. E. Rosenstein (2010). "Physiology of circadian entrainment." Physiological reviews **90**(3): 1063-1102.

Gomez-Santos, C., P. Gomez-Abellan, J. A. Madrid, J. J. Hernandez-Morante, J. A. Lujan, J. M. Ordovas and M. Garaulet (2009). "Circadian rhythm of clock genes in human adipose explants." Obesity (Silver Spring) **17**(8): 1481-1485.

Gong, R., D. J. Morris and A. S. Brem (2008). "Human renal 11 β -hydroxysteroid dehydrogenase 1 functions and co-localizes with COX-2." Life Sci **82**(11-12): 631-637.

Gonze, D., S. Bernard, C. Waltermann, A. Kramer and H. Herzl (2005). "Spontaneous Synchronization of Coupled Circadian Oscillators." Biophysical Journal **89**(1): 120-129.

Gotoh, T., M. Vila-Caballer, C. S. Santos, J. Liu, J. Yang and C. V. Finkielstein (2014). "The circadian factor Period 2 modulates p53 stability and transcriptional activity in unstressed cells." Molecular biology of the cell **25**(19): 3081-3093.

Goussis, D. A. and H. N. Najm (2006). "Model reduction and physical understanding of slowly oscillating processes: the circadian cycle." Multiscale Modeling & Simulation **5**(4): 1297-1332.

Grazio, S., D. B. Naglic, B. Anic, F. Grubisic, D. Bobek, M. Bakula, H. S. Kavanagh, A. T. Kuna and S. Cvijetic (2015). "Vitamin D serum level, disease activity and functional ability in different rheumatic patients." Am J Med Sci **349**(1): 46-49.

Hadlow, N. C., S. Brown, R. Wardrop and D. Henley (2014). "The effects of season, daylight saving and time of sunrise on serum cortisol in a large population." Chronobiol Int **31**(2): 243-251.

Hahn, A. T., J. T. Jones and T. Meyer (2009). "Quantitative analysis of cell cycle phase durations and PC12 differentiation using fluorescent biosensors." Cell Cycle **8**(7): 1044-1052.

Haimovich, B., J. Calvano, A. D. Haimovich, S. E. Calvano, S. M. Coyle and S. F. Lowry (2010). "In vivo endotoxin synchronizes and suppresses clock gene expression in human peripheral blood leukocytes." Critical care medicine **38**(3): 751.

Hardy, R., E. H. Rabbitt, A. Filer, P. Emery, M. Hewison, P. M. Stewart, N. J. Gittoes, C. D. Buckley, K. Raza and M. S. Cooper (2008). "Local and systemic glucocorticoid metabolism in inflammatory arthritis." Ann Rheum Dis **67**(9): 1204-1210.

Hardy, R. S., A. Filer, M. S. Cooper, G. Parsonage, K. Raza, D. L. Hardie, E. H. Rabbitt, P. M. Stewart, C. D. Buckley and M. Hewison (2006). "Differential expression, function and response to inflammatory stimuli of 11 β -hydroxysteroid dehydrogenase type 1 in human fibroblasts: a mechanism for tissue-specific regulation of inflammation." Arthritis research & therapy **8**(4): R108.

Harno, E. and A. White (2010). "Will treating diabetes with 11beta-HSD1 inhibitors affect the HPA axis?" Trends Endocrinol Metab **21**(10): 619-627.

Harrington, M. (2010). "Location, location, location: important for jet-lagged circadian loops." The Journal of Clinical Investigation **120**(7): 2265-2267.

Harris, H. J., Y. Kotelevtsev, J. J. Mullins, J. R. Seckl and M. C. Holmes (2001). "Intracellular regeneration of glucocorticoids by 11beta-hydroxysteroid dehydrogenase (11beta-HSD)-1 plays a key role in regulation of the hypothalamic-pituitary-adrenal axis: analysis of 11beta-HSD-1-deficient mice." Endocrinology **142**(1): 114-120.

Hassi, J., K. Sikkila, A. Ruokonen and J. Leppaluoto (2001). "The pituitary-thyroid axis in healthy men living under subarctic climatological conditions." J Endocrinol **169**(1): 195-203.

Haus, E., L. Sackett-Lundeen and M. H. Smolensky (2012). "Rheumatoid arthritis: circadian rhythms in disease activity, signs and symptoms, and rationale for chronotherapy with corticosteroids and other medications." Bull NYU Hosp Jt Dis **70 Suppl 1**: 3-10.

Hawley, D. J., F. Wolfe, F. A. Lue and H. Moldofsky (2001). "Seasonal symptom severity in patients with rheumatic diseases: a study of 1,424 patients." J Rheumatol **28**(8): 1900-1909.

Hazlerigg, D. G. and G. C. Wagner (2006). "Seasonal photoperiodism in vertebrates: from coincidence to amplitude." Trends Endocrinol Metab **17**(3): 83-91.

Heiniger, C. D., M. K. Rochat, F. J. Frey and B. M. Frey (2001). "TNF-alpha enhances intracellular glucocorticoid availability." FEBS Lett **507**(3): 351-356.

Heinrich, R. and S. Schuster (1996). Time Hierarchy in Metabolism. The Regulation of Cellular Systems. Boston, MA, Springer US: 112-137.

- Hermann, C., S. von Aulock, O. Dehus, M. Keller, H. Okigami, F. Gantner, A. Wendel and T. Hartung (2006). "Endogenous cortisol determines the circadian rhythm of lipopolysaccharide-- but not lipoteichoic acid--inducible cytokine release." Eur J Immunol **36**(2): 371-379.
- Hirschie Johnson, C., J. A. Elliott and R. Foster (2003). "Entrainment of circadian programs." Chronobiology international **20**(5): 741-774.
- Hughes, K. A., K. N. Manolopoulos, J. Iqbal, N. L. Cruden, R. H. Stimson, R. M. Reynolds, D. E. Newby, R. Andrew, F. Karpe and B. R. Walker (2012). "Recycling Between Cortisol and Cortisone in Human Splanchnic, Subcutaneous Adipose, and Skeletal Muscle Tissues In Vivo." Diabetes **61**(6): 1357-1364.
- Husse, J., G. Eichele and H. Oster (2015). "Synchronization of the mammalian circadian timing system: Light can control peripheral clocks independently of the SCN clock." Bioessays **37**(10): 1119-1128.
- Ichikawa, Y., K. Yoshida, M. Kawagoe, E. Saito, Y. Abe, K. Arikawa and M. Homma (1977). "Altered equilibrium between cortisol and cortisone in plasma in thyroid dysfunction and inflammatory diseases." Metabolism **26**(9): 989-997.
- Ignatova, I. D., R. M. Kostadinova, C. E. Goldring, A. R. Nawrocki, F. J. Frey and B. M. Frey (2009). "Tumor necrosis factor-alpha upregulates 11beta-hydroxysteroid dehydrogenase type 1 expression by CCAAT/enhancer binding protein-beta in HepG2 cells." Am J Physiol Endocrinol Metab **296**(2): E367-377.
- Ihekwa, A. E., D. S. Broomhead, R. L. Grimley, N. Benson and D. B. Kell (2004). "Sensitivity analysis of parameters controlling oscillatory signalling in the NF-kappaB pathway: the roles of IKK and IkappaBalpha." Syst Biol (Stevenage) **1**(1): 93-103.
- Iikuni, N., A. Nakajima, E. Inoue, E. Tanaka, H. Okamoto, M. Hara, T. Tomatsu, N. Kamatani and H. Yamanaka (2007). "What's in season for rheumatoid arthritis patients? Seasonal fluctuations in disease activity." Rheumatology (Oxford) **46**(5): 846-848.
- Ishida, A., T. Mutoh, T. Ueyama, H. Bando, S. Masubuchi, D. Nakahara, G. Tsujimoto and H. Okamura (2005). "Light activates the adrenal gland: timing of gene expression and glucocorticoid release." Cell Metab **2**(5): 297-307.
- Iwasaki, Y., S. Takayasu, M. Nishiyama, M. Tsugita, T. Taguchi, M. Asai, M. Yoshida, M. Kambayashi and K. Hashimoto (2008). "Is the metabolic syndrome an intracellular Cushing state? Effects of multiple humoral factors on the transcriptional activity of the hepatic glucocorticoid-activating enzyme (11beta-hydroxysteroid dehydrogenase type 1) gene." Mol Cell Endocrinol **285**(1-2): 10-18.

Jamieson, P. M., K. E. Chapman and J. R. Seckl (1999). "Tissue- and temporal-specific regulation of 11beta-hydroxysteroid dehydrogenase type 1 by glucocorticoids in vivo." J Steroid Biochem Mol Biol **68**(5-6): 245-250.

Janich, P., A. B. Arpat, V. Castelo-Szekely, M. Lopes and D. Gatfield (2015). "Ribosome profiling reveals the rhythmic liver transcriptome and circadian clock regulation by upstream open reading frames." Genome Res **25**(12): 1848-1859.

Jin, X., L. P. Shearman, D. R. Weaver, M. J. Zylka, G. J. de Vries and S. M. Reppert (1999). "A molecular mechanism regulating rhythmic output from the suprachiasmatic circadian clock." Cell **96**(1): 57-68.

Juan, G., E. Hernando and C. Cordon-Cardo (2002). "Separation of live cells in different phases of the cell cycle for gene expression analysis." Cytometry Part A **49**(4): 170-175.

Jung, C. M., S. B. Khalsa, F. A. Scheer, C. Cajochen, S. W. Lockley, C. A. Czeisler and K. P. Wright, Jr. (2010). "Acute effects of bright light exposure on cortisol levels." J Biol Rhythms **25**(3): 208-216.

Kalsbeek, A., E. Fliers, M. Hofman, D. Swaab and R. Buijs (2010). "Vasopressin and the output of the hypothalamic biological clock." Journal of neuroendocrinology **22**(5): 362-372.

Kalsbeek, A., J. van der Vliet and R. M. Buijs (1996). "Decrease of endogenous vasopressin release necessary for expression of the circadian rise in plasma corticosterone: a reverse microdialysis study." J Neuroendocrinol **8**(4): 299-307.

Kanikowska, D., J. Sugeno, M. Sato, Y. Shimizu, Y. Inukai, N. Nishimura and S. Iwase (2009). "Seasonal variation in blood concentrations of interleukin-6, adrenocorticotrophic hormone, metabolites of catecholamine and cortisol in healthy volunteers." Int J Biometeorol **53**(6): 479-485.

Kawamura, A., N. Tamaki and T. Kokunai (1998). "Effect of Dexamethasone on Cell Proliferation of Neuroepithelial Tumor Cell Lines." Neurologia medico-chirurgica **38**(10): 633-640.

Kawasaki, H., R. Doi, K. Ito, M. Shimoda and N. Ishida (2013). "The circadian binding of CLOCK protein to the promoter of C/ebpalpha gene in mouse cells." PLoS One **8**(3): e58221.

Keenan, D. M., F. Roelfsema and J. D. Veldhuis (2004). "Endogenous ACTH concentration-dependent drive of pulsatile cortisol secretion in the human." Am J Physiol Endocrinol Metab **287**(4): E652-661.

- Keller, M., J. Mazuch, U. Abraham, G. D. Eom, E. D. Herzog, H. D. Volk, A. Kramer and B. Maier (2009). "A circadian clock in macrophages controls inflammatory immune responses." Proc Natl Acad Sci U S A **106**(50): 21407-21412.
- Kent, E., S. Neumann, U. Kummer and P. Mendes (2013). "What Can We Learn from Global Sensitivity Analysis of Biochemical Systems?" PLOS ONE **8**(11): e79244.
- Keul, R., P. C. Heinrich, G. Muller-newen, K. Muller and P. Woo (1998). "A possible role for soluble IL-6 receptor in the pathogenesis of systemic onset juvenile chronic arthritis." Cytokine **10**(9): 729-734.
- Khoo, A. L., L. Y. Chai, H. J. Koenen, F. C. Sweep, I. Joosten, M. G. Netea and A. J. van der Ven (2011). "Regulation of cytokine responses by seasonality of vitamin D status in healthy individuals." Clin Exp Immunol **164**(1): 72-79.
- Klinke, D. J. (2008). "Integrating Epidemiological Data into a Mechanistic Model of Type 2 Diabetes: Validating the Prevalence of Virtual Patients." Annals of Biomedical Engineering **36**(2): 321-334.
- Kostadinova, R. M., A. R. Nawrocki, F. J. Frey and B. M. Frey (2005). "Tumor necrosis factor alpha and phorbol 12-myristate-13-acetate down-regulate human 11beta-hydroxysteroid dehydrogenase type 2 through p50/p50 NF-kappaB homodimers and Egr-1." FASEB J **19**(6): 650-652.
- Kostoglou-Athanassiou, I., D. F. Treacher, M. J. Wheeler and M. L. Forsling (1998). "Bright light exposure and pituitary hormone secretion." Clin Endocrinol (Oxf) **48**(1): 73-79.
- Kotelevtsev, Y., R. W. Brown, S. Fleming, C. Kenyon, C. R. W. Edwards, J. R. Seckl and J. J. Mullins (1999). "Hypertension in mice lacking 11 β -hydroxysteroid dehydrogenase type 2." Journal of Clinical Investigation **103**(5): 683-689.
- Kox, M., M. J. van den Berg, J. G. van der Hoeven, J. P. Wielders, A. J. van der Ven and P. Pickkers (2013). "Vitamin D status is not associated with inflammatory cytokine levels during experimental human endotoxaemia." Clin Exp Immunol **171**(2): 231-236.
- Koyama, K. and Z. Krozowski (2001). "Modulation of 11 beta-hydroxysteroid dehydrogenase type 2 activity in Ishikawa cells is associated with changes in cellular proliferation." Mol Cell Endocrinol **183**(1-2): 165-170.
- Kramer, B. P. and M. Fussenegger (2005). "Hysteresis in a synthetic mammalian gene network." Proc Natl Acad Sci U S A **102**(27): 9517-9522.
- Kumari, M., M. Shipley, M. Stafford and M. Kivimaki (2011). "Association of Diurnal Patterns in Salivary Cortisol with All-Cause and Cardiovascular Mortality: Findings from

the Whitehall II Study." The Journal of Clinical Endocrinology & Metabolism **96**(5): 1478-1485.

Kume, K., M. J. Zylka, S. Sriram, L. P. Shearman, D. R. Weaver, X. Jin, E. S. Maywood, M. H. Hastings and S. M. Reppert (1999). "mCRY1 and mCRY2 are essential components of the negative limb of the circadian clock feedback loop." Cell **98**(2): 193-205.

Laerum, O. D., O. Sletvold and T. Riise (1988). "Circadian and circannual variations of cell cycle distribution in the mouse bone marrow." Chronobiology international **5**(1): 19-35.

Lalanne, M. and J. F. Henderson (1975). "Effects of hormones and drugs on phosphoribosyl pyrophosphate concentrations in mouse liver." Canadian journal of biochemistry **53**(3): 394-399.

Lam, R. W. and R. D. Levitan (2000). "Pathophysiology of seasonal affective disorder: a review." Journal of Psychiatry and Neuroscience **25**(5): 469.

Lancaster, G. I., Q. Khan, P. Drysdale, F. Wallace, A. E. Jeukendrup, M. T. Drayson and M. Gleeson (2005). "The physiological regulation of toll-like receptor expression and function in humans." J Physiol **563**(Pt 3): 945-955.

Langeveld, C., M. Van Waas, J. Stoof, W. Suianto, E. De Kloet, J. Wolbers and J. Heimans (1992). "Implication of glucocorticoid receptors in the stimulation of human glioma cell proliferation by dexamethasone." Journal of neuroscience research **31**(3): 524-531.

Lavery, G. G., E. A. Walker, N. Draper, P. Jeyasuria, J. Marcos, C. H. Shackleton, K. L. Parker, P. C. White and P. M. Stewart (2006). "Hexose-6-phosphate dehydrogenase knock-out mice lack 11 beta-hydroxysteroid dehydrogenase type 1-mediated glucocorticoid generation." J Biol Chem **281**(10): 6546-6551.

Lederbogen, F., J. Hummel, C. Fademrecht, B. Krumm, C. Kühner, M. Deuschle, K. H. Ladwig, C. Meisinger, H. E. Wichmann, H. Lutz and B. Breivogel (2011). "Flattened Circadian Cortisol Rhythm in Type 2 Diabetes." Exp Clin Endocrinol Diabetes **119**(09): 573-575.

Lekstrom-Himes, J. and K. G. Xanthopoulos (1998). "Biological role of the CCAAT/enhancer-binding protein family of transcription factors." J Biol Chem **273**(44): 28545-28548.

Leonard, B. E. (2006). "HPA and immune axes in stress: involvement of the serotonergic system." Neuroimmunomodulation **13**(5-6): 268-276.

- Leproult, R., E. F. Colecchia, M. L'Hermite-Baleriaux and E. Van Cauter (2001). "Transition from dim to bright light in the morning induces an immediate elevation of cortisol levels." J Clin Endocrinol Metab **86**(1): 151-157.
- Li, K. X., R. E. Smith, P. Ferrari, J. W. Funder and Z. S. Krozowski (1996). "Rat 11 beta-hydroxysteroid dehydrogenase type 2 enzyme is expressed at low levels in the placenta and is modulated by adrenal steroids in the kidney." Mol Cell Endocrinol **120**(1): 67-75.
- Li, M.-D., C.-M. Li and Z. Wang (2012). "The Role of Circadian Clocks in Metabolic Disease." The Yale Journal of Biology and Medicine **85**(3): 387-401.
- Liu, B. and E. Taioli (2015). "Seasonal Variations of Complete Blood Count and Inflammatory Biomarkers in the US Population-Analysis of NHANES Data." PloS one **10**(11): e0142382.
- Lochmiller, R. L., M. R. Vestey and S. T. McMurry (1994). "Temporal Variation in Humoral and Cell-Mediated Immune Response in a *Sigmodon Hispidus* Population." Ecology **75**(1): 236-245.
- Loewenstein, W. R. (1979). "Junctional intercellular communication and the control of growth." Biochimica et Biophysica Acta (BBA)-Reviews on Cancer **560**(1): 1-65.
- Lofgren, E., N. H. Fefferman, Y. N. Naumov, J. Gorski and E. N. Naumova (2007). "Influenza seasonality: underlying causes and modeling theories." J Virol **81**(11): 5429-5436.
- Low, S. C., M. P. Moisan, J. M. Noble, C. R. Edwards and J. R. Seckl (1994). "Glucocorticoids regulate hippocampal 11 beta-hydroxysteroid dehydrogenase activity and gene expression in vivo in the rat." J Neuroendocrinol **6**(3): 285-290.
- Lowen, A. C. and J. Steel (2014). "Roles of humidity and temperature in shaping influenza seasonality." J Virol **88**(14): 7692-7695.
- Ma, D., S. Panda and J. D. Lin (2011). "Temporal orchestration of circadian autophagy rhythm by C/EBPbeta." EMBO J **30**(22): 4642-4651.
- Maes, M., W. Stevens, S. Scharpe, E. Bosmans, F. De Meyer, P. D'Hondt, D. Peeters, P. Thompson, P. Cosyns, L. De Clerck and et al. (1994). "Seasonal variation in peripheral blood leukocyte subsets and in serum interleukin-6, and soluble interleukin-2 and -6 receptor concentrations in normal volunteers." Experientia **50**(9): 821-829.
- Majzoub, J. A. (2006). "Corticotropin-releasing hormone physiology." European Journal of Endocrinology **155**(suppl 1): S71-S76.
- Makinen, T. M., R. Juvonen, J. Jokelainen, T. H. Harju, A. Peitso, A. Bloigu, S. Silvennoinen-Kassinen, M. Leinonen and J. Hassi (2009). "Cold temperature and low

humidity are associated with increased occurrence of respiratory tract infections." Respir Med **103**(3): 456-462.

Malavasi, E. L., V. Kelly, N. Nath, A. Gambineri, R. S. Dakin, U. Pagotto, R. Pasquali, B. R. Walker and K. E. Chapman (2010). "Functional effects of polymorphisms in the human gene encoding 11 beta-hydroxysteroid dehydrogenase type 1 (11 beta-HSD1): a sequence variant at the translation start of 11 beta-HSD1 alters enzyme levels." Endocrinology **151**(1): 195-202.

Marcheva, B., K. Moynihan Ramsey, E. D. Buhr, Y. Kobayashi, H. Su, C. H. Ko, G. Ivanova, C. Omura, S. Mo, M. H. Vitaterna, J. P. Lopez, L. H. Philipson, C. A. Bradfield, S. D. Crosby, L. JeBailey, X. Wang, J. S. Takahashi and J. Bass (2010). "Disruption of the Clock Components CLOCK and BMAL1 Leads to Hypoinsulinemia and Diabetes." Nature **466**(7306): 627-631.

Matchock, R. L., L. D. Dorn and E. J. Susman (2007). "Diurnal and seasonal cortisol, testosterone, and DHEA rhythms in boys and girls during puberty." Chronobiol Int **24**(5): 969-990.

Matsuno, F., S. Chowdhury, T. Gotoh, K. Iwase, H. Matsuzaki, K. Takatsuki, M. Mori and M. Takiguchi (1996). "Induction of the C/EBP beta gene by dexamethasone and glucagon in primary-cultured rat hepatocytes." J Biochem **119**(3): 524-532.

Mattern, J., M. W. Büchler and I. Herr (2007). "Cell cycle arrest by glucocorticoids may protect normal tissue and solid tumors from cancer therapy." Cancer biology & therapy **6**(9): 1341-1350.

Mavroudis, P. D., S. A. Corbett, S. E. Calvano and I. P. Androulakis (2014). "Mathematical modeling of light-mediated HPA axis activity and downstream implications on the entrainment of peripheral clock genes." Physiol Genomics **46**(20): 766-778.

Mavroudis, P. D., S. A. Corbett, S. E. Calvano and I. P. Androulakis (2015). "Circadian characteristics of permissive and suppressive effects of cortisol and their role in homeostasis and the acute inflammatory response." Math Biosci **260**: 54-64.

Mavroudis, P. D., J. D. Scheff, S. E. Calvano and I. P. Androulakis (2013). "Systems biology of circadian-immune interactions." J Innate Immun **5**(2): 153-162.

McKay, M. D., R. J. Beckman and W. J. Conover (1979). "A Comparison of Three Methods for Selecting Values of Input Variables in the Analysis of Output from a Computer Code." Technometrics **21**(2): 239-245.

Meijer, J. H., S. Michel, H. T. Vanderleest and J. H. Rohling (2010). "Daily and seasonal adaptation of the circadian clock requires plasticity of the SCN neuronal network." Eur J Neurosci **32**(12): 2143-2151.

Miki, T., T. Matsumoto, Z. Zhao and C. C. Lee (2013). "p53 Regulates Period2 Expression and the Circadian Clock." Nature communications **4**: 2444-2444.

Mitsuyama, K., A. Toyonaga, E. Sasaki, O. Ishida, H. Ikeda, O. Tsuruta, K. Harada, H. Tateishi, T. Nishiyama and K. Tanikawa (1995). "Soluble interleukin-6 receptors in inflammatory bowel disease: relation to circulating interleukin-6." Gut **36**(1): 45-49.

Mohawk, J. A., C. B. Green and J. S. Takahashi (2012). "Central and peripheral circadian clocks in mammals." Annu Rev Neurosci **35**: 445-462.

Morgan, S. A., E. L. McCabe, L. L. Gathercole, Z. K. Hassan-Smith, D. P. Lerner, I. J. Bujalska, P. M. Stewart, J. W. Tomlinson and G. G. Lavery (2014). "11beta-HSD1 is the major regulator of the tissue-specific effects of circulating glucocorticoid excess." Proc Natl Acad Sci U S A **111**(24): E2482-2491.

Morineau, G., A. Boudi, A. Barka, M. Gourmelen, F. Degeilh, N. Hardy, A. al-Halnak, H. Soliman, J. P. Gosling, R. Julien, J. L. Brerault, P. Boudou, P. Aubert, J. M. Villette, A. Pruna, H. Galons and J. Fiet (1997). "Radioimmunoassay of cortisone in serum, urine, and saliva to assess the status of the cortisol-cortisone shuttle." Clin Chem **43**(8 Pt 1): 1397-1407.

Morris, C. J., T. E. Purvis, K. Hu and F. A. J. L. Scheer (2016). "Circadian misalignment increases cardiovascular disease risk factors in humans." Proceedings of the National Academy of Sciences of the United States of America **113**(10): E1402-E1411.

Mosendane, T., T. Mosendane and F. J. Raal (2008). "Shift work and its effects on the cardiovascular system." Cardiovascular Journal of Africa **19**(4): 210-215.

Motzkus, D., U. Albrecht and E. Maronde (2002). "The human PER1 gene is inducible by interleukin-6." J Mol Neurosci **18**(1-2): 105-109.

Mourtzoukou, E. G. and M. E. Falagas (2007). "Exposure to cold and respiratory tract infections." Int J Tuberc Lung Dis **11**(9): 938-943.

N.Appaji Rao, H. S. S., G.S.Jagannatha Rao, S.Seethalakshmi and N.S.Punekar (1987). Kinetic approaches to the study of enzyme regulation. New Delhi, Oxford & IBH Publishing Co.

Nagoshi, E., C. Saini, C. Bauer, T. Laroche, F. Naef and U. Schibler (2004). "Circadian Gene Expression in Individual Fibroblasts: Cell-Autonomous and Self-Sustained Oscillators Pass Time to Daughter Cells." Cell **119**(5): 693-705.

- Nair, R. and A. Maseeh (2012). "Vitamin D: The "sunshine" vitamin." J Pharmacol Pharmacother **3**(2): 118-126.
- Narasimamurthy, R., M. Hatori, S. K. Nayak, F. Liu, S. Panda and I. M. Verma (2012). "Circadian clock protein cryptochrome regulates the expression of proinflammatory cytokines." Proc Natl Acad Sci U S A **109**(31): 12662-12667.
- Neganova, I. and M. Lako (2008). "G1 to S phase cell cycle transition in somatic and embryonic stem cells." Journal of Anatomy **213**(1): 30-44.
- Nelson, R. J. (2004). "Seasonal immune function and sickness responses." Trends Immunol **25**(4): 187-192.
- Newman, L. A., M. T. Walker, R. L. Brown, T. W. Cronin and P. R. Robinson (2003). "Melanopsin forms a functional short-wavelength photopigment." Biochemistry **42**(44): 12734-12738.
- Nguyen, K. D., S. J. Fentress, Y. Qiu, K. Yun, J. S. Cox and A. Chawla (2013). "Circadian gene Bmal1 regulates diurnal oscillations of Ly6C(hi) inflammatory monocytes." Science **341**(6153): 1483-1488.
- Niehof, M., K. Streetz, T. Rakemann, S. C. Bischoff, M. P. Manns, F. Horn and C. Trautwein (2001). "Interleukin-6-induced tethering of STAT3 to the LAP/C/EBPbeta promoter suggests a new mechanism of transcriptional regulation by STAT3." J Biol Chem **276**(12): 9016-9027.
- Nomura, S., M. Fujitaka, N. Sakura and K. Ueda (1997). "Circadian rhythms in plasma cortisone and cortisol and the cortisone/cortisol ratio." Clin Chim Acta **266**(2): 83-91.
- Novak, B. and J. J. Tyson (2008). "Design principles of biochemical oscillators." Nat Rev Mol Cell Biol **9**(12): 981-991.
- Nunez, B. S., F. M. Rogerson, T. Mune, Y. Igarashi, Y. Nakagawa, G. Phillipov, A. Moudgil, L. B. Travis, M. Palermo, C. Shackleton and P. C. White (1999). "Mutants of 11 β -Hydroxysteroid Dehydrogenase (11-HSD2) With Partial Activity." Improved Correlations Between Genotype and Biochemical Phenotype in Apparent Mineralocorticoid Excess **34**(4): 638-642.
- O'Jile, J. R. and T. J. Bartness (1992). "Effects of thyroxine on the photoperiodic control of energy balance and reproductive status in Siberian hamsters." Physiol Behav **52**(2): 267-270.
- Ohlander, J., M.-C. Keskin, J. Stork and K. Radon (2015). "Shift work and hypertension: Prevalence and analysis of disease pathways in a German car manufacturing company." American Journal of Industrial Medicine **58**(5): 549-560.

Olsen, N., T. Sokka, C. L. Seehorn, B. Kraft, K. Maas, J. Moore and T. M. Aune (2004). "A gene expression signature for recent onset rheumatoid arthritis in peripheral blood mononuclear cells." Ann Rheum Dis **63**(11): 1387-1392.

Otsuka, T., M. Goto, M. Kawai, Y. Togo, K. Sato, K. Katoh, M. Furuse and S. Yasuo (2012). "Photoperiod regulates corticosterone rhythms by altered adrenal sensitivity via melatonin-independent mechanisms in Fischer 344 rats and C57BL/6J mice." PLoS One **7**(6): e39090.

Ouyang, Y., C. R. Andersson, T. Kondo, S. S. Golden and C. H. Johnson (1998). "Resonating circadian clocks enhance fitness in cyanobacteria." Proc Natl Acad Sci U S A **95**(15): 8660-8664.

Papaikonomou, E. (1977). "Rat adrenocortical dynamics." J Physiol **265**(1): 119-131.

Patberg, W. R. and J. J. Rasker (2004). "Weather effects in rheumatoid arthritis: from controversy to consensus. A review." J Rheumatol **31**(7): 1327-1334.

Paterson, J. M., M. C. Holmes, C. J. Kenyon, R. Carter, J. J. Mullins and J. R. Seckl (2007). "Liver-selective transgene rescue of hypothalamic-pituitary-adrenal axis dysfunction in 11beta-hydroxysteroid dehydrogenase type 1-deficient mice." Endocrinology **148**(3): 961-966.

Pearl Mizrahi, S., O. Sandler, L. Lande-Diner, N. Q. Balaban and I. Simon (2016). "Distinguishing between stochasticity and determinism: Examples from cell cycle duration variability." BioEssays **38**(1): 8-13.

Perez-Aso, M., J. L. Feig, A. Mediero and B. N. Cronstein (2013). "Adenosine A2A receptor and TNF-alpha regulate the circadian machinery of the human monocytic THP-1 cells." Inflammation **36**(1): 152-162.

Perry, M. G., J. R. Kirwan, D. S. Jessop and L. P. Hunt (2009). "Overnight variations in cortisol, interleukin 6, tumour necrosis factor α and other cytokines in people with rheumatoid arthritis." Annals of the Rheumatic Diseases **68**(1): 63-68.

Persson, R., A. H. Garde, A. M. Hansen, K. Osterberg, B. Larsson, P. Orbaek and B. Karlson (2008). "Seasonal variation in human salivary cortisol concentration." Chronobiol Int **25**(6): 923-937.

Petrovsky, N., P. McNair and L. C. Harrison (1998). "Diurnal rhythms of pro-inflammatory cytokines: regulation by plasma cortisol and therapeutic implications." Cytokine **10**(4): 307-312.

Pidwirny, M. (2006). Earth-Sun Relationships and Insolation. Fundamentals of Physical Geography.

Pierre, K., N. Schlesinger and I. P. Androulakis (2016). "The role of the hypothalamic-pituitary-adrenal axis in modulating seasonal changes in immunity." Physiol Genomics **48**(10): 719-738.

Prendergast, B. J., S. R. Baillie and F. S. Dhabhar (2008). "Gonadal hormone-dependent and -independent regulation of immune function by photoperiod in Siberian hamsters." Am J Physiol Regul Integr Comp Physiol **294**(2): R384-392.

Purich, D. L. (2010). Chapter 11 - Regulatory Behavior of Enzymes. Enzyme Kinetics: Catalysis & Control. Boston, Elsevier: 685-728.

Puttonen, S., K. Viitasalo and M. Härmä (2011). "Effect of Shiftwork on Systemic Markers of Inflammation." Chronobiology International **28**(6): 528-535.

Ramakrishnan, R., D. C. DuBois, R. R. Almon, N. A. Pyszczynski and W. J. Jusko (2002). "Fifth-generation model for corticosteroid pharmacodynamics: application to steady-state receptor down-regulation and enzyme induction patterns during seven-day continuous infusion of methylprednisolone in rats." J Pharmacokinet Pharmacodyn **29**(1): 1-24.

Ramkisoensing, A. and J. H. Meijer (2015). "Synchronization of Biological Clock Neurons by Light and Peripheral Feedback Systems Promotes Circadian Rhythms and Health." Frontiers in Neurology **6**: 128.

Reppert, S. M. and D. R. Weaver (2002). "Coordination of circadian timing in mammals." Nature **418**(6901): 935-941.

Resnitzky, D., M. Gossen, H. Bujard and S. Reed (1994). "Acceleration of the G1/S phase transition by expression of cyclins D1 and E with an inducible system." Molecular and cellular biology **14**(3): 1669-1679.

Robak, T., A. Gladalska, H. Stepien and E. Robak (1998). "Serum levels of interleukin-6 type cytokines and soluble interleukin-6 receptor in patients with rheumatoid arthritis." Mediators Inflamm **7**(5): 347-353.

Rocco, M. B., J. Barry, S. Campbell, E. Nabel, E. F. Cook, L. Goldman and A. P. Selwyn (1987). "Circadian variation of transient myocardial ischemia in patients with coronary artery disease." Circulation **75**(2): 395-400.

Rodriguez-Fernandez, M., J. R. Banga and F. J. Doyle (2012). "Novel global sensitivity analysis methodology accounting for the crucial role of the distribution of input parameters: application to systems biology models." International Journal of Robust and Nonlinear Control **22**(10): 1082-1102.

- Rogatsky, I., J. M. Trowbridge and M. J. Garabedian (1997). "Glucocorticoid receptor-mediated cell cycle arrest is achieved through distinct cell-specific transcriptional regulatory mechanisms." Molecular and cellular biology **17**(6): 3181-3193.
- Rohling, J., L. Wolters and J. H. Meijer (2006). "Simulation of day-length encoding in the SCN: from single-cell to tissue-level organization." J Biol Rhythms **21**(4): 301-313.
- Rüger, M., M. C. M. Gordijn, D. G. M. Beersma, B. de Vries and S. Daan (2006). "Time-of-day-dependent effects of bright light exposure on human psychophysiology: comparison of daytime and nighttime exposure." American Journal of Physiology - Regulatory, Integrative and Comparative Physiology **290**(5): R1413.
- Sage, D., D. Maurel and O. Bosler (2002). "Corticosterone-dependent driving influence of the suprachiasmatic nucleus on adrenal sensitivity to ACTH." American Journal of Physiology-Endocrinology and Metabolism **282**(2): E458-E465.
- Sai, S., C. L. Esteves, V. Kelly, Z. Michailidou, K. Anderson, A. P. Coll, Y. Nakagawa, T. Ohzeki, J. R. Seckl and K. E. Chapman (2008). "Glucocorticoid regulation of the promoter of 11beta-hydroxysteroid dehydrogenase type 1 is indirect and requires CCAAT/enhancer-binding protein-beta." Mol Endocrinol **22**(9): 2049-2060.
- Salah, B., A. T. Dinh Xuan, J. L. Fouilladieu, A. Lockhart and J. Regnard (1988). "Nasal mucociliary transport in healthy subjects is slower when breathing dry air." Eur Respir J **1**(9): 852-855.
- Salman, H., M. Bergman, H. Bessler, S. Alexandrova, B. Beilin and M. Djaldetti (2000). "Hypothermia affects the phagocytic activity of rat peritoneal macrophages." Acta Physiol Scand **168**(3): 431-436.
- Sapolsky, R. M., L. M. Romero and A. U. Munck (2000). "How do glucocorticoids influence stress responses? Integrating permissive, suppressive, stimulatory, and preparative actions." Endocr Rev **21**(1): 55-89.
- Schaap, J., H. Albus, H. T. VanderLeest, P. H. Eilers, L. Detari and J. H. Meijer (2003). "Heterogeneity of rhythmic suprachiasmatic nucleus neurons: Implications for circadian waveform and photoperiodic encoding." Proc Natl Acad Sci U S A **100**(26): 15994-15999.
- Scheer, F. A. and R. M. Buijs (1999). "Light affects morning salivary cortisol in humans." J Clin Endocrinol Metab **84**(9): 3395-3398.
- Scheff, J. D., S. E. Calvano, S. F. Lowry and I. P. Androulakis (2010). "Modeling the influence of circadian rhythms on the acute inflammatory response." J Theor Biol **264**(3): 1068-1076.

- Scheff, J. D., P. D. Mavroudis, S. E. Calvano, S. F. Lowry and I. P. Androulakis (2011). "Modeling autonomic regulation of cardiac function and heart rate variability in human endotoxemia." Physiol Genomics **43**(16): 951-964.
- Scheiermann, C., Y. Kunisaki and P. S. Frenette (2013). "Circadian control of the immune system." Nat Rev Immunol **13**(3): 190-198.
- Schlesinger, N. and M. Schlesinger (2005). "Seasonal variation of rheumatic diseases." Discov Med **5**(25): 64-69.
- Schmal, C., J. Myung, H. Herzog and G. Bordyugov (2015). "A theoretical study on seasonality." Frontiers in neurology **6**: 94.
- Seckl, J. R. and B. R. Walker (2001). "Minireview: 11 β -Hydroxysteroid Dehydrogenase Type 1— A Tissue-Specific Amplifier of Glucocorticoid Action." Endocrinology **142**(4): 1371-1376.
- Sephton, S. E., R. M. Sapolsky, H. C. Kraemer and D. Spiegel (2000). "Diurnal Cortisol Rhythm as a Predictor of Breast Cancer Survival." Journal of the National Cancer Institute **92**(12): 994-1000.
- Shafiqat, N., B. Elleby, S. Svensson, J. Shafiqat, H. Jornvall, L. Abrahmsen and U. Oppermann (2003). "Comparative enzymology of 11 beta -hydroxysteroid dehydrogenase type 1 from glucocorticoid resistant (Guinea pig) versus sensitive (human) species." J Biol Chem **278**(3): 2030-2035.
- Sharma, A. and W. J. Jusko (1998). "Characteristics of indirect pharmacodynamic models and applications to clinical drug responses." Br J Clin Pharmacol **45**(3): 229-239.
- Shearman, L. P., S. Sriram, D. R. Weaver, E. S. Maywood, I. Chaves, B. Zheng, K. Kume, C. C. Lee, G. T. van der Horst, M. H. Hastings and S. M. Reppert (2000). "Interacting molecular loops in the mammalian circadian clock." Science **288**(5468): 1013-1019.
- Sherr, C. J. (1994). "G1 phase progression: cycling on cue." Cell **79**(4): 551-555.
- Silver, A. C., A. Arjona, W. E. Walker and E. Fikrig (2012). "The circadian clock controls toll-like receptor 9-mediated innate and adaptive immunity." Immunity **36**(2): 251-261.
- Sinclair, J. A. and R. L. Lochmiller (2000). "The winter immunoenhancement hypothesis: associations among immunity, density, and survival in prairie vole (*Microtus ochrogaster*) populations." Canadian Journal of Zoology **78**(2): 254-264.
- Smals, A. G., H. A. Ross and P. W. Kloppenborg (1977). "Seasonal variation in serum T3 and T4 levels in man." J Clin Endocrinol Metab **44**(5): 998-1001.

- So, A. Y., T. U. Bernal, M. L. Pillsbury, K. R. Yamamoto and B. J. Feldman (2009). "Glucocorticoid regulation of the circadian clock modulates glucose homeostasis." Proc Natl Acad Sci U S A **106**(41): 17582-17587.
- Son, G. H., S. Chung, H. K. Choe, H.-D. Kim, S.-M. Baik, H. Lee, H.-W. Lee, S. Choi, W. Sun, H. Kim, S. Cho, K. H. Lee and K. Kim (2008). "Adrenal peripheral clock controls the autonomous circadian rhythm of glucocorticoid by causing rhythmic steroid production." Proceedings of the National Academy of Sciences **105**(52): 20970-20975.
- Sorrells, S. F. and R. M. Sapolsky (2007). "An inflammatory review of glucocorticoid actions in the CNS." Brain Behav Immun **21**(3): 259-272.
- Sosniyenko, S., D. Parkanová, H. Illnerová, M. Sládek and A. Sumová (2010). "Different mechanisms of adjustment to a change of the photoperiod in the suprachiasmatic and liver circadian clocks." American Journal of Physiology-Regulatory, Integrative and Comparative Physiology **298**(4): R959-R971.
- Sothorn, R., R. Smaaland and J. Moore (1995). "Circannual rhythm in DNA synthesis (S-phase) in healthy human bone marrow and rectal mucosa." The FASEB journal **9**(5): 397-403.
- Spengler, M. L., K. K. Kuropatwinski, M. Comas, A. V. Gasparian, N. Fedtsova, A. S. Gleiberman, Gitlin, II, N. M. Artemicheva, K. A. Deluca, A. V. Gudkov and M. P. Antoch (2012). "Core circadian protein CLOCK is a positive regulator of NF-kappaB-mediated transcription." Proc Natl Acad Sci U S A **109**(37): E2457-2465.
- Srinivasan, V., G. J. Maestroni, D. P. Cardinali, A. I. Esquifino, S. R. Perumal and S. C. Miller (2005). "Melatonin, immune function and aging." Immun Ageing **2**: 17.
- Sriram, K., M. Rodriguez-Fernandez and F. J. Doyle, 3rd (2012). "Modeling cortisol dynamics in the neuro-endocrine axis distinguishes normal, depression, and post-traumatic stress disorder (PTSD) in humans." PLoS Comput Biol **8**(2): e1002379.
- Stevenson, T. J., K. G. Onishi, S. P. Bradley and B. J. Prendergast (2014). "Cell-autonomous iodothyronine deiodinase expression mediates seasonal plasticity in immune function." Brain Behav Immun **36**: 61-70.
- Stevenson, T. J. and B. J. Prendergast (2015). "Photoperiodic time measurement and seasonal immunological plasticity." Front Neuroendocrinol **37**: 76-88.
- Stewart, P., J. Corrie, C. Shackleton and C. Edwards (1988). "Syndrome of apparent mineralocorticoid excess. A defect in the cortisol-cortisone shuttle." Journal of Clinical Investigation **82**(1): 340.
- Straub, R. H., L. Paimela, R. Peltomaa, J. Scholmerich and M. Leirisalo-Repo (2002). "Inadequately low serum levels of steroid hormones in relation to interleukin-6 and tumor

necrosis factor in untreated patients with early rheumatoid arthritis and reactive arthritis." Arthritis Rheum **46**(3): 654-662.

Suzuki, S., K. Koyama, A. Darnel, H. Ishibashi, S. Kobayashi, H. Kubo, T. Suzuki, H. Sasano and Z. S. Krozowski (2003). "Dexamethasone upregulates 11beta-hydroxysteroid dehydrogenase type 2 in BEAS-2B cells." Am J Respir Crit Care Med **167**(9): 1244-1249.

Takahashi, J. S., H. K. Hong, C. H. Ko and E. L. McDearmon (2008). "The genetics of mammalian circadian order and disorder: implications for physiology and disease." Nat Rev Genet **9**(10): 764-775.

Takeda, N. and K. Maemura (2011). "Circadian clock and cardiovascular disease." Journal of cardiology **57**(3): 249-256.

Tass, P., M. G. Rosenblum, J. Weule, J. Kurths, A. Pikovsky, J. Volkmann, A. Schnitzler and H. J. Freund (1998). "Detection of $\mathit{n}:\mathit{m}$ Phase Locking from Noisy Data: Application to Magnetoencephalography." Physical Review Letters **81**(15): 3291-3294.

Terada, Y., T. Kobayashi, H. Kuwana, H. Tanaka, S. Inoshita, M. Kuwahara and S. Sasaki (2005). "Aldosterone stimulates proliferation of mesangial cells by activating mitogen-activated protein kinase 1/2, cyclin D1, and cyclin A." Journal of the American Society of Nephrology **16**(8): 2296-2305.

Tibshirani, R., G. Walther and T. Hastie (2001). "Estimating the number of clusters in a data set via the gap statistic." Journal of the Royal Statistical Society: Series B (Statistical Methodology) **63**(2): 411-423.

Tiemann, C. A., J. Vanlier, M. H. Oosterveer, A. K. Groen, P. A. Hilbers and N. A. van Riel (2013). "Parameter trajectory analysis to identify treatment effects of pharmacological interventions." PLoS Comput Biol **9**(8): e1003166.

Toettcher, J. E., A. Loewer, G. J. Ostheimer, M. B. Yaffe, B. Tidor and G. Lahav (2009). "Distinct mechanisms act in concert to mediate cell cycle arrest." Proceedings of the National Academy of Sciences **106**(3): 785-790.

Toh, K. L. (2008). "Basic science review on circadian rhythm biology and circadian sleep disorders." Ann Acad Med Singapore **37**(8): 662-668.

Tornheim, K. and J. M. Lowenstein (1975). "The purine nucleotide cycle. Control of phosphofructokinase and glycolytic oscillations in muscle extracts." Journal of Biological Chemistry **250**(16): 6304-6314.

- Tyson, J. J., K. C. Chen and B. Novak (2003). "Sniffers, buzzers, toggles and blinkers: dynamics of regulatory and signaling pathways in the cell." Curr Opin Cell Biol **15**(2): 221-231.
- Uson, J., A. Balsa, D. Pascual-Salcedo, J. A. Cabezas, J. M. Gonzalez-Tarrio, E. Martin-Mola and G. Fontan (1997). "Soluble interleukin 6 (IL-6) receptor and IL-6 levels in serum and synovial fluid of patients with different arthropathies." J Rheumatol **24**(11): 2069-2075.
- VanderLeest, H. T., T. Houben, S. Michel, T. Deboer, H. Albus, M. J. Vansteensel, G. D. Block and J. H. Meijer (2007). "Seasonal encoding by the circadian pacemaker of the SCN." Curr Biol **17**(5): 468-473.
- Voice, M. W., J. R. Seckl, C. R. Edwards and K. E. Chapman (1996). "11 beta-hydroxysteroid dehydrogenase type 1 expression in 2S FAZA hepatoma cells is hormonally regulated: a model system for the study of hepatic glucocorticoid metabolism." Biochem J **317** (Pt 2): 621-625.
- Vondrasova, D., I. Hajek and H. Illnerova (1997). "Exposure to long summer days affects the human melatonin and cortisol rhythms." Brain Res **759**(1): 166-170.
- Walker, B. R. and R. Andrew (2006). "Tissue production of cortisol by 11beta-hydroxysteroid dehydrogenase type 1 and metabolic disease." Ann N Y Acad Sci **1083**: 165-184.
- Walker, B. R., R. Best, J. P. Noon, G. C. Watt and D. J. Webb (1997). "Seasonal variation in glucocorticoid activity in healthy men." J Clin Endocrinol Metab **82**(12): 4015-4019.
- Walker, J. J., J. R. Terry and S. L. Lightman (2010). "Origin of ultradian pulsatility in the hypothalamic-pituitary-adrenal axis." Proc Biol Sci **277**(1688): 1627-1633.
- Weber, B., S. Lewicka, M. Deuschle, M. Colla, P. Vecsei and I. Heuser (2000). "Increased diurnal plasma concentrations of cortisone in depressed patients." J Clin Endocrinol Metab **85**(3): 1133-1136.
- Welsh, D. K., S.-H. Yoo, A. C. Liu, J. S. Takahashi and S. A. Kay (2004). "Bioluminescence Imaging of Individual Fibroblasts Reveals Persistent, Independently Phased Circadian Rhythms of Clock Gene Expression." Current biology : CB **14**(24): 2289-2295.
- Wen, J. C., F. S. Dhabhar and B. J. Prendergast (2007). "Pineal-dependent and -independent effects of photoperiod on immune function in Siberian hamsters (*Phodopus sungorus*)." Horm Behav **51**(1): 31-39.

White, P. C. (2001). "11beta-hydroxysteroid dehydrogenase and its role in the syndrome of apparent mineralocorticoid excess." Am J Med Sci **322**(6): 308-315.

Whitehouse, L., A. Tomlin and M. Pilling (2004). "Systematic reduction of complex tropospheric chemical mechanisms, Part II: Lumping using a time-scale based approach." Atmospheric Chemistry and Physics **4**(7): 2057-2081.

Wikelski, M., L. B. Martin, A. Scheuerlein, M. T. Robinson, N. D. Robinson, B. Helm, M. Hau and E. Gwinner (2008). "Avian circannual clocks: adaptive significance and possible involvement of energy turnover in their proximate control." Philosophical Transactions of the Royal Society B: Biological Sciences **363**(1490): 411-423.

Williams, L. J., V. Lyons, I. MacLeod, V. Rajan, G. J. Darlington, V. Poli, J. R. Seckl and K. E. Chapman (2000). "C/EBP regulates hepatic transcription of 11beta - hydroxysteroid dehydrogenase type 1. A novel mechanism for cross-talk between the C/EBP and glucocorticoid signaling pathways." J Biol Chem **275**(39): 30232-30239.

Wu, M. X., L. M. Zhou, L. D. Zhao, Z. J. Zhao, W. H. Zheng and J. S. Liu (2015). "Seasonal variation in body mass, body temperature and thermogenesis in the Hwamei, *Garrulax canorus*." Comp Biochem Physiol A Mol Integr Physiol **179**: 113-119.

Yamamoto, T., Y. Nakahata, M. Tanaka, M. Yoshida, H. Soma, K. Shinohara, A. Yasuda, T. Mamine and T. Takumi (2005). "Acute physical stress elevates mouse period1 mRNA expression in mouse peripheral tissues via a glucocorticoid-responsive element." Journal of Biological Chemistry **280**(51): 42036-42043.

Yazmalar, L., L. Ediz, M. Alpayci, O. Hiz, M. Toprak and I. Tekeoglu (2013). "Seasonal disease activity and serum vitamin D levels in rheumatoid arthritis, ankylosing spondylitis and osteoarthritis." Afr Health Sci **13**(1): 47-55.

Yellon, S. M. and L. T. Tran (2002). "Photoperiod, reproduction, and immunity in select strains of inbred mice." J Biol Rhythms **17**(1): 65-75.

Yin, M., S. Q. Yang, H. Z. Lin, M. D. Lane, S. Chatterjee and A. M. Diehl (1996). "Tumor necrosis factor alpha promotes nuclear localization of cytokine-inducible CCAAT/enhancer binding protein isoforms in hepatocytes." J Biol Chem **271**(30): 17974-17978.

Yoshida, K., A. Hashiramoto, T. Okano, T. Yamane, N. Shibamura and S. Shiozawa (2013). "TNF-alpha modulates expression of the circadian clock gene Per2 in rheumatoid synovial cells." Scand J Rheumatol **42**(4): 276-280.

Zallocchi, M. L., L. Matkovic, J. C. Calvo and M. C. Damasco (2004). "Adrenal gland involvement in the regulation of renal 11beta-hydroxysteroid dehydrogenase 2." J Cell Biochem **92**(3): 591-602.

Zhang, Q., S. Bhattacharya and M. E. Andersen (2013). "Ultrasensitive response motifs: basic amplifiers in molecular signalling networks." Open Biol **3**(4): 130031.

Zhang, X. Y., M. N. Trame, L. J. Lesko and S. Schmidt (2015). "Sobol Sensitivity Analysis: A Tool to Guide the Development and Evaluation of Systems Pharmacology Models." CPT Pharmacometrics Syst Pharmacol **4**(2): 69-79.

Zhou, J., R. F. Riemersma, U. A. Unmehopa and et al. (2001). "Alterations in arginine vasopressin neurons in the suprachiasmatic nucleus in depression." Archives of General Psychiatry **58**(7): 655-662.

Zi, Z. (2011). "Sensitivity analysis approaches applied to systems biology models." IET systems biology **5**(6): 336-346.

Zi, Z., K. H. Cho, M. H. Sung, X. Xia, J. Zheng and Z. Sun (2005). "In silico identification of the key components and steps in IFN-gamma induced JAK-STAT signaling pathway." FEBS Lett **579**(5): 1101-1108.

Zibera, C., N. Gibelli, G. Butti, P. Pedrazzoli, M. Carbone, L. Magrassi and d. C. G. Robustelli (1991). "Proliferative effect of dexamethasone on a human glioblastoma cell line (HU 197) is mediated by glucocorticoid receptors." Anticancer research **12**(5): 1571-1574.

APPENDIX

Table A1.

Parameter	Value	Units	Description/Reference
$V_{\text{season}}, C_{\text{season}}, n_{\text{season}}$ winter	1.5		Maximum SCN activity, Seasonal coefficient for Michaelis constant of cortisol production, Hill Coefficient/ estimated
$V_{\text{season}}, C_{\text{season}}, n_{\text{season}}$ spring	1		Maximum SCN activity, Seasonal coefficient for Michaelis constant of cortisol production, Hill Coefficient/ estimated
$V_{\text{season}}, C_{\text{season}}, n_{\text{season}}$ summer	0.75		Maximum SCN activity, Seasonal coefficient for Michaelis constant of cortisol production, Hill Coefficient/ estimated
$V_{\text{season}}, C_{\text{season}}, n_{\text{season}}$ autumn	1.2		Maximum SCN activity, Seasonal coefficient for Michaelis constant of cortisol production, Hill Coefficient/ estimated
k_{p1}	0.7965	$\mu\text{M}\cdot\text{h}^{-1}$	Rate constant of CRH production/(Mavroudis, Corbett et al. 2014)
I_{CRH}	1	μM	Strength of input signals on CRH production/ estimated
K_{p1}	1.0577	μM	Dissociation constant for CRH production/(Mavroudis, Corbett et al. 2014)
V_{d1}	0.5084	$\mu\text{M}\cdot\text{h}^{-1}$	Rate of CRH enzymatic degradation/(Mavroudis, Corbett et al. 2014)
K_{d1}	1.9627	μM	Michaelis constant of CRH enzymatic degradation/(Mavroudis, Corbett et al. 2014)
k_{fp}	0.15	μM^{-1}	Efficiency of P on ACTH and F stimulation/ estimated
k_{p2}	0.6857	$\mu\text{M}\cdot\text{h}^{-1}$	Rate of ACTH production/(Mavroudis, Corbett et al. 2014)
K_{p2}	1.0577	μM	Dissociation constant for ACTH production/(Mavroudis, Corbett et al. 2014)

V_{d2}	0.5129	$\mu\text{M}\cdot\text{h}^{-1}$	Rate of ACTH enzymatic degradation/(Mavroudis, Corbett et al. 2014)
K_{d2}	0.3069	μM	Michaelis constant of ACTH enzymatic degradation/(Mavroudis, Corbett et al. 2014)
K_{d2}	0.3069	μM	Michaelis constant of ACTH enzymatic degradation/(Mavroudis, Corbett et al. 2014)
k_{p3}	1.0302	$\mu\text{M}\cdot\text{h}^{-1}$	Rate of F central production/ estimated
K_{p3}	0.9608	μM	Michaelis constant of F central production/ estimated
V_{d3}	0.3618	$\mu\text{M}\cdot\text{h}^{-1}$	Rate of F central enzymatic degradation/(Mavroudis, Corbett et al. 2014)
K_{d3}	0.4695	μM	Michaelis constant of F central enzymatic degradation/(Mavroudis, Corbett et al. 2014)
$k_{\text{syn}_{Rm}}$	2.9	$\text{fmol}\cdot\text{g}^{-1}\cdot\text{h}^{-1}$	Synthesis rate or glucocorticoid receptor mRNA/(Ramakrishnan, DuBois et al. 2002)
$I_{c50_{Rm}}$	26.2	$\text{nmol}\cdot\text{L}^{-1}\cdot\text{mgprotein}^{-1}$	Concentration of FR(N) at which mRNA, R synthesis drops to its half/(Ramakrishnan, DuBois et al. 2002)
R_0	540.7	$\text{nmol}\cdot\text{L}^{-1}\cdot\text{mgprotein}^{-1}$	Baseline value of free cytosolic glucocorticoid receptor/(Ramakrishnan, DuBois et al. 2002)
R_{m0}	25.8	$\text{fmol}\cdot\text{g}^{-1}$	Baseline value of glucocorticoid receptor mRNA/(Ramakrishnan, DuBois et al. 2002)
$k_{\text{dgr}_{Rm}}$	$k_{\text{syn}_{Rm}}/R_{m0}$		Degradation rate of glucocorticoid receptor mRNA/(Ramakrishnan, DuBois et al. 2002)
k_{dgr_R}	0.0572	h^{-1}	Degradation rate of cytosolic glucocorticoid receptor/(Ramakrishnan, DuBois et al. 2002)
k_{syn_R}	$(R_0/R_{m0})\cdot k_{\text{dgr}_R}$		Synthesis rate of free cytosolic receptor/(Ramakrishnan, DuBois et al. 2002)
R_f	0.49		Fraction of cortisol recycled/(Ramakrishnan, DuBois et al. 2002)

k_{re}	0.57	h^{-1}	Rate of receptor recycling from nucleus to cytoplasm/(Ramakrishnan, DuBois et al. 2002)
k_{on}	0.00329	$L.nmol^{-1}.h^{-1}$	Second order rate constant of glucocorticoid receptor binding/(Ramakrishnan, DuBois et al. 2002)
k_t	0.63	h^{-1}	Rate of receptor translocation to the nucleus/(Ramakrishnan, DuBois et al. 2002)
$k_{F,MR}$	1.1011	1	Maximum extent of $F_{periphery}$ mediated activation of MR/(Mavroudis, Corbett et al. 2015)
$K_{F,MR}$	0.5	nM	Michaelis constant for $F_{periphery}$ mediated activation of MR/(Mavroudis, Corbett et al. 2015)
$k_{F,GR}$	15	1	Maximum extent of $F_{periphery}$ mediated activation of GR/(Mavroudis, Corbett et al. 2015)
$K_{F,GR}$	30	nM	Michaelis constant for $F_{periphery}$ mediated activation of GR/(Mavroudis, Corbett et al. 2015)
k_{MR}	0.34	$nM.h^{-1}$	Base production rate of MR/(Mavroudis, Corbett et al. 2015)
MR_T	1.45	nM	Total MR concentration/(Mavroudis, Corbett et al. 2015)
K_{MR}	0.21	nM	Michaelis constant for MR production/(Mavroudis, Corbett et al. 2015)
$k_{MR,deg}$	0.70	$nM.h^{-1}$	Degradation rate for MR/(Mavroudis, Corbett et al. 2015)
$k_{b,MR}$	0.00329	$nM^{-1}.h^{-1}$	Rate of mineralocorticoid receptor removal due to binding/(Mavroudis, Corbett et al. 2015)
$k_{r,MR}$	0.001	h^{-1}	Ratio of mineralocorticoid receptor recycled \times rate of recycling/(Mavroudis, Corbett et al. 2015)
$k_{b,GR}$	0.00329	$nM^{-1}.h^{-1}$	Rate of glucocorticoid receptor removal due to binding/(Mavroudis, Corbett et al. 2015)

$k_{r,GR}$	0.001	h^{-1}	Ratio of glucocorticoid receptor recycled \times rate of recycling /(Mavroudis, Corbett et al. 2015)
$k_{on,MR}/ k_{on,GR}$	1	h^{-1}	Binding rate between cortisol and the MR/GR receptor/(Mavroudis, Corbett et al. 2015)
$k_{T,MR}/ k_{T,GR}$	1	h^{-1}	Translocation rate of the activated cortisol-receptor complex/(Mavroudis, Corbett et al. 2015)
$k_{re,MR}/ k_{re,MR}$	1	h^{-1}	Rate of receptor recycling from the nucleus to the cytoplasm /(Mavroudis, Corbett et al. 2015)
$K_{MR,deg}$	1.65	nM	Michaelis constant for degradation of MR/(Mavroudis, Corbett et al. 2015)
k_{GR}	1.18	$nM \cdot h^{-1}$	Base production rate of GR/(Mavroudis, Corbett et al. 2015)
GR_T	1.81	nM	Total GR concentration/(Mavroudis, Corbett et al. 2015)
K_{GR}	0.74	nM	Michaelis constant for GR production/(Mavroudis, Corbett et al. 2015)
$k_{GR,deg}$	1.52	$nM \cdot h^{-1}$	Degradation rate for GR/(Mavroudis, Corbett et al. 2015)
$K_{GR,deg}$	1.05	nM	Michaelis constant for degradation of GR/(Mavroudis, Corbett et al. 2015)
k_f	1.2	nM^{-1}	Efficiency of P on transcription of Per-Cry/estimated
k_c	0.009	$nM \cdot h^{-1}$	Coupling strength/estimated
v_{1b}	9	$nM \cdot h^{-1}$	Maximal rate of Per-Cry transcription/(Becker-Weimann, Wolf et al. 2004)
k_{1b}	1	nM	Michaelis constant of Per-Cry transcription/(Becker-Weimann, Wolf et al. 2004)
k_{1i}	0.56	nM	Inhibition constant of Per-Cry transcription/(Becker-Weimann, Wolf et al. 2004)

c	0.01	nM	Concentration of constitutive activator/(Becker-Weimann, Wolf et al. 2004)
p	8		Hill coefficient of inhibition of Per-Cry transcription/(Becker-Weimann, Wolf et al. 2004)
k _{1d}	0.12	h ⁻¹	Degradation rate of Per-Cry mRNA/(Becker-Weimann, Wolf et al. 2004)
k _{2b}	0.3	nM ⁻¹ .h ⁻¹	Complex formation rate of Per-Cry mRNA/(Becker-Weimann, Wolf et al. 2004)
q	2		No. of PER-CRY complex forming subunits/(Becker-Weimann, Wolf et al. 2004)
k _{2d}	0.05	h ⁻¹	Degradation rate of cytoplasmic PER-CRY/(Becker-Weimann, Wolf et al. 2004)
k _{2t}	0.24	h ⁻¹	Nuclear import rate of the PER-CRY complex/(Becker-Weimann, Wolf et al. 2004)
k _{3t}	0.02	h ⁻¹	Nuclear export rate of PER-CRY complex/(Becker-Weimann, Wolf et al. 2004)
k _{3d}	0.12	h ⁻¹	Degradation rate of the nuclear PER-CRY complex/(Becker-Weimann, Wolf et al. 2004)
v _{4b}	3.6	nM.h ⁻¹	Maximal rate of Bmal1 transcription/(Becker-Weimann, Wolf et al. 2004)
k _{4b}	2.16	nM	Michaelis constant of Bmal1 transcription/(Becker-Weimann, Wolf et al. 2004)
r	3		Hill coefficient of activation of Bmal1 transcription/(Becker-Weimann, Wolf et al. 2004)
k _{4d}	0.75	h ⁻¹	Degradation rate of Bmal1 mRNA/(Becker-Weimann, Wolf et al. 2004)
k _{5b}	0.24	h ⁻¹	Translation rate of BMAL1/(Becker-Weimann, Wolf et al. 2004)

k_{5d}	0.06	h^{-1}	Degradation rate of cytoplasmic BMAL1/(Becker-Weimann, Wolf et al. 2004)
k_{5t}	0.45	h^{-1}	Nuclear import rate of BMAL1/(Becker-Weimann, Wolf et al. 2004)
k_{6t}	0.06	h^{-1}	Nuclear export rate of BMAL1/(Becker-Weimann, Wolf et al. 2004)
k_{6d}	0.12	h^{-1}	Degradation rate of nuclear BMAL1/(Becker-Weimann, Wolf et al. 2004)
k_{7a}	0.003	h^{-1}	Deactivation rate of CLOCK-BMAL1/(Becker-Weimann, Wolf et al. 2004)
k_{7d}	0.09	h^{-1}	Degradation rate of CLOCK-BMAL1/(Becker-Weimann, Wolf et al. 2004)
$k_{mRNA_{P_{in}}}$	7.3	$\mu M \cdot h^{-1}$	Base transcription rate of mRNA _P /(Mavroudis, Corbett et al. 2015)
$k_{P_{LPSR^*TLR4}}$	59.81	μM^{-1}	Efficiency of LPSR mediated transcription of mRNA _P /(Mavroudis, Corbett et al. 2015)
k_{fr}	1.07	1	Maximum extent of FGR(N) mediated suppression of mRNA _P /(Mavroudis, Corbett et al. 2015)
K_{fr}	1	μM	Michaelis constant for FGR(N) mediated suppression of mRNA _P /(Mavroudis, Corbett et al. 2015)
k_{pc}	0.3	1	Maximum extent of BMAL1 mediated suppression of mRNA_P and mRNA_{TLR4^*} / estimated
K_{pc}	25	μM	Michaelis constant for BMAL1 mediated suppression of mRNA_P and mRNA_{TLR4^*} / estimated
$k_{mRNA_{P_{out}}}$	2.89	h^{-1}	Degradation rate of mRNA _P /(Mavroudis, Corbett et al. 2015)
k_{in_p}	0.29	h^{-1}	Translation rate of P/(Mavroudis, Corbett et al. 2015)
k_{out_p}	1.06	h^{-1}	Degradation rate of P/(Mavroudis, Corbett et al. 2015)

$k_{mRNA_{Rp_{in}}}$	0.61	$\mu M \cdot h^{-1}$	Base transcription rate of $mRNA_{Rp}$ /(Mavroudis, Corbett et al. 2015)
k_{fr2}	0.8	1	Maximum extent of FMR(N) mediated transcription of $mRNA_{Rp}$ /(Mavroudis, Corbett et al. 2015)
K_{fr2}	0.5	μM	Michaelis constant for FMR(N) mediated transcription of $mRNA_{Rp}$ /(Mavroudis, Corbett et al. 2015)
$k_{mRNA_{Rp_{out}}}$	0.19	h^{-1}	Degradation rate of $mRNA_{Rp}$ /(Mavroudis, Corbett et al. 2015)
$k_{in_{Rp}}$	1.11	h^{-1}	Translation rate of R_p /(Mavroudis, Corbett et al. 2015)
k_d	0.14	$\mu M^{-1} \cdot h^{-1}$	P- R_p binding rate constant/(Mavroudis, Corbett et al. 2015)
$k_{out_{Rp}}$	0.26	h^{-1}	Degradation rate of R_p /(Mavroudis, Corbett et al. 2015)
$k_{out_{pRp}}$	1.3	h^{-1}	Degradation rate of PR_p /(Mavroudis, Corbett et al. 2015)
$k_{LPS,1}$	4.5	h^{-1}	Growth rate of LPS/(Scheff, Calvano et al. 2010)
$k_{LPS,2}$	6.79	h^{-1}	Clearance rate of LPS/(Scheff, Calvano et al. 2010)
$k_{LPS,3}$	0.0914	$\mu M \cdot h^{-1}$	Base transcription rate of $mRNA_{TLR4^*}$ /(Scheff, Calvano et al. 2010)
$k_{mRNA_{TLR4^*}}$	1.74	μM^{-1}	Efficiency of PR_p mediated transcription of $mRNA_{TLR4^*}$ /(Scheff, Calvano et al. 2010)
$k_{LPS,4}$	0.32	h^{-1}	Decay rate of $mRNA_{TLR4^*}$ /(Scheff, Calvano et al. 2010)
k_{syn}	0.02	h^{-1}	Translation rate of R_{TLR4}^* /(Scheff, Calvano et al. 2010)
k_{deg}	0.02	h^{-1}	Degradation rate of R_{TLR4}^* /(Scheff, Calvano et al. 2010)
k_2	0.04	h^{-1}	Dissociation rate between LPS and of R_{TLR4}^* /(Scheff, Calvano et al. 2010)

k_1	3	$\mu\text{M}^{-1}\cdot\text{h}^{-1}$	Binding rate between LPS and of R_{TLR4}^* /(Scheff, Calvano et al. 2010)
k_3	5	h^{-1}	Degradation rate of $LPSR_{TLR4}^*$ /(Scheff, Calvano et al. 2010)

Table A2.

Parameter	Value	Units	Description/Reference
n_{season} winter	1.5		Seasonal adrenal sensitivity to <i>ACTH</i> /(Pierre, Schlesinger et al. 2016)
n_{season} spring	1		Seasonal adrenal sensitivity to <i>ACTH</i> /(Pierre, Schlesinger et al. 2016)
n_{season} summer	0.75		Seasonal adrenal sensitivity to <i>ACTH</i> /(Pierre, Schlesinger et al. 2016)
n_{season} autumn	1.2		Seasonal adrenal sensitivity to <i>ACTH</i> /(Pierre, Schlesinger et al. 2016)
k_{fp2}	0.06	μM^{-1}	Efficiency of <i>P</i> on $F_{periphery}$ stimulation/estimated
K_{p2}	2.3978	μM	Dissociation constant for <i>ACTH</i> production/estimated
K_{p3}	1.1299	μM	Michaelis constant of $F_{periphery}$ production/estimated
V_{d3}	0.3444	$\mu\text{M}\cdot\text{h}^{-1}$	Rate of $F_{periphery}$ enzymatic degradation/estimated
k_{8a}	0.7132	$\mu\text{M}\cdot\text{h}^{-1}$	Base transcription rate of $11\beta - \text{HSD1}_{mRNA}$ /estimated
k_{8b}	0.1942	1	Maximum extent of <i>FGR(N)</i> mediated activation of $11\beta - \text{HSD1}_{mRNA}$ /estimated
K_{8b}	1.1400	μM	Michaelis constant of <i>FGR(N)</i> mediated activation of $11\beta - \text{HSD1}_{mRNA}$ /estimated
k_{8c}	0.0744	1	Maximum extent of <i>CLOCK – BMAL1</i> mediated activation of $11\beta - \text{HSD1}_{mRNA}$ /estimated
K_{8c}	0.4774	μM	Michaelis constant of <i>CLOCK – BMAL1</i> mediated activation of $11\beta - \text{HSD1}_{mRNA}$ /estimated

k_{8p}	1.4450	μM^{-1}	Maximum extent of P mediated activation of $11\beta - \text{HSD1}_{mRNA}$ /estimated
k_{8d}	2.4134	h^{-1}	Degradation rate of $11\beta - \text{HSD1}_{mRNA}$ /estimated
k_{9a}	1.3382	h^{-1}	Translation rate of $11\beta - \text{HSD1}$ /estimated
k_{9d}	6.2035	h^{-1}	Degradation rate of $11\beta - \text{HSD1}$ /estimated
k_{10a}	8.1253	$\mu\text{M}.\text{h}^{-1}$	Maximum transcription rate of $11\beta - \text{HSD2}_{mRNA}$ /estimated
K_{10a}	0.3392	μM	Michaelis constant of $11\beta - \text{HSD2}_{mRNA}$ transcription/estimated
k_{10b}	0.0337	μM^{-1}	Maximum extent of P mediated suppression of $11\beta - \text{HSD1}_{mRNA}$ transcription/estimated
k_{10d}	1.3789	h^{-1}	Degradation rate of $11\beta - \text{HSD2}_{mRNA}$ /estimated
k_{11a}	13.6271	h^{-1}	Translation rate of $11\beta - \text{HSD2}$ /estimated
k_{11d}	0.7775	h^{-1}	Degradation rate of $11\beta - \text{HSD2}$ /estimated
k_{cat1}	16.2	h^{-1}	Turnover number of $11\beta - \text{HSD1}$ /(Castro, Zhu et al. 2007)
K_{mF}	0.8	μM	Michaelis constant of $F_{periphery}$ activation/(Shafqat, Elleby et al. 2003)
k_{cat2}	0.01	h^{-1}	Turnover number of $11\beta - \text{HSD2}$ /(Gong, Morris et al. 2008)
K_{mE}	0.055	μM	Michaelis constant of E production/(Brown, Chapman et al. 1993)
k_{12d}	0.2441	h^{-1}	Degradation rate of E /estimated

Table A3.

Parameter	Value	Units	Description/Reference
v_{sd}	0.05355	$\mu\text{M.h}^{-1}$	Base activation rate of <i>CYCD</i>/estimated
k_{fd}	1.9025	1	Maximum extent of <i>FMR(N)</i> mediated activation of <i>CYCD</i>/estimated
K_{fd}	0.81	μM	Michaelis constant of <i>FMR(N)</i> mediated activation of <i>CYCD</i>/estimated
V_{dd}	0.245	$\mu\text{M.h}^{-1}$	Maximum degradation rate of cyclin D/Cdk4–6 complex/(Gérard and Goldbeter 2011)
K_{dd}	0.1	μM	Michaelis constant for the degradation of cyclin D/Cdk4–6/(Gérard and Goldbeter 2011)
V_{1e2f}	0.805	h^{-1}	Rate constant for activation of E2F by cyclin D/Cdk4–6 and cyclin E/Cdk2 complexes/(Gérard and Goldbeter 2011)
$E2F_{tot}$	3	μM	Total concentration of the transcription factor E2F/(Gérard and Goldbeter 2011)
K_{1e2f}	0.01	μM	Michaelis constant for E2F activation by cyclin D/Cdk4–6 and cyclin E/Cdk2 complexes/(Gérard and Goldbeter 2011)
k_{fe2f}	0.707	1	Maximum extent of <i>FGR(N)</i> mediated inhibition of <i>E2F</i>/estimated
K_{fe2f}	7.9436	μM	Michaelis constant of <i>FGR(N)</i> mediated activation of <i>E2F</i>/estimated
V_{2e2f}	0.7	h^{-1}	Rate constant for inactivation of E2F by the cyclin A/Cdk2 complex/(Gérard and Goldbeter 2011)
K_{2e2f}	0.01	μM	Michaelis constant for E2F inactivation by the cyclin A/Cdk2 complex/(Gérard and Goldbeter 2011)

v_{se}	0.21	h^{-1}	Rate constant for synthesis of cyclin E/Cdk2 induced by the transcription factor E2F/(Gérard and Goldbeter 2011)
V_{dE}	0.35	h^{-1}	Rate constant for the degradation of cyclin E/Cdk2 by cyclin A/Cdk2/(Gérard and Goldbeter 2011)
K_{de}	0.1	μM	Michaelis constant for the degradation of cyclin E/Cdk2/(Gérard and Goldbeter 2011)
v_{sa}	0.175	h^{-1}	Rate constant for synthesis of cyclin A/Cdk2 induced by the transcription factor E2F/(Gérard and Goldbeter 2011)
V_{da}	0.245	h^{-1}	Rate constant for the degradation of the cyclin A/Cdk2 complex by the protein Cdc20/(Gérard and Goldbeter 2011)
V_{da}	0.245	h^{-1}	Rate constant for the degradation of the cyclin A/Cdk2 complex by the protein Cdc20/(Gérard and Goldbeter 2011)
v_{sb}	0.21	h^{-1}	Rate constant for synthesis of cyclin B/Cdk1 induced by cyclin A/Cdk2/(Gérard and Goldbeter 2011)
K_{cb}	1.0568	μM	Michaelis constant of <i>CLOCK – BMAL1</i> mediated inhibition of <i>CYCB</i>/estimated
V_{db}	0.28	h^{-1}	Rate constant for the degradation of the cyclin B/Cdk1 complex by the protein Cdc20/(Gérard and Goldbeter 2011)
K_{db}	0.005	μM	Michaelis constant for the degradation, activated by Cdc20, of cyclin B/Cdk1/(Gérard and Goldbeter 2011)
V_{1cdc20}	0.21	h^{-1}	Rate constant for activation of Cdc20 through phosphorylation by cyclin B/Cdk1/(Gérard and Goldbeter 2011)
$Cdc20_{tot}$	5	μM	Total concentration of the protein Cdc20/(Gérard and Goldbeter 2011)

K_{1cdc20}	1	μM	Michaelis constant for Cdc20 activation through phosphorylation by cyclin B/Cdk1/(Gérard and Goldbeter 2011)
V_{2cdc20}	0.35	$\mu\text{M}\cdot\text{h}^{-1}$	Maximum rate constant for inactivation of Cdc20 through dephosphorylation/(Gérard and Goldbeter 2011)
K_{2cdc20}	1	μM	Michaelis constant for Cdc20 inactivation through dephosphorylation/(Gérard and Goldbeter 2011)